Mud volcanism and fluid emissions in Eastern Mediterranean neotectonic zones

Tiphaine A. C. Zitter

VRIJE UNIVERSITEIT

MUD VOLCANISM AND FLUID EMISSIONS IN EASTERN MEDITERRANEAN NEOTECTONIC ZONES

ACADEMISCH PROEFSCHRIFT

ter verkrijging van de graad van doctor aan
de Vrije Universiteit Amsterdam,
op gezag van de rector magnificus
prof.dr. T. Sminia,
in het openbaar te verdedigen
ten overstaan van de promotiecommissie
van de faculteit der Aard- en Levenswetenschappen
op dinsdag 23 maart 2004 om 15.45 uur
in de aula van de universiteit,
De Boelelaan 1105

door

Tiphaine Amandine Célia Zitter

geboren te Clamart, Frankrijk

promotor: prof.dr. W. Schlager
copromotor: dr. J.M. Woodside

À mon fils,

If we knew what it was we were doing, it would not be called research, would it?
Albert Einstein.

The research reported in this thesis was carried out at the:

Department of Sedimentology and Marine Geology
Free University of Amsterdam
Faculty of Earth and Life Science
De Boelelaan 1085
1081HV Amsterdam
The Netherlands

Financial support for this research was provided by the Netherlands Organisation for Scientific Research (NWO) through the MEDMUD (809.63.010), MEDISED (809.63.011), MEDINAUT/MEDINETH (750.199.01) and ANAXIPROBE (750.195.02) projects.

This is a Netherlands Research School of Sedimentary Geology (NSG) publication.

ISBN 90-9017859-7

Cover: 3D bathymetric view of the Anaxagoras Seamount (Anaximander Mountains area) with superimposed imagery from EM12Dual multibeam data, developed by IFREMER.

Contents

Acknowledgements

First of all I would like to thank warmly my copromotor John Woodside who initiated this project. As marine geologists, we met on a boat, and I would like to thank him for having offered me the opportunity of carrying out this research. He was always ready for helpful scientific discussions or just for a little chat to cheer you up. His continuous support, through science and life, his thoughtfulness towards the well-being of his PhD students made him the best supervisor I could ever have wished to have.

I also thank my promotor Prof. Wolfgang Schlager for his guidance and advice through the completion of this thesis.

I am grateful to the members of the reading committee for their constructive reviews and comments which improved the final version of this manuscript: Jean Mascle (who also introduced me to the world of marine geology by offering me the opportunity of my first scientific cruise), Achim Kopf (we met on a boat too), Alain Rabaute and Johan ten Veen (who I also thank for his help with the Dutch summary).

Chapters 3-6 from this thesis are based on published manuscripts, articles in press or in preparation, and I would like to thank all my co-authors, Sjerry van der Gaast, Caroline Huguen, Brechtje Jelsma, Jean Mascle, Johan ten Veen, and John Woodside as well as reviewers Martin Hovland, Achim Kopf, Alastair Robertson and other anonymous referees for their suggestions that contributed to substantial improvements of the publications.

A person I would like to mention here in particular is Caroline Huguen. Her scientific input was of great value for this thesis. We had a lot of fun together and I appreciated her hospitality in Villefranche/Mer. But above all, I thank her for her inestimable friendship and support, her help every time I needed it.

As this thesis was accomplished within an international multidisciplinary framework, I would like to thank all the medmudders and medinauters (people from MEDMUD and MEDINAUT), Vanni Aloisi, Ioanna Bouloubassi, Jean-Luc Charlou, Anke Dählmann, Gert De Lange, Aline Fiala, Jean-Paul Foucher, Yves Fouquet, Ralf Haese, Sander Heijs, Pierre Henry, Caroline Huguen, Jean Mascle, Karine Olu-Leroy, Rich Pancost, Catherine Pierre, Myriam Sibuet, Alina Stadnitskaia, and Joe Werne, for fruitful discussions and collaborations, and their welcoming hospitality during my visits to the different institutes in Brest, Villefranche/Mer, Groningen, Utrecht, Texel.

This thesis is based on geophysical and geological marine data, so I am particularly grateful to the captains, the crews, the technical teams, the IFREMER/GENAVIR technical crews and the shipboard scientific parties of the R/V Gelendzhik (ANAXIPROBE 96-TTR6), of the R/V Professor Logachev (MEDINETH expedition), of the R/V L'Atalante (PRISMED II and ANAXIPROBE cruises), of the R/V Nadir (MEDINAUT expedition), and of the submersible Nautile (MEDINAUT expedition).

During conferences, I had the opportunity to meet very interesting people. I would like to thank here the people I met in Malta, Isparta, Gent, Tromsø, Nice, San Fransisco, and during the TTR11-Leg 2 expeditions in Black Sea. Special thanks to: Yildirim Dilek, Gunay Cifci, Michael Ivanov, Martin Flower, Jeff Priest, André Poisson, Bruno Vrielynck, and Dilek Yaman.

For their help in processing the multibeam and sonar data, as well as the video recordings with the IFREMER software CARAIBES and ADELIE, I would like to thank Jean-Marie Augustin, Jean-Marc Sinquin, Benoît Loubrieu and Fabrice Lecornu. The technical support from the computer group in the Vrije Universiteit, Arie Bikker, Frans Stevens, Joska Lebis and the helpdesk was essential for getting along with computers. In addition I would like to thank the sedsec (sedimentology secretariat), as well as Alwien and Els for their help with administrative stuff.

In the Vrije Universiteit, I would like to thank all my colleagues, from the E2 corridor and from all the Earth (and later Earth and Life) Science Faculty, for the nice working environment, sharing lunches, borrels, and a lot of dinners and parties: first my 2 roommates, Hendrick and Sam (with his micro-wave, by the way thank also to Lotte for this useful present), Guido, Erwin, Remke, Elmer, Giovanna, Vale, Ute, Florian, Bart, Bram, Klaas, Heiko, Nadifa, Johan, Liesbeth, Marten, Adrian, Jeroen, Anne, Stephanie, Jorge, Tristan, Daniel, Sevgi, Jeroen (the nearly French guy), Gideon, Dimitrios, Joaquim, Barbara, Nina, Geoffrey, Jurgen, Glenn, Melanie, Tibor, Alex, Ana Maria, and Viktor.

My special thanks are also going to the French connection, in Amsterdam, Stephanie with whom I discover so much nice Amsterdam restaurants, Geoffrey, Martine, and abroad, Eric, Max, Jerome, Omar, and many others.

In Amsterdam, housing shortage made me discover for the first time the joys of sharing so an apartment. I would like to thank my dearest roommates, first Nina who always made home “gezellig” and then Giovanna who knew better than anyone to decipher my secret moods.

Speaking about accommodation, thanks to Marcel and his hospitability on Texel, to Melek for hosting me in Turkey, to Lies and her welcome in Villefranche/Mer, and thanks a lot to everyone that offered me a roof when I had to come back to Amsterdam for completing my thesis after having moved abroad: Vale and Jurgen, Stephanie, Daniel, and Giovanna.

Je voudrais également remercier mes parents pour leur soutien durant mes études et mes sœurs pour leurs fréquentes visites à Amsterdam. Merci Maman de m’avoir aider avec le bébé durant les derniers moments de la mise au point de cette thèse.

Enfin, je voudrais remercier celui auprès de qui je vis, et qui m’a attendue et soutenue, à la fin de cette thèse et ce malgrè la distance. Merci de tout mon cœur Olive de ton amour, et du merveilleux cadeau que tu m’as donné. Il s’appelle Théodore et il a été très sage pour me permettre de finir la rédaction de ce manuscrit.

Summary

Mud volcanoes result from the extrusion of fluid-rich mud flows and have long been known onshore or at sea, mainly within active belts but also on highly sedimented passive margins. However, the interest of the scientific community in submarine mud volcanoes and associated phenomena has increased as their potential importance for several processes has recently been recognized. These processes include ocean margin shaping, the release of greenhouse gases and induced climate change, energy production for chemosynthetic based life, petroleum genesis, and gas hydrates accumulation, which is seen as a potential energy resource. Therefore, a multidisciplinary approach is required to understand mud volcanism and the inter-relationships among gases, bacteria, benthic communities, sediment stability, debris flow, tectonics and the geophysical and geochemical signature of the mud volcanic products.

This thesis is part of the MEDINAUT and MEDMUD programmes, both international and national multidisciplinary research initiatives, which focussed on the Eastern Mediterranean Sea as a natural laboratory for mud volcanism and fluid emissions. The principal goal of this thesis is to determine the geological controls on mud volcanism in this area and the physical origins of the acoustic signature of the mud volcano deposits. The dataset, collected during several marine expeditions (ANAXIPROBE, PRISMED II, MEDINAUT, MEDINETH), is presented in Chapter 2 and comprises multibeam bathymetry and imagery, seismic profiles, gravity data, sidescan sonar records, submersible video records, and sedimentary cores. The thesis is divided in two parts: the first part (Chapters 3 and 4) examines the geology and sedimentology of mud volcanoes in the Eastern Mediterranean Sea, whereas the second part (Chapters 5 and 6), more specifically focusses on the Anaximander Mountains area, south of Turkey and deals with the current stress field and active deformation at the junction between the Hellenic and Cyprus Arcs, and its relation with the evolution of mud volcanism.

Sedimentology and geology of Eastern Mediterranean mud volcano deposits - In Chapter 3, the in situ observations of mud volcanoes at the seafloor (as analysed from video recordings from the submersible "Nautile" and from deep tow video) have revealed common characteristics at cold seeps, such as carbonate crust constructions and specific chemosynthetic-based fauna. The mapping of the seafloor characteristics and the degree of colonization by benthic fauna can be correlated with the observed backscatter variations. Mud volcanism activity presents a high variability related to the intensity of the fluid fluxes and, probably, the ages of the mud flows and seeps. Therefore the geophysical signature can be related to spatial and temporal variations of mud volcanism. Recognition of mud volcanic activity also depends on the type of phenomenon considered (e.g. fluid emissions, mud eruptions, biological activity) and on the scale of observation.

Chapter 4 discusses the depositional environment, age, and depth of the lithological units from which the mud breccia is extruded. The clay mineralogy of all the studied samples of the mud matrix reveals a common assemblage that is dominated by the presence of smectite (up to 90% of the total clay mineral content) and is comparable with smectite-rich terrigeneous

units of Messinian age. The absence of diagenetic transformations indicate a shallow depth for the remobilization of the mud reservoir. This is of direct relevance (as a constraint) to geochemical research into the depth of origin of seep fluids.

Tectonic control of mud volcanism: examples from the Anaximander Mountains at the junction between the Hellenic and the Cyprus Arcs - The Anaximander Mountains, a complex of three distinct seamounts rising more than 1000 m above the surrounding sea-floor, are formed by crustal blocks rifted from southern Turkey. Together with the surrounding areas (the Florence Rise and the Isparta Angle in SW Turkey) they form a tectonic accommodation zone between active deformation in the Aegean-SW Turkey region and the tectonically quieter Cyprus region. The structural pattern of the area is examined in Chapter 5 and suggests that progressive adjustment to incipient collision developed into a broad zone of NW-SE transpressive wrenching. The mud volcanoes are observed along the dominant structures of the western Cyprus Arc (the eastern Anaximander Mountains and the Florence Rise) where major longitudinal N150°-trending normal/oblique faults as well as crosscutting N070°-oriented sinistral strike slip faults occur.

Chapter 6 presents a detailed analysis of the relationship between the occurrence of mud volcanoes and tectonic features detected in O.R.E.Tech deep-tow sidescan sonar and subbottom profiler data, which were obtained during the 1999 MEDINETH expedition. The fault mapping indicates that several mud volcanoes in the Anaximander Mountains and along the Florence Rise are structurally controlled. The faults are inferred to provide pathways for over-pressured mud and fluids, and mud volcanoes appear related to both major and secondary faults within the regional stress field associated with plate convergence. This analysis reveals the a fundamental role of for transcurrent and extensional tectonics faulting, suggesting that extension generated by normal faults, and to some extent by strike-slip faults, facilitates mud extrusion.

Chapter 7 reviews the principal results from Chapter 3 to 6 and integrates them with geochemical and microbiological analyses also carried out within the MEDMUD programme to give insight into the emplacement and evolution of mud volcanoes as well as the origin of both the fluids and the solid phase of the expelled material.

Samenvatting

Moddervulkanen en vloeistoflekken in tektonisch actieve gebieden in de Oostelijke Middellandse Zee

Moddervulkanen ontstaan door de uitstoot van vloeistofrijke modderstromen en zijn reeds lang bekend op land en in zee, langs actieve plaatgrenzen en op dik gesedimenteerde passieve plaatranden. Een recente toename in de wetenschappelijke interesse voor submariene moddervulkanen en geassocieerde fenomenen is toe te schrijven aan het onderkennen van hun belang voor diverse processen. Deze processen omvatten de vorming van oceaan randen, de uitstoot van broeikasgassen en daaraan gerelateerde klimaatveranderingen, de energie huishouding voor chemosynthetische organismen, het ontstaan van olie en de vorming van gas hydraten, welke als potentiele nieuwe energie bron worden gezien. Het onderzoek naar moddervulkanen vereist daarom een multidisciplinaire aanpak, teneinde een beter begrip te krijgen van de relatie tussen gasvorming, bacteriën, benthische leefvormen, de stabiliteit van de zeebodem, tektoniek en de geofysische en geochemische karakteristieken van moddervulkaan afzettingen.

Dit proefschrift vormt een onderdeel van de MEDINAUT en MEDMUD programma's; beide gericht op internationaal en nationaal, multidisciplinair onderzoek in de Oostelijke Middellandse Zee, die fungeert als een natuurlijk laboratorium voor de studie van moddervulkanisme en vloeistoflekken. Het belangrijkste doel van dit onderzoek is om voor dit gebied enerzijds de geologische factoren te bepalen die leiden tot moddervulkanimse en anderzijds de fysische achtergrond van de acoustische kenmerken van moddervulkaan afzettingen te leren doorgronden. De hiervoor gebruikte dataset is verzameld tijdens diverse mariene expedities (ANAXIPROBE, PRISMED II, MEDINAUT, MEDINETH), welke beschreven worden in Hoodstuk 2. De verkregen dataset bevat multibeam bathymetrie en bathymetrische beelden, seismische profielen, zwaartekracht data, sidescan sonar records, duikboot video opnamen en sediment kernen. Het proefschrift is onderverdeeld in twee delen. Het eerste gedeelte (Hoofdstuk 3 en 4) bestudeert de geologie en sedimentologie van moddervulkanen in de Oostelijke Middellandse Zee. Het tweede gedeelte (Hoofdstuk 5 en 6) richt zich specifiek op de Anaximander Mountains die zich ten zuiden van Turkije bevinden, ter hoogte van de verbinding tussen de Helleense en Cypriotische Bogen. Voor dit gebied wordt de relatie tussen het voorkomen van moddervulkanen en breuken beschreven en gekoppeld aan actieve plaatgebewegingen.

Sedimentologie en geologie van moddervulkaan afzettingen in de Oostelijke Middelandse Zee - Hoofdstuk 3 geeft een analyse van in situ waarnemingen van moddervulkanen op de zeebodem aan de hand van videobeelden gemaakt vanuit de duikboot "Nautinil" en "deep-tow" video opnamen. Hieruit blijkt dat moddervulkaan depressies veel gemeenschappelijke kenmerken vertonen, zoals het voorkomen van kalkkorsten en chemo-synthetische fauna (schelpen en wormen). Diverse karakteristieken van de zeebodem en de mate van kolonisatie door bodem fauna kunnen direct gerelateerd worden aan variaties in backscatter in de side-scan sonar records. De vele variaties zijn gerelateerd aan de intensiteit waarmee vloeistof vrijkomt en, waarschijnlijk, de ouderdom van de moddervulkaan en het

vloeistoflek. Op deze manier kunnen de geofysische signaturen van moddervulkanen gekoppeld worden hun variatie in ruimtelijke en tijd. Voorts zal het herkennen van moddervulkaan activiteit sterk afhangen van het type fenomeen dat wordt bestudeerd (zoals bijvoorbeeld de vloeistoflekken, de modder uitstoot, of biologische activiteit) en de observatieschaal.

In Hoofdstuk 4 wordt de herkomst van de uitgestoten modderbreccias beschreven in termen van afzettingsmilieu, ouderdom en de diepte van het oorspronkelijke gesteente. Voor alle bestudeerde monsters toont de klei mineralogie aan dat de modder matrix een gelijke samenstelling heeft voornamelijk bestaande uit smectiet (tot 90%). Deze samenstelling komt overeen met smectiet-rijke terrigene sedimenten van Messinian ouderdom. Het ontbreken van diagenetische omzetting van de modder matrix suggereert dat de modder vanaf relatief kleine diepte is geremobiliseerd. Dit feit is van direct belang voor het geochemische onderzoek naar de herkomstdiepte van vloeistoflekken.

Tektonische controle op moddervulkanisme: voorbeelden van de Anaximander Mountains op de verbinding tussen de Helleense en Cypriotische Bogen - De Anaximander Mountains omvatten een complex van drie seamounts (submariene bergen) die meer dan 1000 m boven de omliggende zeebodem oprijzen. Deze seamounts zijn ontstaan door het loskomen en zuidwaarts bewegen van stukken korst van zuid Turkije. Samen met de omliggende gebieden (de Florence Rise en de Isparta Angle in zuidwest Turkije) vormen zij een zone van tektonische accommodatie tussen zones met actieve deformatie in het Egeïsche gebied en west Turkije en het tektonisch rustigere Cyprus gebied. Het structurele patroon van de Anaximander Mountains wordt beschreven in Hoofdstuk 5 en suggereert dat de geleidelijke aanpassing aan de actieve botsing met het Afrikaanse continent leidt tot de ontwikkeling van NW-ZO georiënteerde strike-slip zones. De moddervulkanen zijn voornamelijk geassocieerd met de dominante strukturen van de westelijke Cyprus Boog (in de oostelijke Anaximander Mountains en de Florence Rise), zoals N150°-georiënteerde normale/oblique breuken en N070°-georiënteerde strike-slip breuken.

Hoofdstuk 6 behandelt de relatie tussen moddervulkanen en tektonische fenomenen, welke zijn ontdekt in de O.R.E.Tech deep-tow side-scan sonar en subbottom profiler data, verkregen tijdens de 1999 MEDINETH expeditie. Het uitkarteren van breuken bevestigt dat het voorkomen van moddervulkanen in de Oostelijke Middellandse Zee, zowel in de Anaximander Mountains en langs de Florence Rise, wordt bepaald door breuken. In dit scenario vormen de breuken paden waarlangs de modder en vloeistof onder overdruk uitstromen. De moddervulkanen zijn geassocieerd met zowel hoofd- en secundaire breuken. Verder blijkt dat een fundamentele rol is weggelegd voor strike-slip- en extensie breuken, hetgeen suggereert dat de langs deze breuken, in meer of mindere mate, gegenereerde rek de uitstoot van modder vergemakkelijkt.

Hoofdstuk 7 geeft een overzicht van de belangrijkste resultaten van Hoofstukken 3 tot en met 6 en integreert deze met geochemische en microbiologische analyses uitgevoerd in het kader van het MEDMUD programma. Deze integratie van onderzoeksresultaten geeft inzicht in de evolutie en verplaatsing van moddervulkanen alsmede in de herkomst van de uitgestoten vloeistoffen en vaste stoffen.

Résumé

Le volcanisme boueux et les émissions de fluides dans les zones néotectoniques de Méditerranée Orientale

Les volcans de boue, résultant de l'extrusion en surface de coulées boueuses riches en fluides, sont depuis longtemps étudiés à terre et en mer, principalement au sein des marges actives mais également sur les marges passives fortement sédimentées. L'intérêt de la communauté scientifique pour les volcans de boue sous-marins s'est développé du fait de leur importance potentielle dans de nombreux domaines, parmi lesquels : la stabilité des marges continentales (déstabilisations sédimentaires, risques sismique), les variations climatiques à plus ou moins long terme (dégagement de gaz à effet de serre dans l'hydrosphère et l'atmosphère), l'évolution des communautés biologiques profondes. L'analyse et la compréhension de ces structures présente enfin un fort intérêt économique notamment comme indicateurs de la présence et du comportement des hydrocarbures en offshore profond, ainsi qu'à travers le stockage d'une quantité de méthane importante sous forme d'hydrates de gaz, pouvant représenter une source énergétique potentielle.

Cette thèse fait partie des programmes internationaux et nationaux MEDINAUT et MEDINETH, dédiés à l'étude pluridisciplinaire du volcanisme boueux et des émissions de fluides en Méditerranée Orientale. En effet, une approche multidisciplinaire est requise pour comprendre les processus physico-chimiques d'interaction entre argilocinèse et phénomènes tels que : émissions de gaz, bactéries et communautés benthiques, stabilité des sédiments (débris flow) et tectonique récente ou active.

Le principal objectif de ce travail a été de déterminer les contrôles géologiques du volcanisme boueux dans cette région et les origines de la signature acoustique des produits de l'argilocinèse à travers l'acquisition, le traitement et l'interprétation de données géophysiques et géologiques aussi diverses que bathymétrie multifaisceaux, imagerie acoustique, sismique réflexion, gravimétrie, enregistrements de sonar tracté, ou encore vidéos et prélèvements "in situ" issus de plongées profondes. Ces données qui furent collectées durant diverses campagnes marines (ANAXIPROBE, PRISMED II, MEDINAUT, MEDINETH) sont détaillées au Chapitre 2. Cette thèse est divisée en deux parties: la première (Chapitres 3 et 4) examine la géologie et sédimentologie des dépôts argilocinétiques en Méditerranée Orientale, tandis que la seconde (Chapitre 5 et 6) est plus spécifiquement axée sur la déformation actuelle dans la région des Monts Anaximandre (à la jonction de l'Arc Héllenique et de l'Arc de Chypre) et ses relations avec la mise en place et l'évolution du volcanisme boueux.

Sédimentologie et géologie des dépôts d'argilocinèse en Méditerranée Orientale - Au Chapitre 3, les observations "in situ" de la surface des volcans de boue (analysées au travers des enregistrements vidéo acquis par caméra tractée ou submersible) ont révélé des caractéristiques communes aux suintements de fluides froids, tels qu'encroûtements carbonatées et faunes spécifiques. Les variations de rétrodiffusion du fond, observées sur les données acoustiques, ont pu être corrélées, grâce aux observations directes, à des variations d'activité des volcans de boue, exprimées par des changements lithologiques et des variations

du degré de colonisation par la faune benthique. L'activité du volcanisme boueux présente en effet une grande variabilité liée à l'intensité des flux de fluides et, probablement, à l'âge des coulées boueuses et des suintements. La signature géophysique peut donc être directement attribuée aux variations d'activité du volcanisme boueux, mises en évidence à travers un certain nombre de paramètres principaux tels qu'émanations de fluides, éruptions de boue et peuplements biologiques, contrôlés par des dynamiques spatio-temporelles à différentes échelles.

Le Chapitre 4 discute l'environnement de dépôt, ainsi que l'âge et la profondeur de l'unité lithologique dont la brèche de boue est issue. L'analyse minéralogique de la matrice boueuse révèle un assemblage argileux similaire pour tous les échantillons, et dominé par la présence de smectite (jusqu'à 90% de la totalité des minéraux argileux). Ce cortège argileux est comparable aux unités terrigènes riches en smectite d'âge Messinien et démontre l'absence de transformations diagénétique, indiquant donc une faible profondeur de remobilisation pour le réservoir boueux.

Le contrôle tectonique du volcanisme boueux: exemple des Monts Anaximandre à la jonction de l'Arc Héllenique et de l'Arc de Chypre - Les Monts Anaximandre, représentent un complexe de trois monts sous-marins de plus de 1000 m de dénivelé détachés de la marge Turque. Ils forment avec les structures avoisinantes (la Ride de Florence et l'Angle d'Isparta au SW de la Turquie) une zone d'accommodation tectonique entre les déformations de la région Egéenne-Turque et la région chypriote. La déformation récente de la région est analysée dans le Chapitre 5 et indique que l'ajustement progressif de la collision s'effectue le long d'une large zone transpressive orientée NW-SE. Les volcans de boue se situent le long de la branche occidentale de l'Arc de Chypre (partie orientale des Monts Anaximandre et Ride de Florence) en association avec un réseau de failles normales à composante dextre orientées N150° parallèlement à la structure et de failles décrochantes senestres orientées N070°.

Le Chapitre 6 se concentre sur une analyse détaillée des relations entre les volcans de boue et les structures tectoniques à partir de données de sonar tracté couplé à un sondeur de sédiments (type O.R.E.Tech), obtenues lors de la campagne MEDINETH. La cartographie des failles associées à plusieurs volcans de boue des Monts Anaximandres et de la Ride de Florence indique que ceux-ci sont contrôlés structuralement. Les failles font office de conduit préférentiel pour l'expulsion de la boue et des fluides sous pression. Une relation avec les accidents majeurs et secondaires dans le champ de contraintes associé à la convergence a été mise en évidence. Cette analyse révèle le rôle fondamental des failles normales et décrochantes, suggérant que les contraintes extensives facilitent la remontée de la boue.

Le Chapitre 7 résume les principaux résultats des Chapitres 3 à 6 et les intègre dans le cadre du programme MEDMUD avec les résultats des analyses géochimiques et microbiologiques afin de déterminer les mécanismes à l'origine de l'apparition et de l'évolution des volcans de boue, ainsi que l'origine des phases solides et fluides du matériel extrudé.

Chapter 1. General Introduction

1.1. Significance of mud volcanism

1.1.1. Mud volcanism as a natural process

Mud mobilization phenomena comprising mud intrusion (mud diapirs) and extrusion (mud volcanoes; Figure 1.1) is common worldwide. The term mud volcanism refers to an array of sedimentary processes that result in the extrusion of argillaceous material on the Earth's surface or at the seafloor (Maksimovich 1940; Higgins and Saunders 1974). The extruded material is composed of a mixture of fine-grained sediments, water and gases, generally incorporating rock fragments from the deeper section. It is called either diapiric melange, argille scaliose or more commonly mud breccia (Cita *et al*. 1981) and forms characteristic elongate outflowing masses or mudflows (Figure 1.2a). The resulting geological structures are topographic elevations (Figure 1.1) of various sizes and shapes, which show a rough analogy with the morphology and activity of igneous volcanoes and therefore are named mud volcanoes. Usually mud breccia is extruded from a central vent or feeder channel, and in some cases from parasitic vents or gryphons (Figure 1.1 and 1.2b). This phenomena can occur at every scale (e.g. with eruptive cones from centimeters to hundreds of meters high and mud flows from decimeters to kilometers long). From time to time, major damaging eruptions of mud may occur. Fluid emissions are a common associated phenomenon, but may also occur outside the mud volcanoes along deep faults. Gases are expelled at localized venting sites, either as free gas in the case of terrestrial mud volcanoes (Figure 1.2c), or dissolved in pore waters and/or trapped as gas hydrates in the case of submarine mud volcanoes (Reed *et al.* 1990; Milkov 2000).

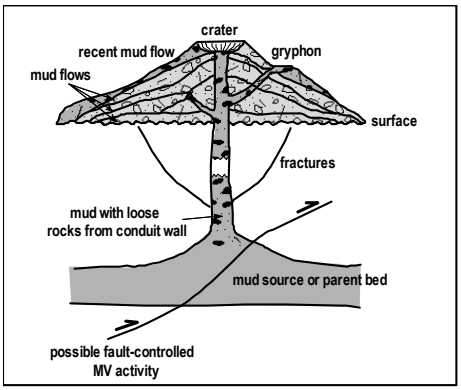

Figure 1.1: Theoretical and scale-independent cross-section of a mud volcano (modified after Dimitrov 2002; Kopf 2002).

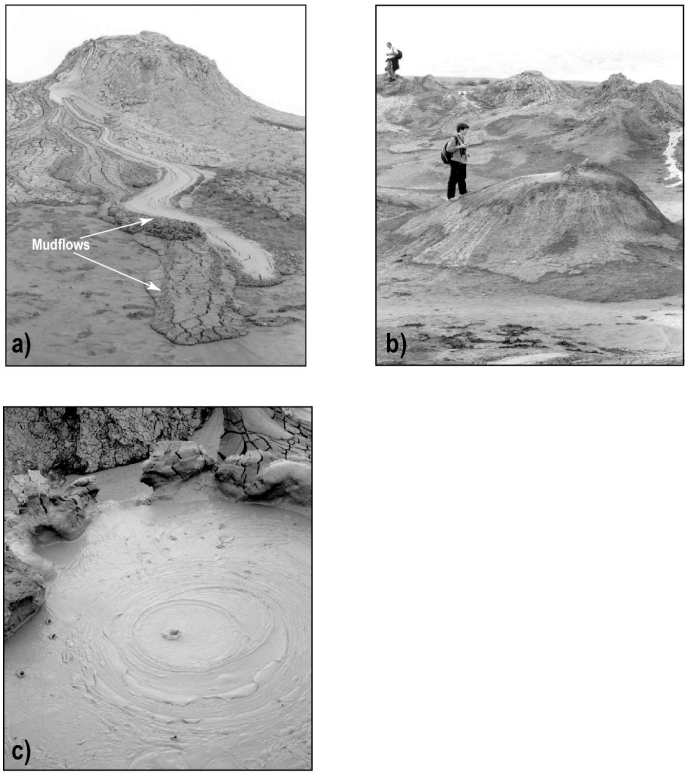

Figure 1.2: Pictures of Dashgil Mud Volcano, Azebaijan (courtesy of John Woodside) showing: a) an eruptive centre with several mud flows erupted from a 2-m high cone., b) several gryphons of about 1 m high within the main mud volcano crater, c) a mud pool with the rings created by a gas bubble.

1.1.2. Worldwide distribution of mud volcanism areas

As shown in Figure 1.3, mud volcanoes are found almost everywhere around the world, onshore as well as offshore. Higgins and Saunders (1974) reported many occurrences of mud volcanoes, but twice as many are presently known. This is due to the increasing number of submarine mud volcanoes surveyed thanks to the wide use of more advanced equipment for underwater exploration in the last ten years. It is probable that a significant number of mud volcanic fields are still to be discovered.

Mud volcanoes and fluid vents occur predominantly at active margins (Figure 1.3). They are mostly found along the Alpine-Himalayan collisional belt, extending from the Mediterranean Sea (Cita *et al*. 1981; Limonov *et al*. 1996; Woodside *et al*. 1997a; Robertson *et al*. 1998), over the Black and Caspian Sea (Ivanov *et al.* 1992; Woodside *et al*. 1997b), the Crimea and Taman peninsula, Azerbaijan (which has the biggest land mud volcanoes in the world; Hovland *et al.* 1997; Fowler *et al.* 2000), Turkmenistan and Iran, as far as into the Makran coast (Wiedicke *et al.* 2001). Further south, mud volcanoes occur along collision zones in most parts of the Indian Ocean and along the Indonesia and Banda fore-arc islands

(Wiedicke *et al.* 2002). Mud volcanoes can be found on Sumatra, Borneo (van Rensbergen *et al.* 1999), Timor (Barber *et al.* 1986), Taiwan and in the Nankai trench (Chamot-Rooke *et al*. 1992). Mud volcanoes are also numerous on the Barbados accretionary prism (Brown and Westbrook 1988; Le Pichon *et al*. 1990), on Trinidad island and the southern Caribbean thrust belts (Vernette *et al*. 1992; Reed *et al*. 1990), as well as along the northeastern American coast (Orange *et al*. 1999).

On passive margins, mud volcanoes are mainly associated with highly sedimented environments such as deep-sea fan and deltaic systems: on the Niger delta (Graue 2000), in the Gulf of Mexico (Sager *et al*. 2003), in the Nile deep-sea fan (Bellaiche *et al*. 2001) and in the Norway Sea (Vogt *et al*. 1991, 1999). They also occur on less sedimented margins such as in the Alboran sea (Perez-Belzuz *et al*. 1997) and Gulf of Cadiz (Kenyon *et al.* 2000, 2001).

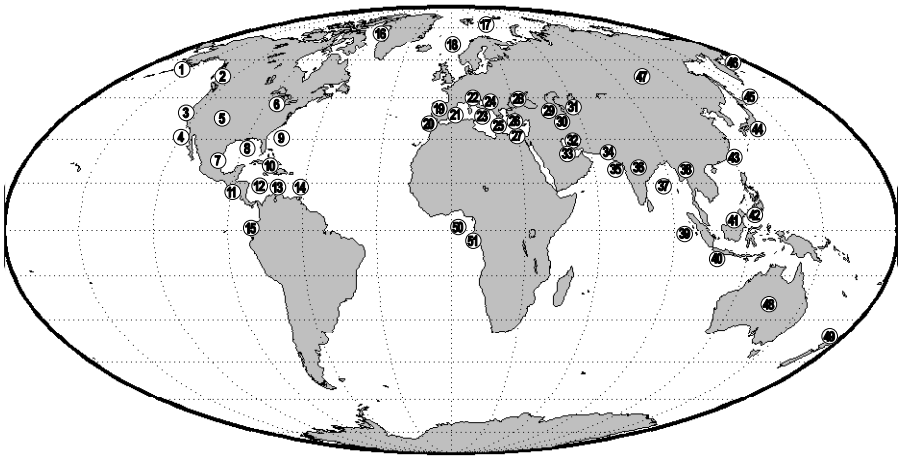

① Aleutian Trench, Alaska margin
② British Columbia, Canadia
③ Cascadia Margin
④ Monterey Bay, offshore California
⑤ Yellowstone, Wyoming
⑥ Lake Michigan
⑦ Mexico
⑧ Mississippi Delta, Gulf of Mexico
⑨ Offshore North Carolina
⑩ Barbados
⑪ Costa Rica
⑫ offshore Panama
⑬ Colombia Margin
⑭ Venuzuela,Trinidad
⑮ Ecuador
⑯ Greenland
⑰ Barents Sea
⑱ North Sea
⑲ Spain
⑳ Gulf of Cadiz
㉑ Alboran Sea
㉒ Appenines
㉓ Sicily
㉔ Adriatic Sea
㉕ Mediterranean Ridge
㉖ Anaximander Mountains
㉗ Nile Fan
㉘ Black Sea
㉙ Azerbaijan
㉚ Caspian Sea
㉛ Turkmenistan
㉜ Iran
㉝ Persian gulf
㉞ Pakistan
㉟ Makran Coast
㊱ India
㊲ Bay of Bengal
㊳ Burma
㊴ Sumatra, Java
㊵ Timor Arc
㊶ Borneo
㊷ Malaysia, offshore Borneo
㊸ Taiwan
㊹ Nankai Trench
㊺ Japan Trench
㊻ Bering Sea
㊼ Baikal Lake
㊽ Australia
㊾ New Zealand
㊿ Niger Delta
51 Angola

Figure 1. 5: Worldwide occurrence of mud volcanoes modified after Milkov 2001; Kopf 2002.

Most of the mud volcanic fields are closely associated to areas where hydrocarbons have been or are actively generated (e.g. Azerbaijan, Caucasus, Indonesia, Carribean, North Sea). The ubiquity of modern mud volcanoes also suggests that there should be many in the geological records. In fact, some paleo-cones are imaged at depth on seismic sections (Fowler *et al.* 2000). Some deposits such as melanges or debris flows might need to be re-evaluated for a better interpretation in terms of mud volcanoes (Barber *et al*. 1986). However, the vulnerability towards erosion of this object makes it difficult to preserve through geological times.

1.1.3. The mechanisms of mud volcano formation

The primary mechanism for the ascent of buried sediments is density inversion or buoyancy force (Brown 1990); it is the main driving force for the ascent of diapirs but this is often not sufficient for vigorous mud extrusion. On the other hand, rapid flow of pore fluids through a sedimentary mass (caused by gas or water flux, gas expansion or shearing stresses) may cause fluidisation (Brown 1990) and provoke buoyancy without any density contrast (diatremes). Actually, the major factor for the formation of mud volcanoes seems to be the overpressuring of a light, plastic, undercompacted fined-grained layer in the deeper sedimentary section. Mud extrusion occurs when pore-fluid pressure exceeds the lithostatic pressure causing hydraulic fracturing. Several processes, which may act simultaneously in mud volcanism areas, can induce such high pore-fluid pressure within the sediments (Barber *et al*. 1986; Dimitrov 2002; Kopf 2002):

- sediment loading (high sedimentation rate, slumps and debris flows);
- tectonic loading (lateral tectonic shortening, accretion and overthrusting);
- hydrocarbons formation;
- diagenetic phenomena (smectite dehydration);
- gas hydrate dissociation;
- hydrothermal pressuring.

The geographical distribution of mud volcanoes show that they all occur in environments where the above processes dominate (i.e. accretionary prisms, deep-sea fans, hydrocarbon provinces). Additionally, some events such as seismic activity or fault generation may trigger mud eruption.

1.1.4. Scientific issues related to fluid venting activity

Mud volcanoes have a large significance in degassing and dewatering deeply buried sediments (Kopf *et al*. 2001; Dimitrov 2002). Therefore they play a major role in the fluid and gas budget and in the geochemical cycle within the subduction factory (Kopf and Deyhle 2002). In particular, mud volcanoes may be a significant natural source of emitted atmospheric methane through massive episodic eruptions or dissociation of associated shallow gas hydrates. The contribution and role of mud volcanoes to the world greenhouse gas budget should thus be

considered in climate change and environmental studies. Mud volcanoes are also of particular interest for giving easy access to the stratigraphical and geological history, because they act as a window on deep sedimentary sequences, bringing material from deeper sections onto the surface. Many other scientific issues might be addressed, such as the role of fluid flow in sediment stability, the interplay between microbial life and fluid seepage, or the dynamics of the gas hydrate system.

1.2. Goal and scope of this research

The eastern Mediterranean Sea is an outstanding area to address the general issue of gas in sediments, due to the widespread occurrence of fluid emissions through the seafloor and the abundance of mud volcanoes there. More specifically, this research focuses on different mud volcanic fields of the eastern Mediterranean Sea (see Chapter 2): the central part of the Mediterranean Ridge (Cita *et al.* 1981, 1989, Cita and Camerlenghi 1990; Robertson *et al.* 1998; Mascle *et al.* 1999; Huguen 2001), the Anaximander Mountains (Woodside *et al* 1998), and the Florence Rise (Woodside *et al* 2002).

The principal objectives are 1/ to describe the sediments associated with mud volcanoes and fluid vents (mud flows, debris flows, authigenic carbonate crusts, brine lake deposits) and their depositional environments; 2/ to determine the processes which formed or modified these deposits (origin of mud and fluids, mechanisms of extrusion, unstable sediments and associated deformation); 3/ to investigate the nature of acoustic backscattering by correlating the observed sedimentary facies and their geophysical signature.

In particular, this research addresses these general questions:

- Can mud volcanism activity (episodicity/frequency of mud eruption, abundance of methane, type of seeps, geographical repartition of fluid vents) be defined and quantified?
- What is the relationship of mud volcanoes with tectonic structures?
- In how far is the occurrence of mud volcanoes and the presence of gas hydrates predictable?

1.3. A multidisciplinary investigation

This research is a component of both the NWO-funded MEDMUD (809.63.010) and MEDINAUT (750.199.01) projects, respectively national and international projects studying mud volcanism and cold seeps with a multidisciplinary approach. The multidisciplinary aspect is essential to link all the diagenetic processes associated with fluid flow, such as biological and geochemical activity at mud volcanoes. These projects provide in this way an unique opportunity to work out the inter-relationships among gas, gas hydrates, bacteria, benthic ecology, stability of sediments, debris flows and tectonics at cold seeps and mud volcanoes.

Within the Dutch MEDMUD (Mediterranean Mud volcanism) project, the different participating groups are roughly defined by their scientific specialities: geochemistry (RUU),

sedimentology and geophysics (VU/this research), engineering and geotechnical properties (WLDelft), microbiology (RUG) and carbon isotopic geochemistry (NIOZ). The French-Dutch MEDINAUT project, for the investigation of the Mediterranean mud volcanoes with the submersible NAUTILE (see Chapter 2), involves French counterparts for geological/geophysical aspects (Géosciences Azur, Villefranche-sur-Mer), isotopic studies (LODYC, Paris), geothermal and methane fluxes (IFREMER, Brest), and biological aspects (IFREMER, Brest, and OOB, Banyuls-sur-Mer).

Within the geological/geophysical collaboration, this research was more particularly focused on the Anaximander and Florence Rise areas French concentration was on the Mediterranean Ridge accretionary prism mud volcanoes (Olimpi field; Huguen 2001). Joint work on both areas integrated these studies for the purpose of comparison and generalisation.

1.4. Outline of the thesis

To begin with, Chapter 2 introduces the geodynamic and geological settings of the eastern Mediterranean basin and presents the data set used and the methods of acquisition and processing. These methods may be reminded and detailed throughout the different chapters when needed. After that, this thesis is divided into two parts.

The first part, grouping Chapters 3 and 4, discusses the geology and sedimentology of mud volcanoes in the Eastern Mediterranean Sea. Chapter 3 presents the geology of mud volcanoes through combined sidescan sonar and submersible observations from the MEDINAUT/MEDINETH expeditions. In Chapter 4, an X-ray clay mineral analysis of the mud matrix provides insights into the depositional environment, age, and depth of the lithological unit from which the mud breccia is extruded.

The second part, Chapters 5 and 6, focuses on the current stress field and active deformation at the junction between the Hellenic and Cyprus Arcs and their relationship with the development of mud volcanism there. Chapter 5 presents an analysis of the tectonic evolution of the area from multibeam bathymetry and imagery, seismic profiling, and gravity data. Chapter 6 discusses the tectonic control on mud volcanism and fluid emissions from combined analysis of swath multibeam imagery, seismic profiling, and sidescan sonar data. This chapter integrates the observations of mud volcanism activity, mechanisms of extrusion, and the distribution of the mud volcanic sediments.

In conclusion, Chapter 7 presents the integration of these new results with geochemical/ microbiological analysis from the MEDMUD program and gives insights into emplacement and evolution of mud volcanoes, and origin of both the fluids and solid phase of the expelled material.

Chapter 2. Introducing the Eastern Mediterranean Basin and the survey techniques

2.1. Tectonic setting of the Eastern Mediterranean Sea

2.1.1. Kinematic evolution from Jurassic to present time

The boundary between Africa and Eurasia has a long and complex tectonic history associated with different episodes of opening-closing seas, usually referred to as Tethys for the Mesozoic and Palaeozoic times, and the Mediterranean since the Tertiary (Dewey *et al*. 1973; Dercourt *et al*. 1993). The development of the Tethyan region is intimately linked with the opening of the Atlantic Ocean, to the west, that began during the Jurassic period. From Santonian time (80 Ma) to present, the main relative motion of Africa with respect to Eurasia was a N-S convergence (Figure 2.1), which led to the progressive closure of the Tethys and the creation of the Alpine-Himalayan orogenic belt. By late Cretaceous times (65 Ma) most ophiolite complexes were emplaced (Himalayan, Oman, Turkey). Compression in the whole Mediterranean region was associated with coalescent back-arc extension, with the opening and closing of numerous disconnected basins (Dercourt *et al*. 1993). In Early Miocene (Aquitanian 20 Ma), the opening of the western Mediterranean Basins (Liguro-Provençal and Tyrrhenian Basins) as well as the Aegean Sea initiated (Figure 2.2).

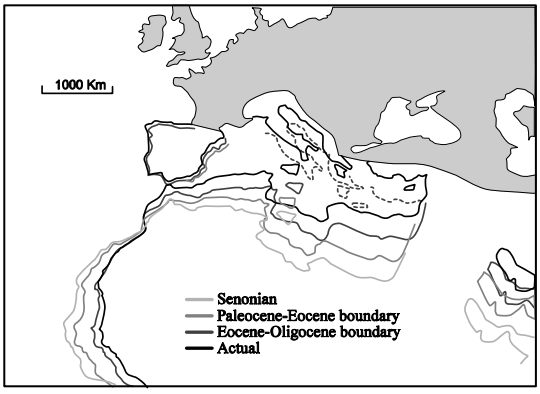

Figure 2.1: Convergent motion of Africa relative to Eurasia from Senonian to present time, from Jolivet *et al.* (1982).

In Mid to Late Miocene times, a drastic change occurred in the eastern Mediterranean tectonics, as the relative plate motion between Africa and Eurasia shifted from N-S to more NE-SW (Le Pichon and Angelier 1979). Linked to the opening of the Red Sea, the collision of the Arabian and Eurasian plates in eastern Turkey and in the Caucasus led to the closure of the seaways between the Mediterranean and the Indian Ocean. It also resulted in the westward

extrusion of the Anatolian microplate (Figure 2.3), the reorganisation of the Cyprus-Hellenic subduction zone into two separate arcs and the increase of extensional tectonics in the Aegean and western Turkey. Also in Late Miocene times, closure of the Betic strait and Rifian Corridor (former Gibraltar seaway) between the Atlantic and Mediterranean completely isolated the Mediterranean waters, causing the so-called Mediterranean salinity crisis (Hsü *et al*. 1973). This caused important environmental changes, leading to intense evaporation and deposition of thick halite and gypsum layers in the deep basins (Cita and Wright 1979).

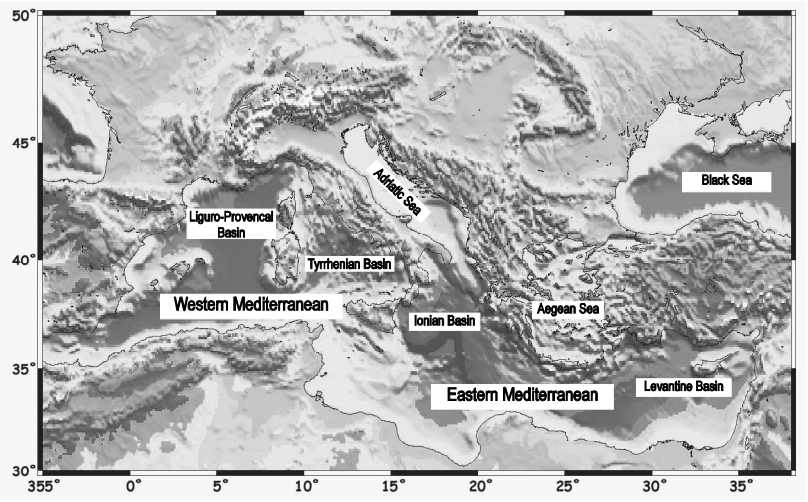

Figure 2.2: Map of the Mediterranean Basins and cited features.

The kinematic model for the present-day eastern Mediterranean tectonics involves two microplates between the African and Eurasian plate (Figure 2.3): the Anatolian microplate moving westward and the Aegean microplate moving southwestward (Mc Kenzie 1972). The partitioning of plate movements in the Anatolian-Aegean region has been recently clarified and quantified using GPS and SLR geodetic data (Le Pichon *et al*. 1995; Reilinger *et al.* 1997; McClusky *et al.* 2000). In a Eurasian fixed reference frame, the African and Arabian plate velocities are respectively of 6 mm y^{-1} and 18 mm y^{-1} (McClusky *et al.* 2000). The resulting westward extrusion of the Anatolian plate (central Turkey) can be described by a coherent counterclockwise rotation around a pole of rotation located approximately NE of the Nile delta, with a velocity of about 20 mm y^{-1} (Le Pichon *et al*. 1995). In contrast, the southwest Aegean-Peloponnisos plate is moving faster (30 mm.y^{-1}) southwestward relative to Eurasia (McClusky *et al.* 2000), increasing the relative convergence rate in the Cretan region. As a consequence, these two microplates are separated by a zone of N-S extension that comprises western Turkey, and are bounded to the north with a zone of associated strike-slip and extensional stresses (Figure 2.3).

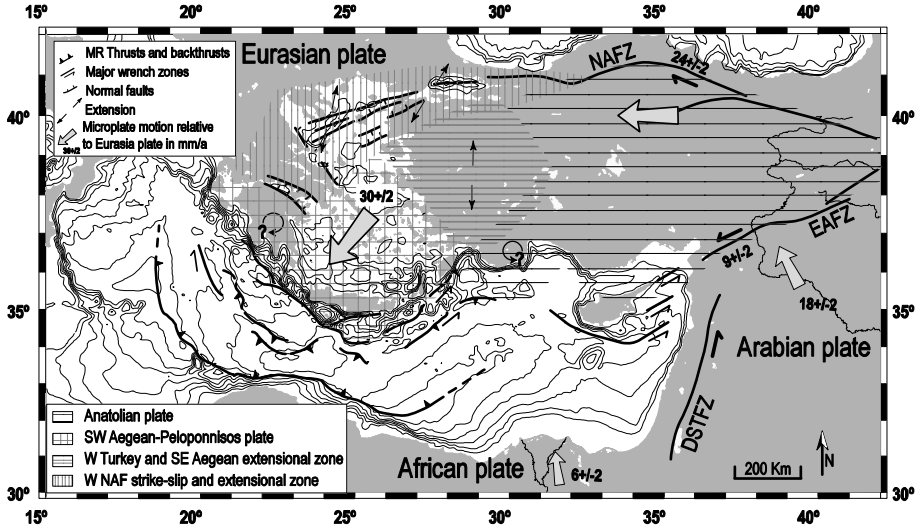

Figure 2.3: Kinematic model of the Eastern Mediterranean convergent zone from the interpretation of geodetic velocities (modified after Mc Clusky et al. 2000). Patterns indicate areas of coherent motion and zones of distributed deformation (see legend). Circular arrows indicate areas of possible rotation. Abbreviations are as follow, EAFZ: East Anatolian fault zone, NAFZ: North Anatolian fault zone, DSTFZ: Dead Sea transform fault zone.

2.1.2. Geodynamic setting of eastern Mediterranean region

The Eastern Mediterranean comprises the Ionian Basin in the west, and the Levantine Basin in the east (Figure 2.2). In contrast to the Western Mediterranean Basins, formed of relatively recent oceanic crust (Miocene), the Eastern Mediterranean Sea may partly be formed of Mesozoic oceanic crust, interpreted as remnant of the Tethyan seafloor, although its extent is still uncertain (De Voogd *et al*. 1992; Truffert et al. 1993; Brönner and Makris 2000; Huguen 2001).

Active subduction is occurring along the Calabrian Arc and along the Hellenic Arc (Figure 2.4), in both cases associated with a volcanic arc. Papazakos and Comminakis (1971) were the first to identify a Wadati-Benioff seismic zone from spatial distribution of earthquake loci below the Aegean region. The geometry of the plunging slab has been further analysed using tomography (Spakman *et al*. 1988, Papazachos *et al*. 1995) and shows two domains: a shallower part dipping 30° and a deeper part dipping 45° (Papazachos *et al*. 2000). The land-locked configuration of the Mediterranean region leads to southward roll-back of the trench system, and extension in back-arc regions (Wortel and Spakman 1992). Ultimately, it results in slab detachment, which may be in process below the Hellenic Arc, whereas it is already completed below the Calabrian Arc (Wortel and Spakman 2000). Several authors interpreted this fragmentation of the down-going slab, as indicative of incipient collision processes (Mascle *et al*. 1982; Nur and Ben-Avraham 1978).

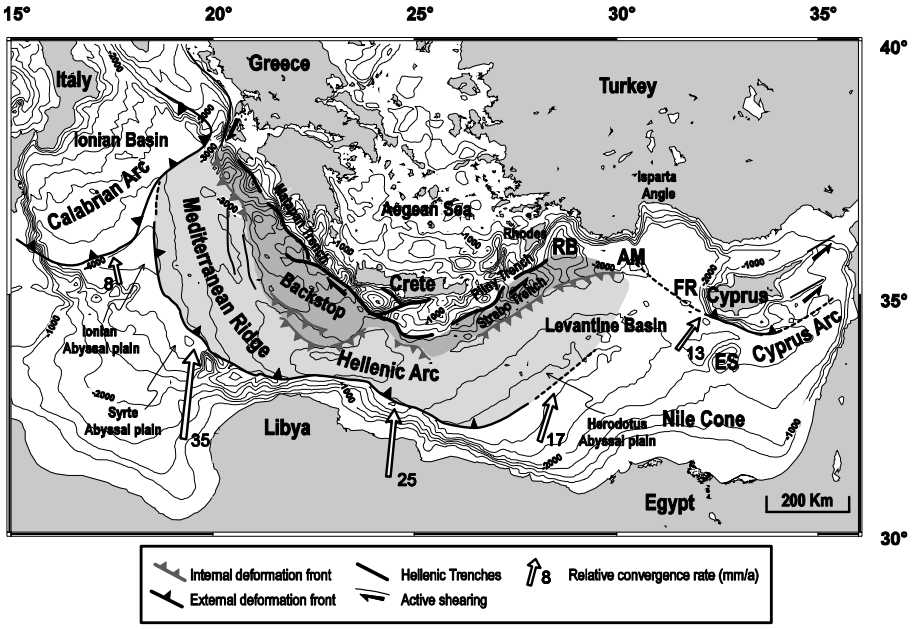

Figure 2.4: General tectonic context of the Eastern Mediterranean Sea with the locations of the main features cited in the text. Abbreviations are as follow: RB: Rhodes Basin, AM: Anaximander Mountains, FR: Florence Rise, ES: Eratosthene Seamount. Big arrows indicate the relative convergence of Africa with respect to the Anatolian microplate (from Loubrieu et al. 2000).

The crustal stretching of the Aegean and southwestern Turkey region, that occurred in late Miocene time, is attributed to the combination of roll-back processes (Le Pichon et Angelier 1979), westward extrusion of Anatolia (Le Pichon *et al*. 1995), and post-orogenic collapse (Jolivet *et al*. 1998). It affected the eastern branch of the Hellenic Arc, both in Crete (ten Veen and Meijer 1998) and Rhodes (ten Veen and Kleinsphen 2002). This extensional phase is also related to the formation of the Rhodes Basin (Woodside *et al*. 2000) and the rifting of the Anaximander Mountains from southern Turkey (Woodside *et al*. 1998). The important obliquity of the convergence due to the increasing curvature of the arc leads to the development of a transtensional stress field in most of these areas, e.g. eastern branch of the Hellenic Arc (Le Quellec and Mascle 1978; Le Pichon *et al.* 1979; Mascle *et al.* 1986), the Isparta Angle in SW turkey (Glover and Robertson 1998), the Anaximander Mountains (ten Veen *et al.* 2003).

Further east, the Hellenic Arc merges with the Cyprus Arc (Ben Avraham *et al*. 1995), which appears to act as a transpressive relay between the Mediterranean subduction zones and the collision zones in Turkey and Iran, Taurides and Zagros area (see Chapter 5). The deformation style along the Cyprus Arc is also complicated by the presence of several interfering blocks (Figure 2.4), either rifted southwards from Europe (i.e. the Anaximander Mountains) or detached from Africa and caught in the collisional process (e.g. the Eratosthenes seamount).

2.1.3. The Mediterranean Ridge accretionary prism

The Mediterranean Ridge (Figure 2.4) is an important accretionary prism, outlining the Hellenic subduction (Le Pichon *et al*. 1982a; Ryan *et al.* 1982). It is an arcuate belt of deformed sediments extending over 1500 km from W to E with a relief of about 1 to 2 km. To the south, the external deformation front is outlined by a series of small abyssal plains (Ionan abyssal plain, Syrte abyssal plain and Herodotus abyssal plain). It is assumed that the accretionary complex (outer and central units) is thrusted northwards over the backstop (or inner unit) (De Voogd *et al* 1992; Truffert *et al*. 1993; Chaumillon and Mascle 1995). To the north, the backstop is bordered by the Hellenic trenches (the Matapan trench to the west and the Pliny and Strabo trenches to the east), which are troughs up to 5000m deep. Two zones of ductile layers could be envisioned as décollement levels within the prism: the Messinian halite layer and, deeper, in the Cretaceous shales (Ryan *et al*. 1982; Camerlenghi *et al.* 1992). From the analysis of high-resolution multichannel seismic profiles, Mascle and Chaumillon (1998) proposed two phases of accretion for the Mediterranean ridge: (a) a pre-Messinian prism (the inner unit) accreted on a décollement level situated within the Aptian shales and (b) a post-Messinian accretion (the outer unit) built on a décollement level within the Messinian ductile layer.

2.2. The marine expeditions

This research integrates a large geophysical and geological dataset acquired during numerous marine expeditions (Figure 2.5).

The Dutch ANAXIPROBE project (750.195.02) mapped and sampled the mud volcanoes and gas seep zones of the Anaximander Mountains region through two marine expeditions. The ANAXIPROBE 95 expedition, carried out on board the R/V L'Atalante (Figure 2.6a) in 1995, provided high-resolution seismic profiling, Simrad EM12D multibeam bathymetry and acoustic imagery, gravity and magnetic data (Woodside *et al*. 1998). The ANAXIPROBE 96-TTR6 expedition, carried out on board the R/V Gelendhzik in 1996, provided cores and dredge samples, as well as MAK-1 sidescan sonar data (Woodside *et al*. 1997a).

The French PRISMED II expedition, carried out on board the R/V L'Atalante in 1998, mapped a large area around the Olimpi mud volcanic field, on the central part of the Mediterranean Ridge (Mascle *et al*. 1999) and identified new areas of mud volcanism, particularly through the mapping of the Florence Rise area, west of Cyprus (Woodside *et al*. 2002). It provided high-resolution seismic profiling, Simrad EM12D multibeam bathymetry and acoustic imagery, gravity and magnetic data.

The MEDINAUT/MEDINETH project (750.199.01) aimed at a multidisciplinary investigation of cold seeps and mud volcanism areas in the Eastern Mediterranean Sea, through two marine expeditions (MEDINAUT/MEDINETH shipboard scientists 2000). The joint French-Dutch expedition with the manned submersible Nautile (Figure 2.7b), on board the R/V Nadir in 1998, performed twenty deep-dives and provided video observations, geological and biological samples, and "in situ" chemical measurements. The Dutch MEDINETH expedition,

on board the R/V Professor Logachev in 1999, provided coring and O.R.E.Tech sidescan sonar data (Figure 2.9).

Additionally, data from the 13 years on-going Training Through Research program (Ivanov *et al*. 1992, 1996; Limonov *et al*. 1994, Woodside *et al*. 1997a) were incorporated in the dataset. They provided mainly high-resolution seismic and MAK-1 sidescan sonar data.

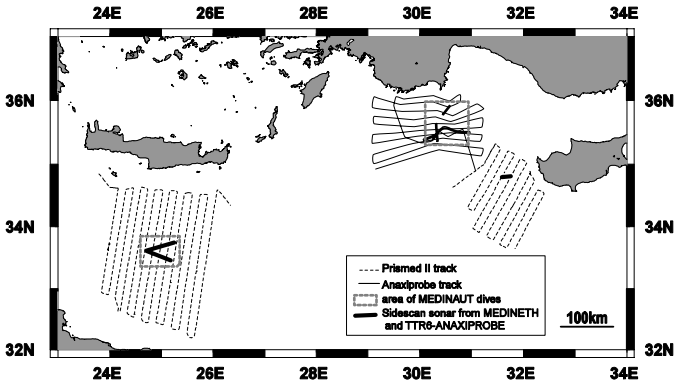

Figure 2.5: Location of the different data integrated with this study.

2.3. Acquisition and processing parameters

2.3.1. The Simrad EM12Dual

The Simrad EM12Dual is a multibeam echosounder providing both bathymetry and acoustic imagery of the seafloor. It operates at 13kHz with 162 beams (Figure 2.6b) allowing a coverage of about seven times the water-depth, i.e. 15 km for a depth of 2000 m. The bathymetry is calculated from the two-way travel time, whereas imagery is deduced from the backscattered energy. Expandable bathythermographs (XBTs) were deployed frequently (4 to 10 per day) to determine the sound velocity profile in the water column. Accurate positioning is given by the ship's GPS system. Data processing was accomplished on board and additionally on land using CARAIBES software (©Ifremer).

Bathymetry

The bathymetry data were obtained as follows: the beams flagged as "bad" by the echosounder during acquisition were automatically eliminated from further processing. Time series of bathymetry data were initially merged with the logged navigation. Gridding was based on a nearest-neighbours simple average. The grid spacing depended on the scale of the mapped area, and was chosen in a range between 80 m to 250 m. Filtering was performed either using a spline, or a Gaussian weighed average scheme. The final bathymetry grids were constructed by combining gridded data from ANAXIPROBE and PRISMED II surveys. GMT (Generic Maping Tool) was also used for display and plotting the final bathymetric maps (Wessel and Smith 1991).

Imagery

Using the different raw data files (navigation, bathymetry data and imagery data) the pixel of the imagery mosaic were calculated and geographically positioned. The size of the pixel usually depended on the opening angle of the echosounder, speed of the ship and shallowest depths of the area. It was set at 45 m in our case. The imagery was then interpolated with a sliding window.

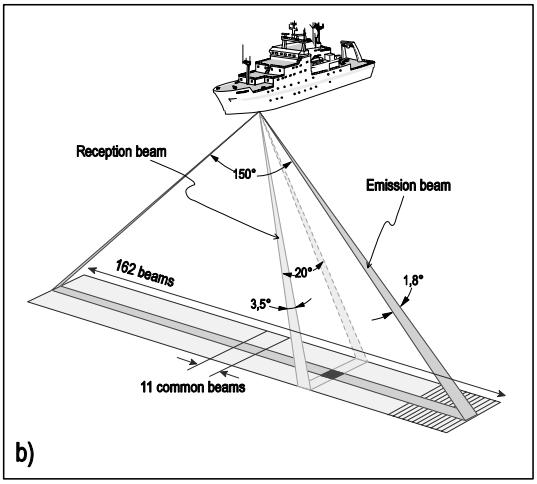

Figure 2.6: a) Picture of the R/V L"ATALANTE (courtesy IFREMER) and b) the acquisition parameters of its hull-mounted EM12Dual multibeam system.

2.3.2. The MAK-1 and O.R.E.Tech sidescan sonar

Both sonar devices were operated in Long-Range mode at 30 kHz frequency, and towed approximately 150 m above the seafloor at a speed of 1.5-2 knots (Figure 2.7a). These devices are able to insonify a swath 2000 m wide (1000 m to each side). The vehicle (or fish) is also equipped with a sub-bottom profiler (SBP) operating at a 6 kHz frequency. The position of the fish is located simultaneously with the onboard positioning system (GPS and GLONASS satellite configurations) and an acoustic short baseline underwater navigation system (SBS). This would theoretically lower the error in positioning to 1-2% of the water depth. However, because of the distance between the ship and the fish, this error is usually around 100 m.

2.3.3. The Nautile dives

The submersible Nautile (Figure 2.8b) allows direct viewing of the seafloor thanks to three port holes along with six flood lights. During the dives, video and still camera shots were recorded and manipulation, sampling and measurements were made using two retractable arms with specific tools. Surface positioning used either a long baseline system (beacons on the sea bed) or an ultra-short baseline system (sensor aboard support ship).

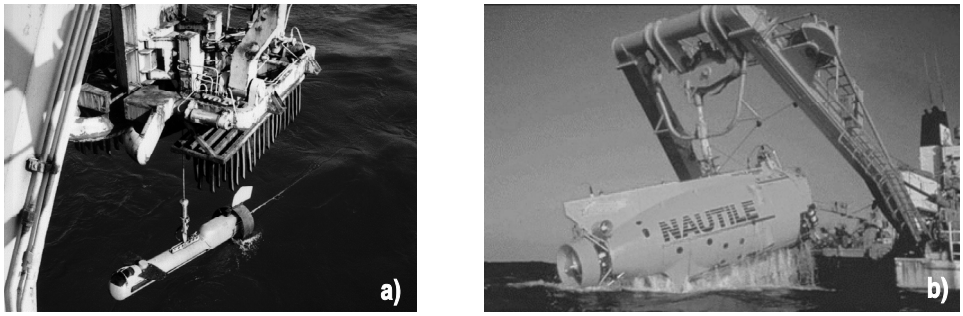

Figure 2.7: Pictures of the launching of a) the O.R.E.Tech sidescan sonar; b) the Nautile submersible from its support ship, the R/V NADIR (Courtesy IFREMER).

Processing was accomplished using ADELIE software, (©Ifremer). Based on ArcView® Geographic Information System (distributed by ESRI), ADELIE helps to import recorded data, which can be visualised and synchronized with the corresponding video. First, the navigation was filtered in order to eliminate outliers, as well as recordings of descent and ascent of the submersible. This filtering was based on: 1) the speed of the submersible, which could not exceed 2 m/s and 2) a navigation data quality factor flagged during acquisition. The dive track was then represented geographically in a view. Additional data such as dive observations, sampling sites, geochemical measurements or any point which can be localized either by a time or by its coordinates, may be plotted on the map as well. The resulting interpreted geological map with dive navigation was then superimposed on a bathymetric contour map previously imported into ADELIE.

Part I

Sedimentology and geology of Eastern Mediterranean mud volcano deposits

Chapter 3. Geology of mud volcanoes in the Eastern Mediterranean from combined sidescan sonar and submersible surveys

Abstract

Submersible observations and seafloor mapping over areas of mud volcanism in the eastern Mediterranean Sea reveal an abundance of methane-rich fluid emissions, as well as specific seeps-associated fauna (e.g. tubeworms, bivalves and chemosynthetic bacteria) and diagenetic deposits (i.e. carbonates crusts). Cold seeps characterized by abundant chemosynthetic bivalves, bacterial mats, and reduced sediments are the surface manifestations of present-day expulsion of methane-rich fluids, whereas massive carbonate crusts with clusters of tubeworms indicate long-term seeping that might be dormant nowadays. The surface characteristics of the mud flows (roughness of the surface, gas escape features, presence of hemipelagic dust, colonization by benthic fauna, development of carbonate crusts) present a high variability related to the intensity and age of seeping, and can be correlated to the observed backscatter variations. The repartition of the mud flows and active seeps is organised concentrically around the centre of the mud volcanoes and potential parasitic cones. Sidescan sonar backscatter patterns are thus indirectly related to spatial and temporal variation of mud volcanism activity.

3.2. Introduction

Mud volcanoes are sedimentary features created where mixed fluid-rich fine-grained sediments, often associated with fragments of rocks or consolidated mud (mud volcano breccia), are expelled at the earth's surface or on the seafloor (Cita *et al.* 1981; Barber *et al.* 1986; Staffini *et al.* 1993). Recognition of this mud breccia sedimentary facies is an essential characteristic for identification of mud volcanoes. However, submarine mud volcanoes are often identified, in the first place, on the basis of their distinctive geophysical signature (Brown and Westbrook, 1988; Henry *et al.* 1990; Fusi and Kenyon 1996; Vogt *et al.* 1991, 1999). They are characterized in acoustic data (e.g. multibeam imagery, sidescan sonar) by high backscattering believed to result from both roughness of the seafloor and volume backscatter of the clasts composing the mud breccia (Volgin and Woodside 1996). In that sense, high backscatter indicates the presence of a mudflow, with mud breccia at outcrop or in the near subsurface (i.e. recent clast-rich mudflows), and the backscatter level decreases with the increasing thickness of the hemipelagic sediments covering the mudflows (i.e. old mudflows). However, submersible observations of the surface of mud volcanoes (Le Pichon *et al.* 1990; Milkov *et al.* 1999; MEDINAUT/MEDINETH shipboard scientists 2000) suggest that the high backscatter could also have other sources such as carbonate crusts that form over seafloor gas seeps typical of this environment.

This chapter is based on TAC Zitter, C Huguen and JM Woodside. 2003. Geology of mud volcanoes in the Eastern Mediterranean from combined sidescan and submersible surveys. Deep Sea Research Part I. *In press.*

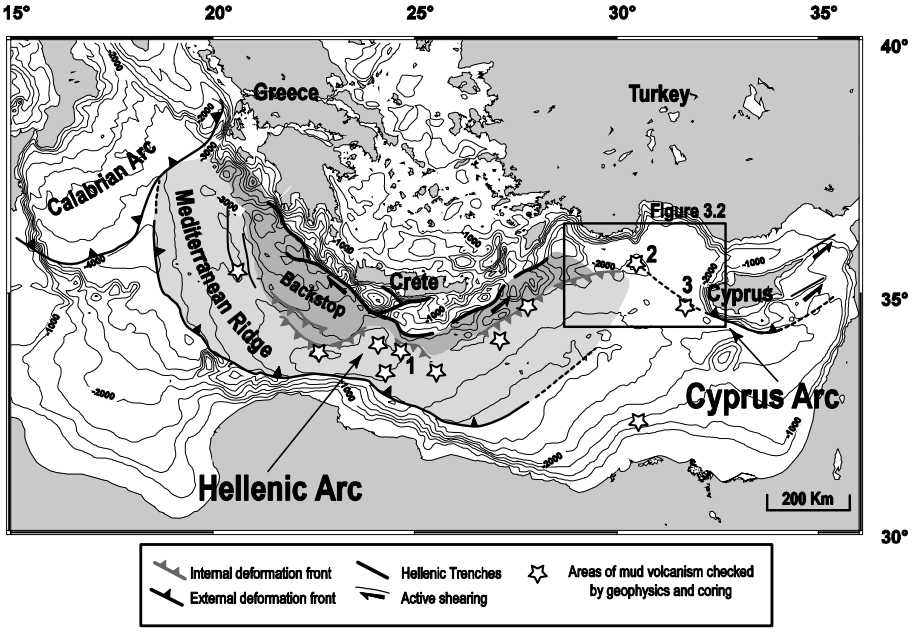

Figure 3.1: a) General tectonic setting of the Eastern Mediterranean Sea. The stars indicate the location of the main mud volcanic fields (from Limonov et al. 1996; Ivanov et al. 1996; Woodside et al. 1998, 2002; Huguen et al. 2001; Kopf et al. 2001; Bellaiche et al. 2001). The mud volcanic fields explored during the MEDINAUT and MEDINETH expeditions are numbered 1: Olimpi field, 2: Anaximander Mountains and 3: Florence Rise. The location of Figure 3.2 is indicated by a box.

Mud volcanism is a common phenomenon in the eastern Mediterranean Sea (Cita *et al*. 1981; Limonov *et al.* 1994; Ivanov *et al.* 1996; Woodside *et al.* 1998, 2002; Huguen, 2001; Kopf *et al.* 2001, Bellaiche *et al.* 2001), partly because of the lateral overpressuring of sediments associated with the convergence of the African and Eurasian plates. Areas of cold seeps and mud volcanism are mostly located within the Mediterranean Ridge, the accretionary prism of the Hellenic Arc subduction zone, but are also encountered further east along the Cyprus Arc and within the Nile deep-sea fan (Figure 3.1). The Dutch-French multidisciplinary project MEDINAUT/MEDINETH investigated mud volcanism through high resolution sidescan sonar and deep submersible dives (MEDINAUT/MEDINETH scientists 2000) focused on two of these areas: the Olimpi field (Cita and Camerlenghi 1990; Camerlenghi *et al.* 1992; Robertson *et al.* 1998; Mascle *et al*. 1999) and the Anaximander Mountains area (Woodside *et al.* 1997a; Woodside *et al.* 1998; see Figure 3.1). The dives with the manned research submersible "Nautile" facilitated an integrated multidisciplinary study, combining sedimentologyl, geochemistry and (micro-)biology. They provided the first *in-situ* observations of mud volcanism in the eastern Mediterranean Sea, although deep-tow video observations were already available over the Olimpi Field from the third Training Through Research (TTR3) expedition (Limonov *et al*. 1994). This dataset was completed by geophysical/acoustic data (deep-tow sidescan sonar and subbottom profiler), deep-tow video camera profiles, and

sediment samples from gravity and piston cores, mainly obtained during the MEDINETH expedition in 1999 and the TTR6-ANAXIPROBE expedition in 1996.

This chapter examines the geology and geomorphology of mud volcanoes through combined observations from high-resolution sidescan sonar and visual seafloor observations, focussing more specifically on the Anaximander Mountains area. We present sidescan sonar mosaics (O.R.E.Tech and MAK1) over five mud volcanoes (MVs) of the Anaximander Mountains area (namely Amsterdam, Kazan, Kula, Tuzlukush and Saint Ouen l'Aumône), interpreted in connection with visual observations (from deep dives or core analysis), when available, to provide "ground-truth" of the reflectivity patterns. The synthesis of the different data, compared with similar studies in the Olimpi mud field (Huguen *et al.* 2003), provides constraints on spatial and temporal variations of mud volcanism and insights into the origin of the geophysical signature.

3.3. Acquisition of data

A large range of acoustic data exists from the Anaximander Mountains area including acoustic imagery from a multibeam swath mapping system (Simrad EM12Dual) and data from deep-towed sidescan sonar and subbottom profiler. Technical details for these devices are given in Chapter 2 (section 2.3.1 and 2.3.2). The EM12D is used as a regional reconnaissance tool. The detailed geomorphologic analysis of the mud volcanoes discussed in this chapter is based essentially on the sidescan sonar and subbottom profiling data. Two types of sidescan sonar were used for this study:

(1) O.R.E.Tech sonar records were acquired during the 1999 MEDINETH expedition along three lines 20 to 30 km long.

(2) MAK deep-tow data from the TTR6-ANAXIPROBE expedition were obtained with a MAK1 sidescan sonar and subbottom profiler, operating similarly to the O.R.E.Tech device in Long Range mode.

The sonar data were reprocessed afterwards and geographically repositioned, to provide better resolution of the geometry of the seafloor structures. For the O.R.E.Tech data, this was done with the help of the Ifremer software CARAIBES©. The analogue MAK1 data were merged using graphical techniques.

The penetration of the different deployed acoustic tools depends on the frequency and on the angle of incidence of the beam on the seafloor. The attenuation of the acoustic signal into sediments may vary from 0.4 –1 dB/m at a frequency of 13 kHz, to 1-3 dB/m at 30 kHz (Mitchell 1993). For the EM12Dual multibeam, the maximal penetration of the acoustic signal does not exceed a few meters. Typically for beams with an angle of incidence as low as 15°, a loss of 20 dB is attained after 2 to 6 m (calculated on the basis of the acoustic model by Mitchell 1993). In contrast, both deep-tow sidescan devices have a maximun penetration of only about 1 m into the upper sediments (Mitchell 1993), and as little as 0.1 m for very low angles of incidence (Volgin and Woodside 1996). The subbottom profiler (SBP), operating at 6 kHz, can penetrate up to 70 m below the seafloor under optimal sedimentary conditions.

Underwater navigation and observations were processed with the help of Ifremer ADELIE software©. The deep-dives were recorded with both mobile and fixed video cameras, but the video analysis discussed here is based on the fixed camera, which recorded images directly in front of the submarine. The area of observation depends on the altitude of the submersible, but in general is 2-3 m wide and several meters deep. Most images resolve objects of centimeter-scale in size. The surfaces of the mud volcanoes were mapped with respect to the small-scale relief and other characteristics of the seafloor, the distribution and nature of the authigenic crusts, the presence of active seeps, the colonization by benthic fauna, and the orientation of features related to recent deformation (ridges, scarps, faults).

Several piston and gravity cores were used to provide ground-truth for the acoustic data. They comprise samples of the sediments up to a few (about 2 to 3) meters deep, and thus permit a comparison for the penetration of the different acoustic tools. However, the positions of these cores on the seafloor are accurate only within a scope of about 100 m with respect to the recorded ship's position.

3.4. Geological framework

The Anaximander Mountains are detached continental blocks from southern Turkey (Woodside *et al.* 1997a, 1998; Zitter *et al.* 2003) located at the junction between the Hellenic and the Cyprus Arc (Figure 3.1 and 3.2). Although mud volcanoes occur within a strong compressional context in this area, they are not directly associated with an accretionary prism, as it is the case for the Olimpi field (Cita *et al.* 1981). The Anaximander Mountains are formed of much older consolidated sediments compared to the accreted marine pelagic sediments composing the sedimentary sequence of the Mediterranean ridge. The deformation style of the Anaximander Mountains and along the western branch of the Cyprus Arc was revealed by multibeam mapping and seismic profiling (Woodside *et al.* 2002; Zitter *et al.* 2003; ten Veen *et al.* 2003) and shows mainly a transpressional and transtensional strain pattern. An important point to note is that the Messinian evaporites, which was deposited in most deep Mediterranean Basins during the Messinian salinity crisis (Hsü *et al.* 1979), is absent throughout the Anaximander Mountains and the Rhodes basin (Woodside *et al.* 2000). Brine seepages are thus not observed in the area, in contrast to the Mediterranean Ridge where evaporites are present in the subsurface and where mud volcanism is often associated with brine seeps (Woodside and Volgin 1996; MEDINAUT/MEDINETH shipboard scientists 2000).

3.5. Mud volcano observations

Mud volcanoes are characterized in the multibeam acoustic data (Figure 3.3) by rounded to slightly elongated high backscattering patches, usually of one or two kilometers in diameter, except for Amsterdam mud volcano which is up to 3 km across. The mud volcanoes generally appear as variable dome-shaped reliefs of 50 to 100 m, i.e. conical (Tuzlukush), hemispherical (Kula), or irregular (Kazan).

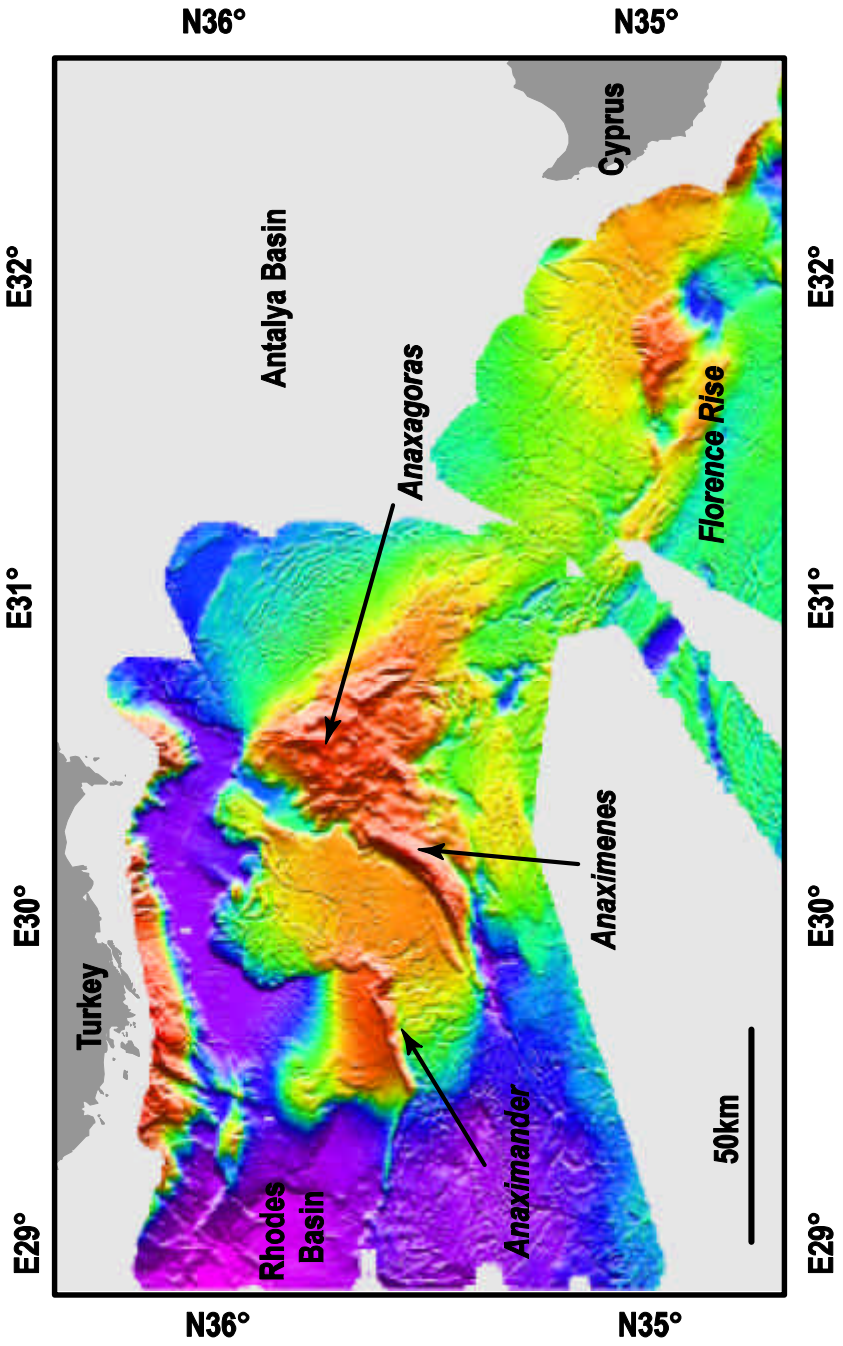

Figure 3.2: Multibeam bathymetry map of the Anaximander Mountains with reference to the main features cited in the text.

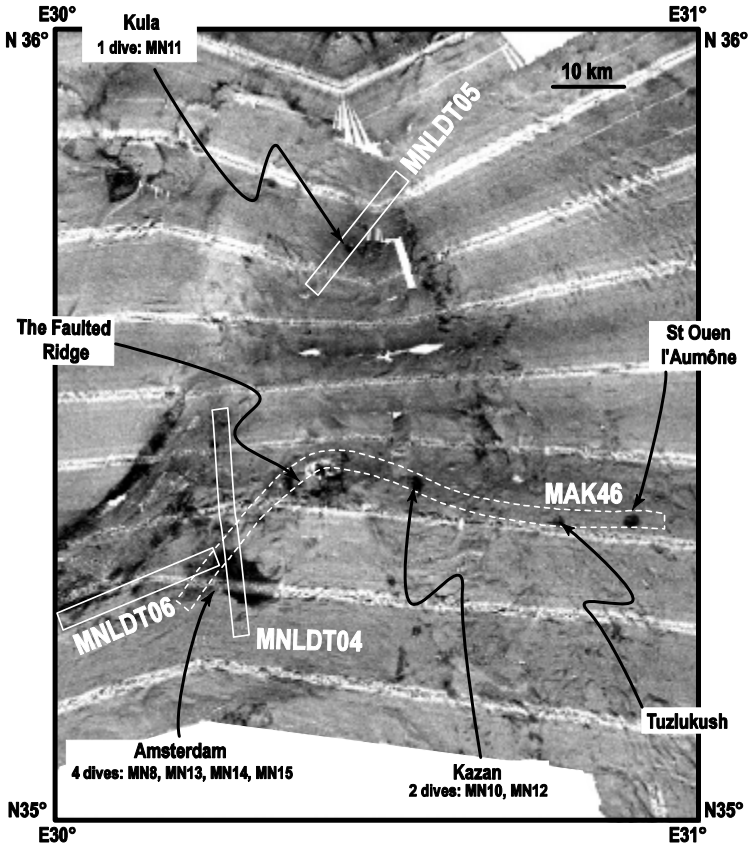

Figure 3.3: Multibeam imagery map of the AnaxagorasSeamount, with the location of the sidescan sonar lines (plain: O.R.E.Tech lines, dashed: MAK1 line). High backscatter is shown as darker shades of grey; thus the relatively large mud flow associated with Amsterdam MV appears as a black patch.

3.5.1. Amsterdam Mud Volcano

Amsterdam mud volcano (MV) is an elliptical seafloor feature up to 3 km across and about 100 m high, with a 2-km wide subcircular plateau for summit (local relief of about 10 m). It is characterized by a flat topography similar to the "mud pie" type recognized in the Barbados accretionary complex (Le Pichon *et al.* 1990), where this terminology describes a large mud accumulation with a flat summit covering an area greater than 50% of the total feature area (Le Pichon *et al.* 1990; Henry *et al.* 1990). These mud pies are believed to form from more fluidized mud than the conical mud volcanoes (Lance *et al.* 1998), or from a wider feeder channel (Kopf 2002). Mud pies often show a concentric zonation of activity, e.g. surface of the seafloor and distribution of fauna (Lance *et al.* 1998).

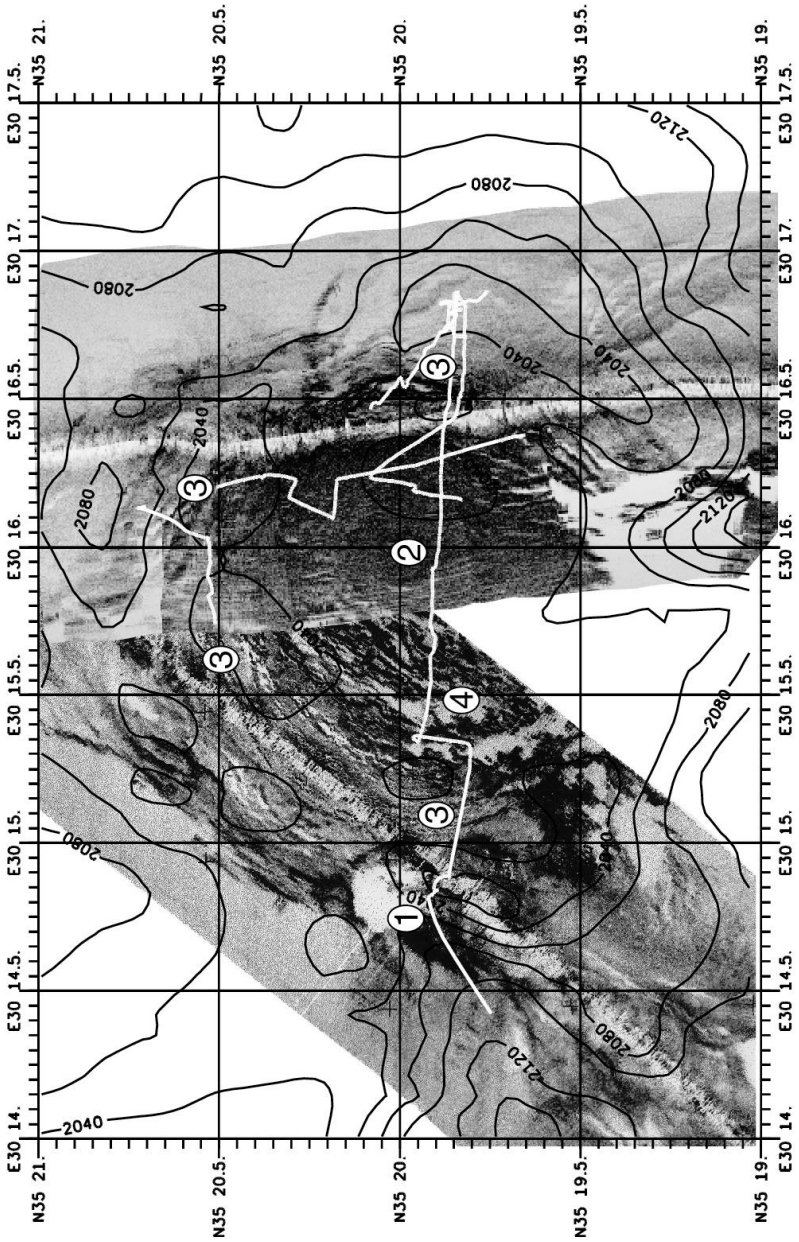

Figure 3.4: Mosaic image of two sidescan sonar lines (MNLDT04 and MAK46) on the summit of Amsterdam Mud Volcano overlying the multibeam bathymetry. The navigation of the submersible during the dives is shown by the white lines. The numbers indicate: ①:eruptive parasitic center, ②: feeder channel, ③: crevasses, ④: ridges.

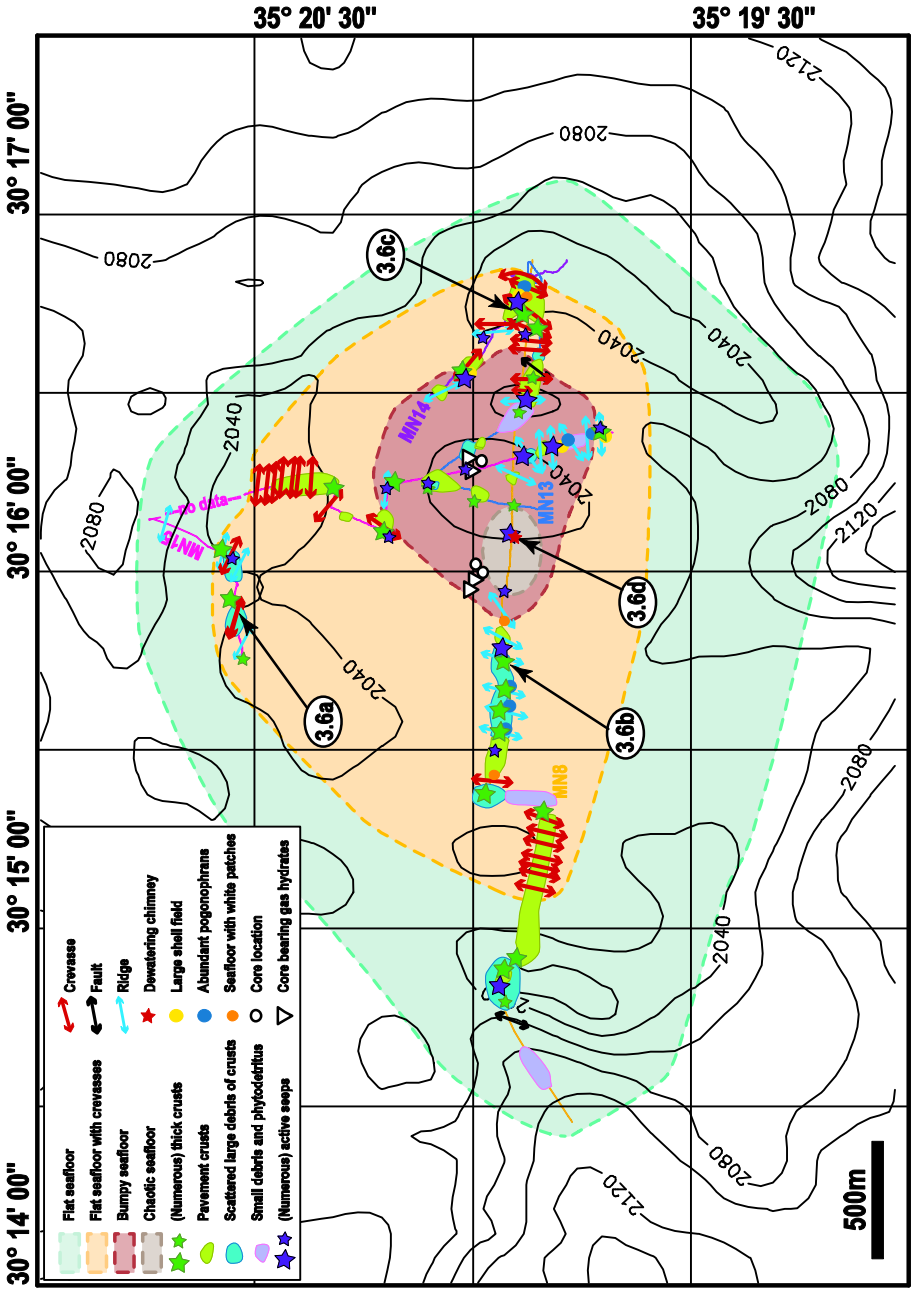

Figure 3.5: Geological map of the summit of Amsterdam MV from the interpretation of the Nautile dives. The location of the cores is also indicated, open triangles stand for the cores that contained gas hydrates and open circles for the others. The numbers refer to the pictures in Figure 3.6.

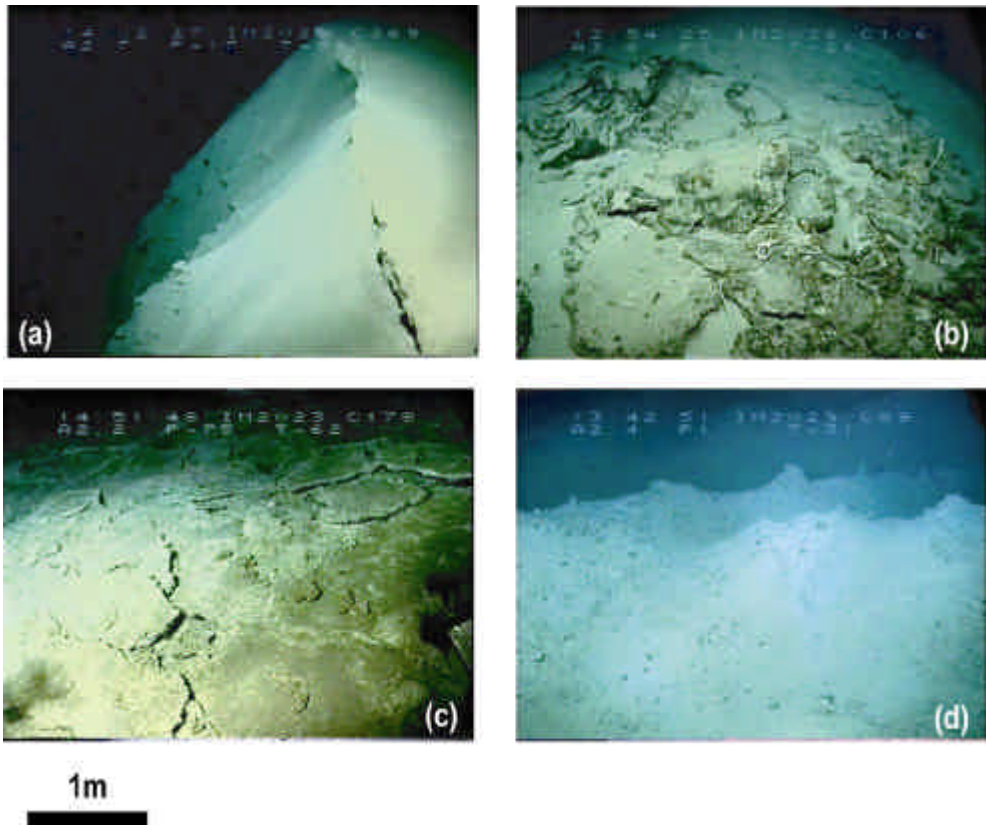

Figure 3.6: Seafloor images of Amsterdam MV showing: (a) one of the 5 to 10 metre deep crevasses that surround the summit of the mud volcano; (b) thick crust and pognophorans found on top of hills/ridges; (c) crust pavements covering the seafloor; (d) young mud flow with dewatering chimneys.

In the multibeam imagery, the high backscattering mudflows from Amsterdam MV cover an area of more than 50 km^2 (Figure 3.3). On the O.R.E.Tech line MNLDT04 record (see Figure 6.5), a mudflow is observed extending downslope to the south of the mud volcano, flowing in a SSE direction as suggested from stream lineations on the image. The flow may comprise at least 12 km^2 of recently erupted mud (MEDINAUT/MEDINETH shipboard scientists 2000), although an area of only 6 km^2 can be observed on the MNLDT04 line. The thickness of Amsterdam mud flows to the southeast has been inferred from seismic profiling to be about 300 m (Woodside *et al.* 1998) and probably results from several erupted flows overlapping and interfingering with hemipelagic sedimentation, as is the case in the Olimpi field for Napoli and Milano MV (Robertson *et al.* 1998). All the cores on the summit of the mud volcano recovered up to 1.5 m of mud breccia from an individual mud eruption event, without any intercalation of hemipelagic sedimentation or episodes of mud breccia oxidation. So the volume of the extruded mud breccia is at least 3.6 km^3 (12 km^2 area per 300 m thick)

and for a single eruption could be as much as 0.018 km^3 (12 km^2 area per 1.5 m thick flow from the last major eruption).

The summit of Amsterdam MV has been mapped with both O.R.E.Tech line MNLDT04, running roughly N-S, and MAK1 line 46, along a N040° direction, which gives a rather complete mosaic image (Figure 3.4). Four Nautile dives run across the summit (Figure 3.4 and 3.5), from west to east (dive 8), south to north (dive 15) and in the eastern part (dives 13 and 14). Its outer region presents alternating enhanced and low backscatter rims (Figure 3.4), associated with a hyperbolic facies on the profiler and corresponding to several meters deep roughly concentric crevasses/gullies and their acoustic shadows. In several locations, the dives (Figure 3.5) run across these features, and show similarly 5 to 10 meters high scarps of mud breccia, with a tens of centimeters thick compacted oxidized mud and/or carbonate crust sitting on top of it (Figure 3.6a). Dive 14 follows one narrow valley formed by these crevasses for several hundreds of meters revealing these to be continuous features, curved in map view. The wider alternating high/low backscatter rims located in the more central part of the summit appear, however, to correlate with long wavelength ridges (Figure 3.4), with thick carbonate crust construction on top of the topographic relief (Figure 3.6b).

The geological interpretation shows a rather concentric organization of mud volcanism activity on the summit of Amsterdam MV. The outer regions of the summit are covered with thin carbonate crust pavement, dusted by hemipelagic sediments, and interpreted as old mud flows (Figure 3.6c). The seafloor is smooth and uneventful in between the main reliefs (crevasses and ridges). However, at the western periphery of the plateau, a weakly reflective (white) circular patch of 450 m diameter corresponds to the acoustic shadow of a small parasitic cone (Figure 3.3), observed with the submarine to be an active fluid eruptions area (MEDINAUT/MEDINETH shipboard scientists 2000). Important fluid expulsions were observed along with numerous seeps recognisable from the very dark grey-purple colour of the reduced sediments and massive (2-3 m across and tens of centimetres-thick) carbonate crusts sitting on the top of this 90 m topographic high. The sonar image shows a higher backscatter level in the surroundings of this parasitic cone than is usual in the outer region of the summit (Figure 3.4). Another important active site, indicated by the presence of large carbonate crusts, numerous bivalves, and some clusters of vestimentiferans is situated in the eastern part of the plateau (Figure 3.5). Living specimens of bivalves were collected over this active site.

In the central part of the mud volcano, the seafloor becomes rougher, bumpy, chaotic or structured by ridges of various orientations. Numerous seeps and/or thick crusts are observed, while the crust pavements become scarce.

Near the centre of the plateau (at about E30° 16', N35° 20') an elliptical area of very high backscatter, about 300 m across, stands out on the sonar image (Figure 3.4 and 6.5). It is inferred to be over the main feeder channel of the volcano. The cores taken in the vicinity of this area (Figure 3.5) recovered dark grey mud breccia with centimetric to pluri-centimetric clasts as well as small disseminated gas hydrate crystals (generally ≤ 1 cm across but up to 2-3 cm for some of them). The dives show an exceptionally chaotic seafloor over this area with exposed clasts and shells on seafloor. This observation together with the absence of carbonate crusts on the seafloor and the observation of dewatering chimneys, and elevated concentrations

of methane in the water column (Charlou *et al.* 2003) suggests this area to be a very recent mud flow (Figure 3.6d) with active fluid seeps through it.

3.5.2. Kazan Mud Volcano

Kazan MV is a small dome 50 m high and 800 m in diameter (Figure 3.7). It is surrounded by broad shallow depressions about 10 m deep and 200 m across. Kazan MV has several very high backscatter tongue-shaped mudflows extending radially about 1 km away from the top of the mud volcano (Figure 3.7). Some different levels of backscattering (from very high to medium backscatter) are noticeable among the mudflows, inferred to indicate several different episodes of eruptions. In contrast to most of the mud volcanoes, part of the summit is characterized by a low backscatter area (Figure 3.7).

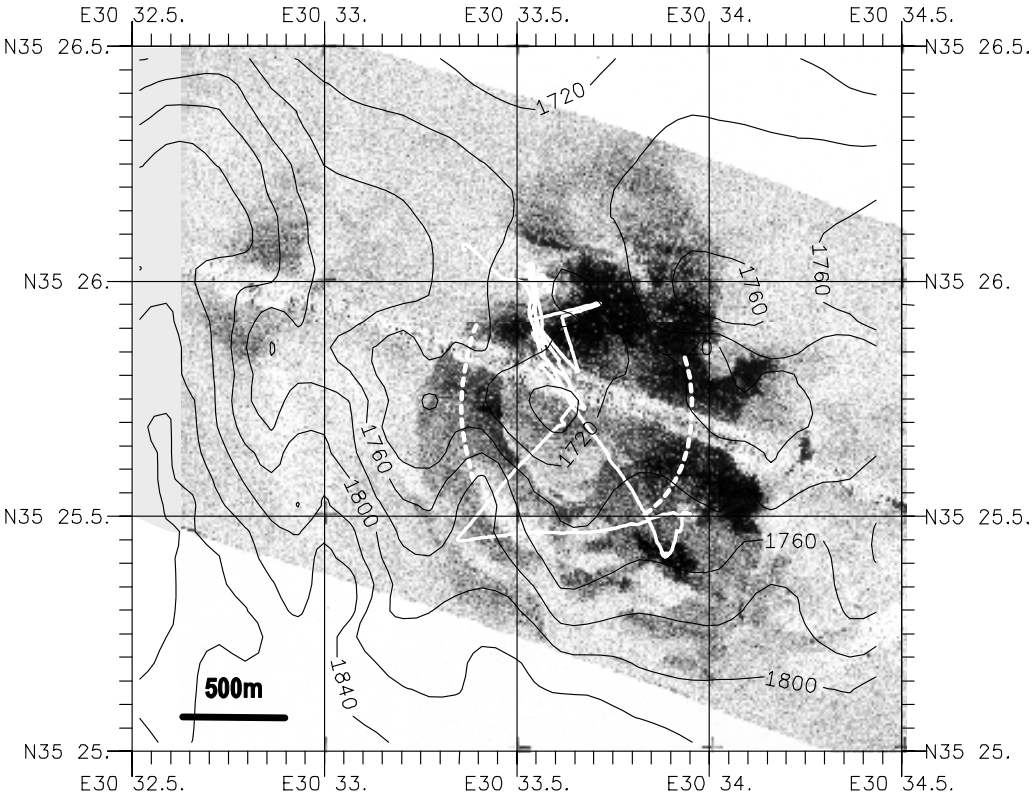

Figure 3.7: Multibeam bathymetry map of Kazan mud volcano with part of MAK 46 sidescan sonar image. The navigation of the submersible during the dives is shown by the white lines. The dashed lines outline the depressions around the mud volcano.

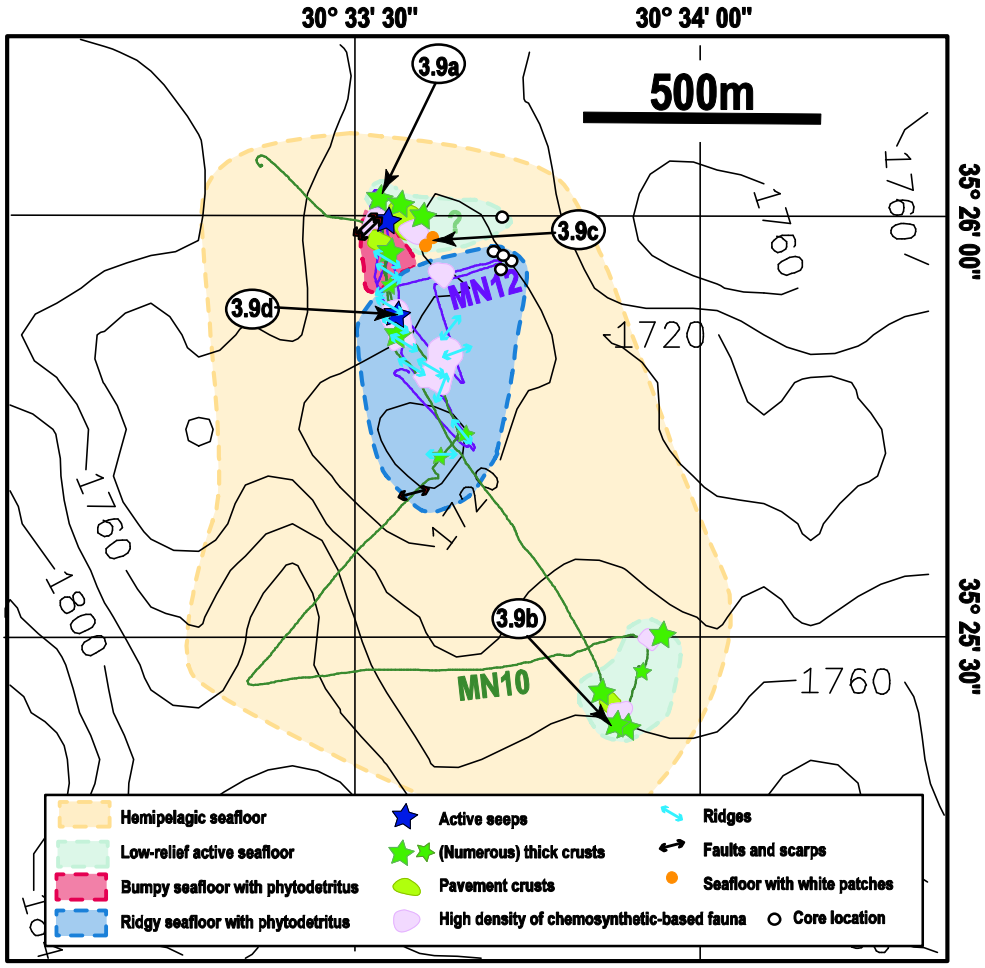

Figure 3.8: Multibeam bathymetry map of Kazan MV with the geological interpretation of the Nautile dives. The locations of the cores are also indicated. The numbers refer to Figure 3.9.

Distribution of fluid seeps, as mapped from the two dives on Kazan MV, is rather unusual (Figure 3.8). Two areas of recent intense seeping activity were discovered, indicated by large numbers of shells covering the seafloor and carbonate crusts built around local fluid expulsion centres (Figure 3.9a and 3.9b). Living bivalves (from the families Vesycomyidae, Thyasiridae, and Lucinidae) were collected from these sites (Olu-Leroy *et al.* 2003; Salas and Woodside 2002). In some places, reduced sediments (of grey-purple color) are observed associated with white patches inferred to be bacterial mats (Figure 3.9c). These two active areas are located on the northwestern part of the summit and on the southeastern flank of the mud volcano (Figure 3.8) and correlate with high backscatter patches. However, the seafloor is quite different from place to place. The summit of the mud volcano exhibits a small-scale relief characterized by ridges and furrows, with phytodetritus concentrated inside the depressions.

Numerous ridges mainly trending NW-SE and NE-SW were mapped (Figure 3.8), as well as faults with steps of several tens of centimetres. In contrast, within the active area on the southeastern flank of the mud volcano the seafloor surface shows relatively low small-scale relief. Within this zone, carbonate crusts are more abundant, mostly thick crusts but also limited crust pavements, sometimes developing a polygonal mosaic pattern. In between these two active areas, no present-day activity was detected.

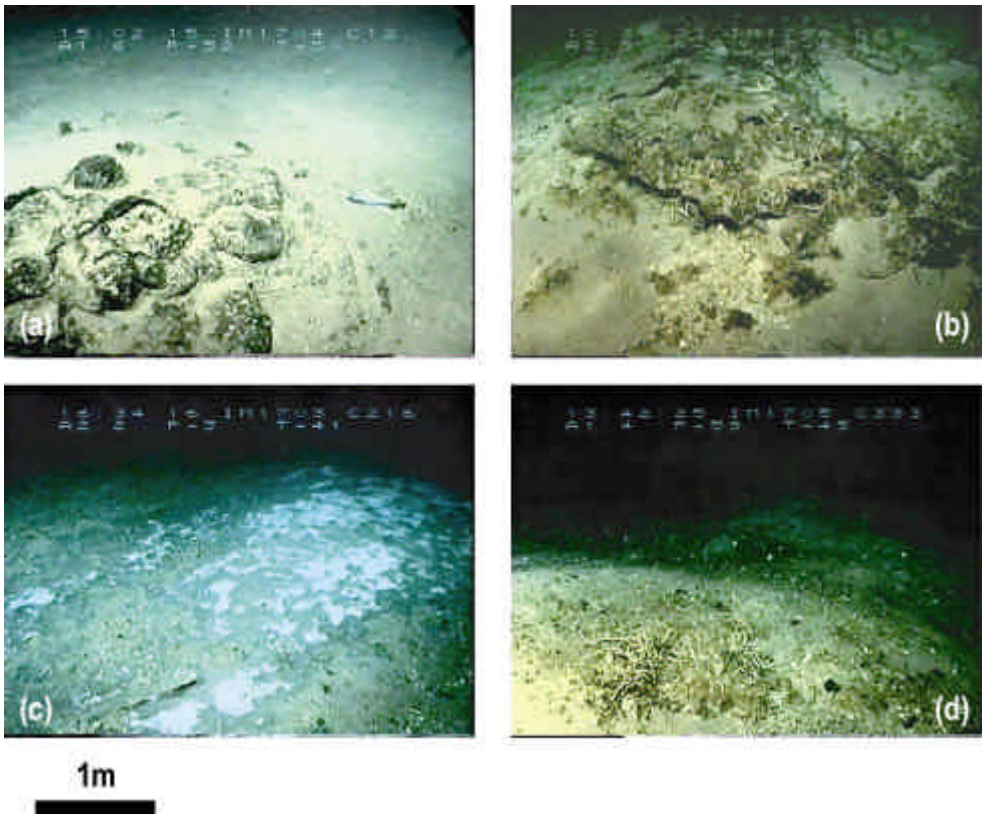

Figure 3.9: Seafloor images of Kazan MV showing: a) a big "champignon type" crust isolated on the hemipelagic sediments; b) an active seeping area, with crusts, tubeworms and shells; c) white patches on reduced sediments, inferred to be bacterial mats; d) cluster of pogonophorans with fields of small shells.

3.5.3. Kula Mud Volcano

Kula Mud Volcano was crossed by O.R.E.Tech line MNLDT05 with a N040? direction (Figure 3.3). It is a dome-shaped feature 80 m high and 1 km across with a smooth summit. Although it appears in the multibeam imagery as having backscatter everywhere, the O.R.E.Tech deep-tow sidescan sonar shows only a very small area (about 500 m across) of high backscattering on the summit of the relief (Figure 3.10). The dive exploration on the

summit area shows an even smaller area (about 250 m wide) of fresh mud flows with exposed clasts on the seafloor. This suggests that part of the mud breccia may be covered by hemipelagic sediments, and indeed various thicknesses of hemipelagic sediments were observed overlying matrix-supported mud breccia during the coring. One core recovered an expanded hemipelagic section 118 cm long, two cores recovered matrix supported mud-breccia under respectively 5 cm and 30 cm of hemipelagic sediments. The three last cores show the mud breccia on the surface. At least three different partly overlapping mudflows (Figure 3.11a) were recognized from different degrees of apparent freshness at their surface. The edges of the flows form scarps of 1 to 2 m in height (suggesting this to be the typical thickness of a mud flow), and the edges of some mud flows (older?) were also visible further downslope. The very localized active area shows a significant number of chemosynthetic-based organisms (tubeworms, and bivalves) scattered on seafloor (Figure 3.11b). Living specimens of bivalves (Lucinidae) were collected during the Nautile dive (Olu-Leroy *et al.* 2003). Moreover, gas hydrates have been sampled from several cores taken in this area (Figure 3.11c). Kula MV appears therefore to have been reactivated relatively recently after a dormant period. Some linear features on the sonogram, associated with vertical displacements of a few metres on the profiler record, are interpreted as minor normal faults. The mud breccia probably also fills some of these faults and fractures, allowing them to be better distinguished because the backscattering is consequently much higher (Figure 3.10). However, the seafloor across these features does not show any outcropping mud breccia, but exhibits a very chaotic surface (Figure 3.11a), with evidence of destabilization characterized by the presence of meter-scale scarps. The chaotic surface areas may be thus the source of part of the high backscattering associated with faulting.

3.5.4. Tuzlukush Mud Volcano

Tuzlukush MV (Figure 3.12) has a conical shape, 80 m high and 900 m wide. A shallow moat of 10 to 20 m deep and 600 m across is observed at the western side of the mud volcano (Figure 3.12). It has a moderate to high backscatter on the sonar image, probably indicating the presence of overlapping older and recent mudflows. The highest backscattering flows extend towards the southeast, southwest and northwest for 200 to 500 m (Figure 3.12a). On the eastern and western sides of the mud volcano, mud flows show less backscatter and are more extensive, up to 1 km long. The core taken from the mud volcano (core 235G) contained 170 cm of Upper Pleistocene and Holocene pelagic sediments at the top, including Sapropel S1 and a tephra layer, overlying grey structureless matrix-supported mud breccia (Woodside *et al.* 1997a). It indicates that this mud volcano is dormant at present.The greater depth of the mud breccia may be the reason why this mud volcano is characterized by moderate backscatter in the deep-tow data. On the SBP, up to 50 m of well-bedded strata can be observed surrounding the mud volcano; they bend down slightly towards the volcano on its eastern side (Figure 3.12) and one mud flow can be seen interfingering with hemipelagic sediments. The cone shows a transparent acoustic facies, slightly disturbed.

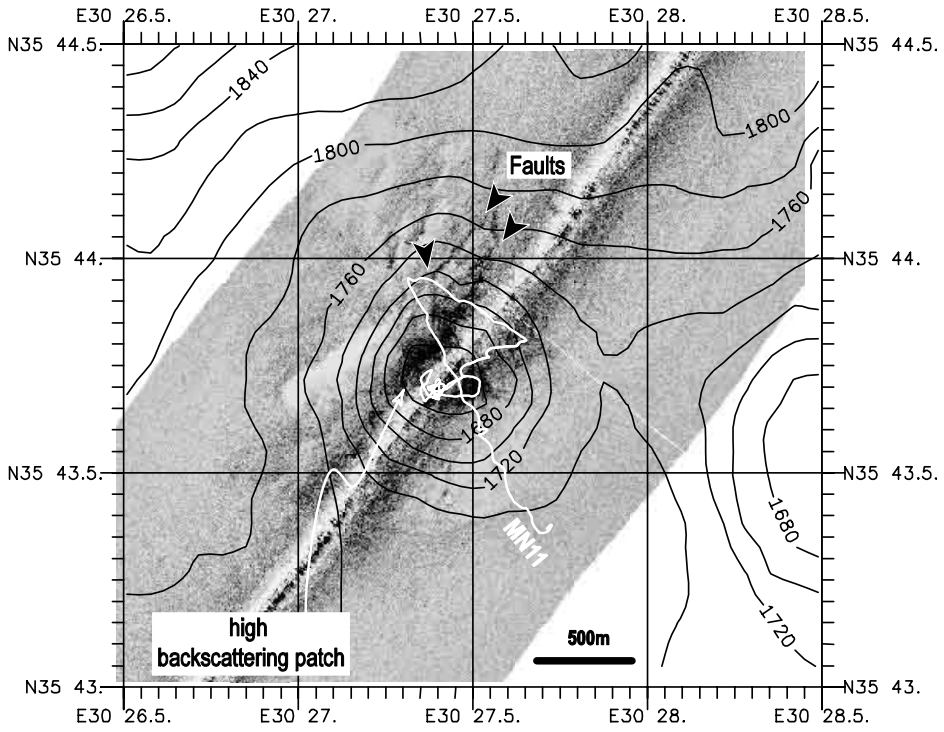

Figure 3.10: Multibeam bathymetry map of Kula Mud Volcano with part of MNLTD05 sidescan sonar image. The navigation of the submersible during the dives is shown by the white lines.

3.5.5. Saint Ouen l'Aumône Mud Volcano

Saint Ouen l'Aumône MV is a circular dome over 1000 m in diameter and 50 m high. It displays very low backscattering on the sonar record (Figure 3.13), although it gives a high backscatter image in the EM12D data (Figure 3.3), indicating that the mud breccia is likely buried under more than 1 m of sediments. In core 236G from this mud volcano, mud breccia was observed at a depth of 2.5 m below normal eastern Mediterranean hemipelagic sediments (Woodside *et al.* 1997a), suggesting Saint Ouen l'Aumône MV to be also dormant at present. Nonetheless, high backscatter patches of about 200 m across are observed on the sonar record, lineated along a N085° trend on the top of the mud volcano, suggesting, in analogy with Kula MV, recent activity related to faulting. The border of the dome exhibits some concentric lines weakly reflective on the sidescan sonar appearing to outline the edge of old mud flows. On the subottom profiler, the mud volcano shows a typically transparent acoustic facies. The western side of the volcano is in sharp contact with up to 30 m of well-stratified sediments, bending down towards the mud volcano. On the eastern side, some acoustically transparent layers, that could indicate buried mud flows, can be observed interfingering with the normally bedded sediments. One of them, extending for 1 km away from the mud volcano, is up to 10 m thick and buried 6 m below the seafloor (Figure 3.13).

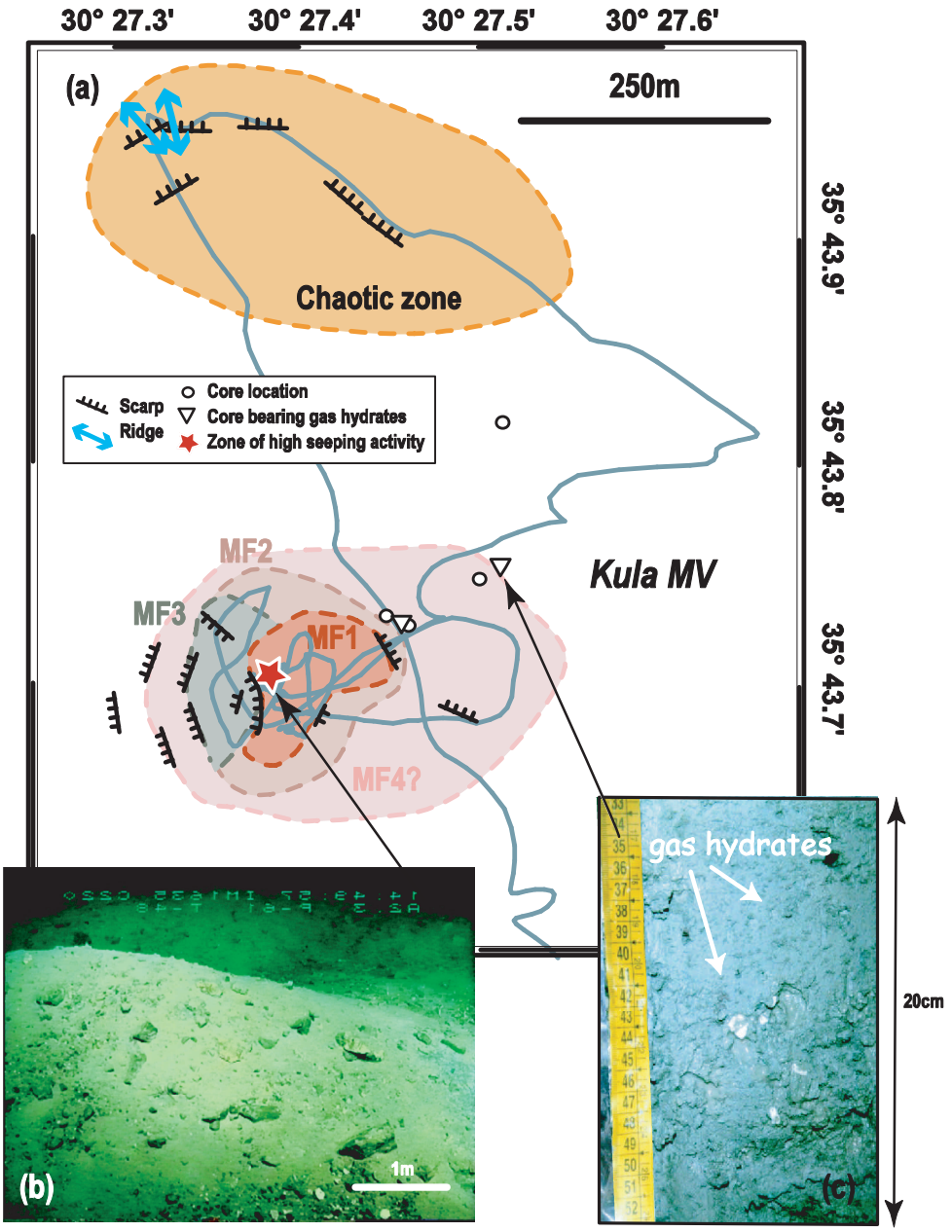

Figure 3.11: a) Geological map from dive MN11 (Kula MV), showing different mud flows (MF1 youngest to MF4 oldest). The locations of the cores are also indicated, open triangles stand for the cores that contained gas hydrates and open circles for all others. The actual core locations are within a radius of about 100m of these ship positions. b) Seafloor image of the recent mud flow. c) Part of core 213G (Woodside et al. 1997), showing crystals of gas hydrates (Photo: courtesy Elena Kozlova).

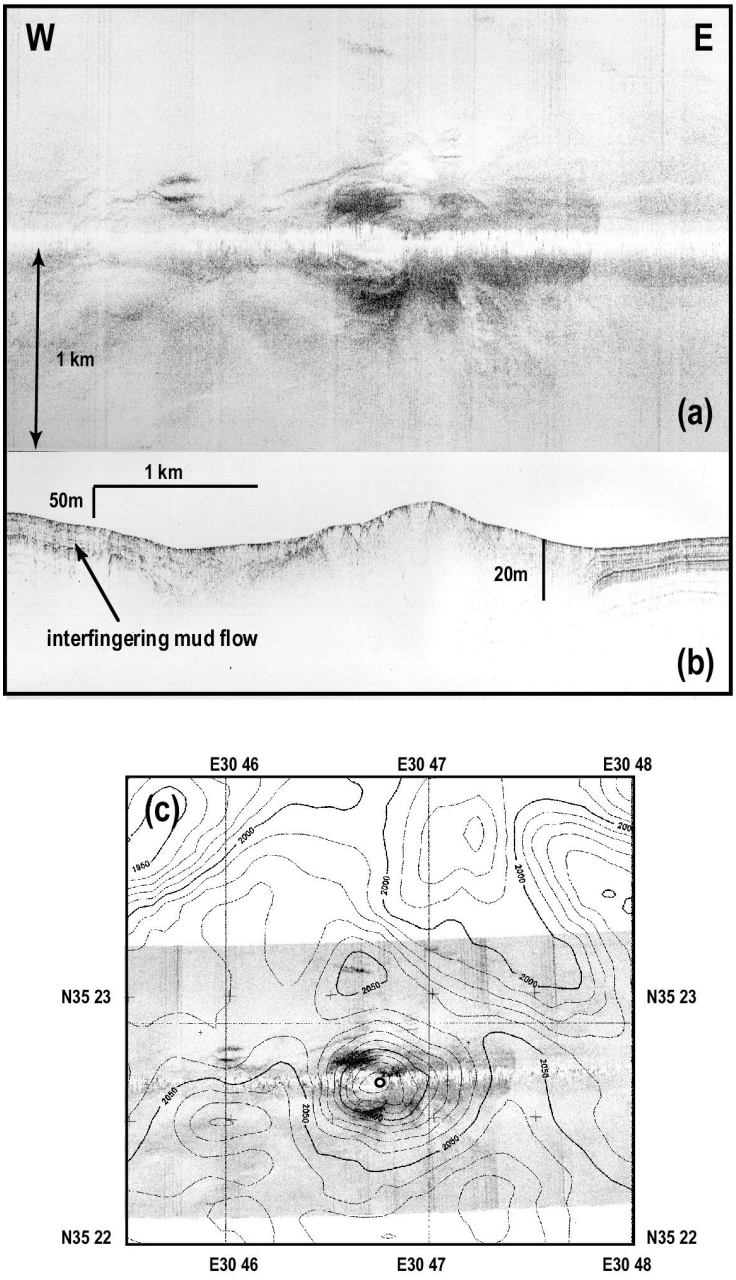

Figure 3.12: Sidescan sonar image (a) and subbottom profiler record (b) of Tuzlukush Mud Volcano. (c) Multibeam bathymetry map of Tuzlukush with part of MAK 46 sidescan sonar image and the position of the core (empty circle).

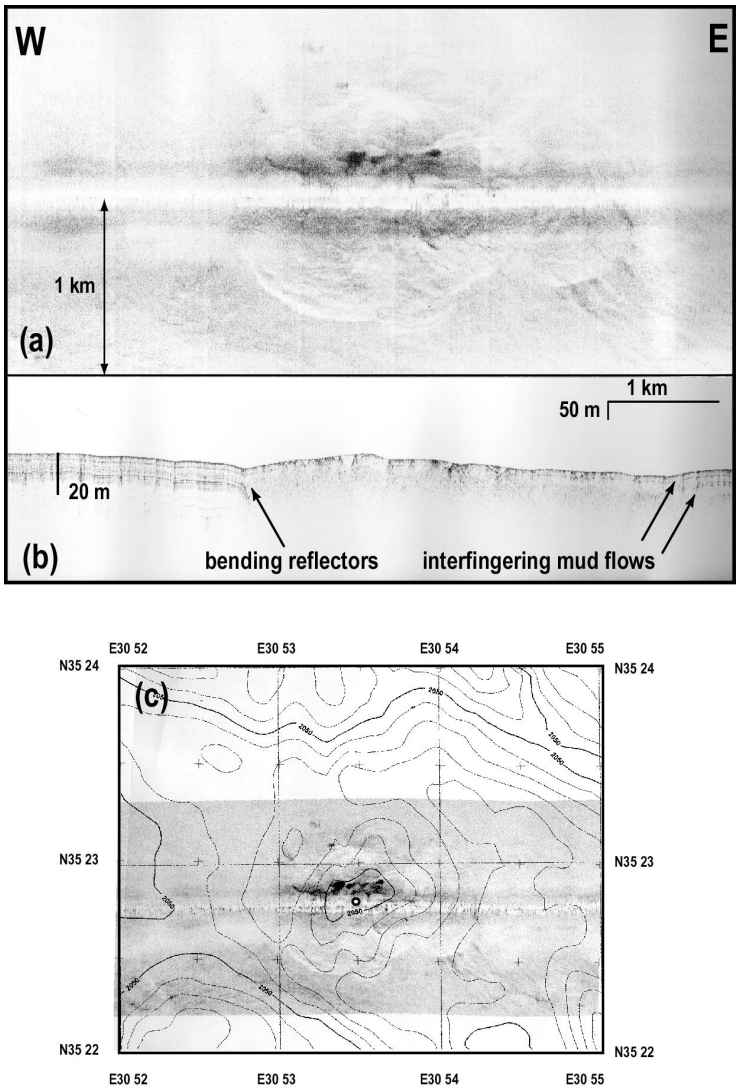

Figure 3.13: Sidescan sonar image (a) and subbottom profiler record (b) of Saint Ouen l'Aumône Mud Volcano. (c) Multibeam bathymetry map of Saint Ouen l'Aumône with part of MAK 46 sidescan sonar image and the position of the core (empty circle).

3.6. Discussion

The Anaximander Mountains mud volcanoes display a large variety of geological and geophysical characteristics. With the exception of the large Amsterdam MV, they are roughly the same size, between 50 and 100 m high and about 1 km across, but present different morphologies (perfect circular features or irregular mound, flat-topped or more conical) and exhibit different backscatter signatures on the sidescan sonar records.

Some mud volcanoes present extensive high backscattering low-viscosity mud flows (e.g. Amsterdam, Kazan, Tuzlukush MVs). Some differences in backscatter level are noticeable from the flows which may partly be caused by different thickness of hemipelagic sediments covering the mud breccia, as proposed by the model of Volgin and Woodside (1996). This indicates different timing of extrusion, with old mud flows showing less backscattering than recent ones. This hypothesis is also supported by piston cores (e.g. up to 2,5 m of hemipelagic sediments observed overlying a mud flow on Saint Ouen l'Aumône MV) and the comparison of the backscatter signature from the different acoustic tools (e.g high backscatter on the EM12D data and low backscatter on the less penetrative sidescan sonar data on Saint Ouen l'Aumône MV). The observations on the SBP of interfingering mudflows within the hemipelagic sediments (Figure 3.12 and 3.13) also confirm the episodic mud eruption activity of the mud volcanoes. Mud flows of different apparent freshness, i.e. of different ages (Table 3.1), were commonly observed during the dives, such as on the summit of Amsterdam MV or Kula MV. Recent mud flows appear to show a higher backscatter, not only because of the absence of hemipelagic sediments but also because of the roughness of the surface of more recently extruded mud flows. However, differences in the backscatter pattern of the mud flows may not only be linked to the age of the flow, but to their intrinsic heterogenity, with respect to size and density of clasts. For instance, on Napoli mud volcano, within the Olimpi field, the proposed reason for the low backscattering was the very fine mud breccia with only millimetric size clasts (Robertson *et al*. 1998), described by Staffini and co-authors (1993) as "mousse-like" mud breccia. Indeed, in contrast to Saint Ouen l'Aumône MV, which presents a different backscatter depending on the acoustic tool used, Napoli MV shows very low backscatter even in the EM12D data.

Methane-derived carbonate crusts that are present around cold seeps are the result of precipitation from diagenetic fluids with the involvement of active microbial consortia (Aloisi *et al.* 2000; 2002). They could also contribute to the acoustic backscatter strength (Orange *et al*. 1999), causing higher acoustic contrasts with the overlying water than soft sediments. Small backscatter patches on the top of weakly reflective mud volcanoes may then correspond to relatively small outcrops of mud breccia or may be related to focused seeps and their associated carbonate crusts rather than to mud flows. The weakly reflective mud volcanoes are not necessarily the less active in terms of fluid expulsion. Napoli MV, in the Olimpi field, shows only a few small patches of high backscattering (probably caused by carbonate crusts) and has very intense fluid seepage as indicated by the presence of numerous seeps and brine lakes (Huguen 2001), as well as by the amount of measured CH_4 in the bottom seawater (Charlou *et al.* 2003). Limited high backscatter areas, restricted to the summit of the mud volcano could also indicate the relatively recent reactivation of the mud volcano after a period of dormancy, as is the case for Kula MV. There, the mud flows outcropping on the seafloor cover a relatively small area (about 300 m by 150 m), but the area of high backscattering in the deep-tow sidescan record is more extensive (about 500m by 500m). Part of the backscatter may also be related to the passive injection along faults of the mud breccia (Figure 3.10), not necessarily exposed on the seafloor, and/or to the surface destabilization associated with faults.

During the recent *in situ* seafloor observations (MEDINAUT/MEDINETH shipboard scientists 2000), authigenic carbonate precipitation appeared a very common phenomenon on

the summit of all the mud volcanoes studied. Different types of crusts have been observed, such as millimetric to pluri-decimetric crust pavements, circular slabs, and metric mounds (Aloisi *et al.* 2000). As suggested by Kulm and Suess (1990), the morphology of carbonate precipitates can be used to infer the intensity and style of fluid expulsion. Thick concentric carbonate crusts are built around local long-term well-established vents. On Kazan MV, these types of crust are predominant (Figure 3.9), with the presence of circular crusts ("plaque d'égoût" or "manhole cover" type) or some large (0.5 to 1.5 m wide) mounds of dark concretions ("champignon" or "mushroom" type) isolated on the surrounding hemipelagic sediments (Figure 3.9a). The long-term time scale of seep activity on Kazan is also indicated by the presence of clusters of vestimentiferans of more than 100 individuals (Olu-Leroy *et al.* 2003) (Figure 3.10d). Amsterdam also presents localized very active venting sites, with large carbonate crusts, clusters of hundreds of tubeworms (Olu-Leroy *et al.* 2003) and typical reduced sediments. On the other hand, the huge area covered by crust pavements on the summit of Amsterdam MV implies some broad areas of diffuse seepages from the degassing mudflows. The important nephelitic layer above Amsterdam MV as well as the more than 200 m high methane plume (Charlou *et al.* 2003) indicate the release of large amounts of methane and turbid fluids from the mud volcano. On Kula MV, such well-established seep zones are lacking and the only source of emitted methane is from the degassing mudflows, as suggested by the scattered tubeworms and shells on the seafloor and the presence in places of thin crust pavement. It does not mean that Kula MV is less active in terms of methane emission, as gas hydrates have been sampled (Figure 3.11b), but the gas seeps are probably younger, as the mud volcano was reactivated after a dormant period.

The distribution of the various types of crusts shows a spatial organisation that also could reflect their age (Table 3.1). Crust pavements develop more extensively on the periphery of the mud volcanoes, in older areas possibly reflecting longer periods of diffuse uniform gas seepage. This implies that old active areas with extensive thick crusts may cause as high backscattering as young areas of recently extruded mud flow, but may not show the same homogeneous pattern (Table 3.1). Another way to differentiate them is their localization with respect to the centre of the mud volcano. The centre of Amsterdam MV shows a complete absence of crust, despite high methane emission (Charlou *et al*. 2003), attesting to the very recent emplacement of the mud flow. In contrast, Napoli and Milano show patches of very thin crust pavement over the active summit area. This indicates the absence of relatively recent mud eruption that could have covered or destroyed the crusts. It is possible that the last mud eruption in Amsterdam MV is much more recent than on these mud volcanoes from the Olimpi field. From the observations of biological communities, i.e. number of living specimens and diversity of species, Olu and co-authors (2003) suggest that the mud volcanoes from the Anaximander Mountains (Amsterdam and Kazan MVs) show higher chemosynthetic activity than those from the Olimpi field (Napoli and Milano MVs). Charlou and co-authors (2003) have also concluded that Amsterdam MV is the most active mud volcano from the amount of CH_4 in seabottom water and the important nephelitic layer. Dating of crusts over seep areas in the Anaximander Mountains by the ^{14}C method gave apparent ages of 8.16 +/-0.15 ka for a thin crust on Kazan MV and 17.405+/-0.38 ka for a massive crust on Amsterdam MV (Aloisi 2000). But these ages are probably overestimated due to enrichment by inactive ^{14}C from fossil hydrocarbon-derived carbon (Aharon *et al.* 1997).

Age	Geology	Biology	Seep activity	Acoustic characteristics	Spatial distribution
1- youngest mud flow	-Seafloor roughness at centimetric to meter scale -Dark grey sediments (not yet oxidized) -Numerous clasts exposed on seafloor -No pelagic sediments -Apparent dewatering	-Dispersed bivalves shells -Few pogonophorans	-Diffuse seepage through mud flow	-Uniform high backscatter -Homogeneous backscatter pattern	-Centres of eruption -Summit of the mud volcano -Parasitic eruptive cones
2	-Seafloor roughness at meter to meters scale -Clasts exposed on seafloor -Dusting of pelagic sedimentation apparent -Thin crust in some places	-Abundant benthic fauna -Dispersed bivalve shells and pogonophorans -Locally bivalve shell clusters bacterial mats	-Diffuse seepage through mud flow -Localized active seeps with purple-grey sediments	-Uniform high-meduim backscatter	-Summit of the mud volcano
3	-Pelagic sediments with bioturbation -Few clasts on seafloor -Some crust pavements -Localised massive crusts crusts slightly broken or fractured by mud movements -Phytodetritus in furrows	-Concentration of benthic fauna in some areas -Bivalve shell fields -Clusters of pogonophorans	-Numerous localised active seeps/ brine lakes -Dormant seeps/ empty brine lakes -Less diffuse seepage	-Medium backscatter with patches of high backscatter	-Summit of the mud volcano -Some areas on the flanks
4-oldest mud flow	-Smooth seafloor with bioturbation -Yellow oxidised sediments -Sometimes fault or crevasse areas -Dark phytodetritus -Some localized massive crusts	-Few living chemosynthetic fauna -Rich in normal bottom fauna -Debris of tubeworms	-Localized active seeps -Dormant seeps	-Low backscatter with small patches of high backscatter -Heterogeneous backscatter pattern	-Periphery of the volcano

Table 3.1: Variation of mud flow and seep characteristics with time after mud breccia extrusion.

Another cause of high backscattering may be internal deformation within the mud volcanoes causing surface destabilisation, such as crevasses around the summit area, very well expressed in the case of Amsterdam MV (Figure 3.5 and 3.6a). This deformation may be due to a modification of the mud rheology (from ductile to brittle) with time, or be the result of elastic rebound after the eruption (expansion/collapse cycles). Gravitational creeping on the flank of the dome may also be responsible for this crevassing. The occurrence of concentric ridges in the centre and crevasses in the outer regions may indicate the evolution of these features. First the mud breccia flow can result in gently undulating crests or long wavelength hummocky topography. Then fractures develop and form escarpments clearly controlled by normal faulting.

Shallow moats and depressions (10 to 20 m deep) surrounding mud volcanoes have been observed in the case of Kazan MV and Tuzlukush MV, and may be related to the loss of material below the mud volcano after the eruption when mud and fluids have been expelled. These deeps are not as developed as the large moats surrounding some Olimpi Field mud volcanoes like Napoli or Maidstone (Robertson *et al*. 1998). However, in the Olimpi field, the angular shape of these moats suggest that they might be fault-controlled (Huguen 2001), and that both subsidence and tectonics play a role in the formation of these depressions. A certain amount of collapsing, probably consecutively to the expulsion of mud and fluids, is also indicated through the bending down of sedimentary layers towards the mud volcano, observed for Tuzlukush and Saint Ouen l'Aumône MV. This "pull-down" effect has been observed in many mud volcanoes, such as in the Black Sea (Limonov *et al*. 1994), and appears as a general characteristic related to mud extrusion mechanisms.

3.7. Conclusion

On a regional as well as a local scale, mud volcanoes and associated mud flows show an important variability in morphology, size, and acoustic characteristics. Most of the mud volcanoes are quite small (less than 1 km wide and less than 100 m high), except for Amsterdam MV, which is up to 3 km across. Nonetheless, they are very active in terms of release of fluids and gases through localized seeps or broad diffuse degassing areas, with the presence of living chemosynthetic-associated fauna, carbonate crusts, and in some cases gas hydrates. There is a relationship between the age of the flows, the amount of visible clasts and crusts on seafloor, the distribution of fauna, the small-scale relief of the seafloor and the pelagic cover. However, the release of methane through localized seeps might be independent of the large scale mud eruptions. Amsterdam and Kazan MVs appear to be very active mud volcanoes, maybe with higher release of methane than in the well known Olimpi field mud volcanoes, Napoli and Milano MVs. The other mud volcanoes of the Anaximander Mountains appear to be less active, and some of them might have been or are in a dormant stage. Ground-truth of the sonar data shows that the geophysical signature of mud volcanoes may be related to spatial and temporal evolution of mud volcanism activity, because the seafloor characteristics (surface of the mud flows, distribution and nature of the crusts) and the degree of colonization by benthic fauna vary with the intensity and age of the fluid seepage.

Acknowledgements

This research was partially funded by the Netherlands Organisation for Scientific Research (NWO) through the MEDISED project (809.63.011), the Anaxiprobe project (750.195.02) and the MEDINAUT/MEDINETH project (750.199.01). It was carried out partly using ADELIE and CARAIBES software IFREMER. We are grateful to the IFREMER/Genavir crew and technical team of the R/V "Nadir" and submersible "Nautile" for their helpful assistance at sea during the MEDINAUT cruise. We thank the captain and crew of R/V "Professor Logachev" for their involvement during the MEDINETH cruise, as well as the MEDINETH/MEDINAUT shipboard scientists. The shipboard scientists, especially Michael Ivanov, as well as the captain and crew of R/V "Gelendzhik" are thanked for the important work at sea during the TTR6/ANAXIPROBE cruise. We deeply thank Jean-Marie Augustin for his help in reprocessing the sonar data. The photograph of gas hydrates from core 213G (Figure 3.11c) was taken by Elena Kozlova who was quick to recognize the significance of the core.

Chapter 4. Clay mineral provenance in mud breccias of Eastern Mediterranean mud volcanoes

4.1. Introduction

In the Eastern Mediterranean Sea, the Olimpi field (Cita *et al.* 1989), located on the crestal part of the Mediterranean Ridge accretionary prism (Figure 3.1), is one of the best studied mud volcano field associated with the on-going subduction of Africa beneath Eurasia (Cita *et al.* 1989, 1990; Camerlenghi *et al.* 1995; Robertson *et al.* 1996; Mascle *et al.* 1999). Mud volcanoes also occur in different settings of the eastern Mediterranean collision zone (Figure 3.1), in the Anaximander Mountains, which are detached continental blocks from southern Turkey (Woodside *et al.* 1997a, 1998; Zitter *et al.* 2003; see Chapter 5), and further southeastwards on the Florence Rise (Woodside *et al.* 2002). The Anaximander Mountains, are formed of much older consolidated sediments than the accreted sediments composing the sedimentary sequence of the Mediterranean Ridge. Another major difference between these areas, also noted in Chapter 3, is that Messinian evaporites occur on the Mediterranean ridge but are absent in the Anaximander Mountains area.

Marine expeditions in different areas of the eastern Mediterranean Sea (Limonov *et al.* 1994, 1995; Ivanov *et al.* 1996; Woodside *et al.* 1997a) and especially the Ocean Drilling Program (ODP) Leg 160 that investigated two mud structures of the Olimpi field (Robertson *et al.* 1998) shed light on many aspects of the mechanisms and evolution of mud volcanism, although many questions remain. Among these, the age and depth of the lithological unit(s) from which the mud is mobilized and extruded is still unclear.

In general, mud volcanoes act as a window for deep sedimentary sequences, because material from the parent bed (or source) and overlying rock fragments are transported to the surface. The material recovered on mud volcanoes is described as mud breccia (Cita *et al.* 1981; Staffini *et al.* 1993) composed of a mud matrix and clasts of variable lithologies. Within the Mediterranean Ridge sedimentary sequence, the origin of the mud matrix is controversial. It has been first proposed to derive from the accretionary prism décollement zone estimated to be at a depth of 5 to 7 km (Camerlenghi *et al.* 1995). In the Olimpi field, most of the clasts are dated from Mid-Miocene age and younger (Premoli-Silva *et al.* 1996; Robertson and Kopf 1998a). However, few Eocene and Cretaceous microfossils, as old as Aptian age, were also found conducting some authors to suggest that the source of the mud originate from Aptian (or older) units (Akmanov 1996; Premoli-Silva *et al.* 1996). Chaumillon and co-authors (1996) suggest that the Mediterranean Ridge is built on several décollement levels, the main one at the base of the Messinian evaporites and an older one, probably located within the Aptian shales, which would therefore act as a possible source of the mud. On the other hand, recent clay mineralogy studies (Jurado-Rodriguez and Martinez-Ruiz 1998) and vitrinite reflectance data on thermal maturity (Kopf *et al.* 2000) indicate a shallower source for the mud material (which could not have been buried more than 2 or 3 km) and several authors proposed a Messinian

origin for the mud matrix (Schulz *et al.* 1997; Robertson and Kopf 1998b; Kopf *et al.* 2000). In the Anaximander Mountains area, the source of the mud is even more enigmatic.

The aim of this chapter is to constrain the original depositional environment of the mud matrix by identifying the clay minerals composing the complex mixture. Clay minerals are indicators of the specific environment of formation (Chamley 1989); and their sedimentary assemblages in marine sediments are useful tracers of their detrital sources from surrounding landmasses, water-mass circulation and dispersal patterns, past and recent sedimentary conditions, as well as alteration processes (Chamley 1989).

We present here the results of an X-ray powder diffraction (XRPD) analysis of the matrix of mud breccia samples recovered during the MEDINETH expedition on board the R/V "Logachev" in 1999 which provided numerous box-cores, gravity-cores, and piston-cores from mud volcanoes in the Eastern Mediterranean Sea. This study focuses on sixteen sub-samples (Table 4.1); fifteen of them were collected from the mud matrix of mud volcanoes located in the Olimpi field (Milano, Napoli, and Moscow), in the Anaximander Mountains (Amsterdam, Kazan) and in the Florence Rise area (Texel), and an additional one was sampled from a hemipelagic core in the Florence Rise area. After discussing the provenance of the different clay minerals, we compare the clay assemblages of the mud matrix with those of the Mediterranean stratigraphic sequence in order to identify the unit from which the mud matrix is derived. The clay assemblages also give information on potential genetic processes, such as diagenetic history or alteration processes within the specific cold-seeps environment of mud volcanoes.

Station	Latitude	Longitude	Area	Bottom target	Recovery (cm)	Subsamples (see Figure 4.1)
MNLBC09	33° 44'.373	24° 46'.639	Olimpi area	Milano MV	40	1
MNLPC03	33° 43'.546	24° 41'.237	Olimpi area	Napoli MV	423	3
MNLGC04	33° 39'.976	24° 34'.950	Olimpi area	Moscow MV	205	6
MNLBC19	35° 25'.950	30° 33'.679	Anaximander Mountains	Kazan MV	34	1
MNLGC11	35° 20'.013	30° 15'.948	Anaximander Mountains	Amsterdam MV	141	2
MNLGC13	34° 8'.254	31° 42'.220	Florence rise	Texel MV	156	2
MNLGC14	34° 47'.188	31° 31'.383	Florence rise	Hemipelagic	2 sections	1

Table 4.1: Location of the MEDINETH cores used within this study.

4.2. Sedimentology of mud volcano cores

Olimpi field

The cores recovered between 40 and 423 cm of grey mud breccia with centimetric clasts and shells, and, for core MNLPC03 on Napoli MV, a mousse-textured mud breccia with degassing structures (Figure 4.1). When possible (in the case of Napoli and Moscow mud volcanoes), subsamples from distinct mudflows within a core were selected on the basis of oxidation events or hemipelagic sediments interlayered within the mud breccia (Figure 4.1). Core MNGC04 from Moscow MV contained three mud flows for a total thickness of 205 cm. The younger mud flow was covered by 2 cm of hemipelagic sediments while the other two mud flows had an oxidized upper surface. Subsamples were selected from within the mud flows and from the transition layers between the mud flows (Figure 4.1). Core MNLPC03 contained a particular black layer between 93 and 99 cm, suggesting pelagic sedimentation in anoxic conditions, possibly a brine lake. A subsample was taken from this interval.

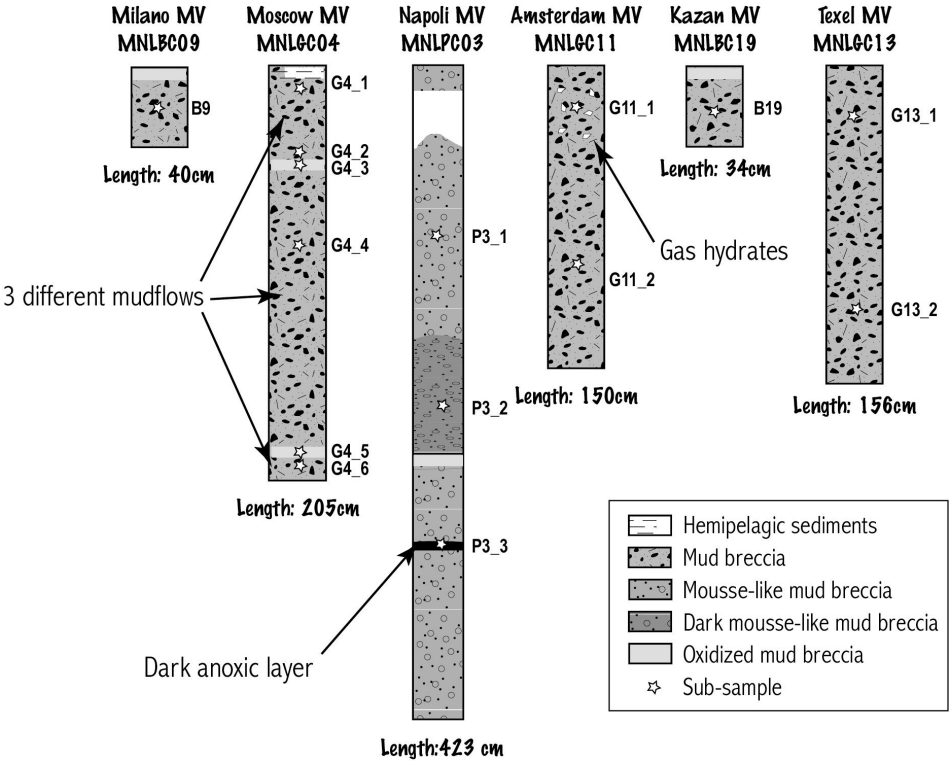

Figure 4.1: Core description and location of the sub-samples used in this study.

The Anaximander Mountains

The cores recovered between 34 and 150 cm of grey mud breccia with millimetric and centimetric clasts and evidence of gas saturation structures. In core MNLGC11, on Amsterdam

MV, small gas hydrate crystals were found throughout the first section (60 cm), which also presented a strong H_2S smell.

Florence Rise area

The MNLGC13 core tested the hypothesis that an unknown dome (now named Texel Mud Volcano) in the Florence Rise area, discovered during the Prismed II cruise, is a mud volcano. The core recovered 156 cm of mud breccia with centimetric clasts. Also present were scattered, millimetric gas hydrate crystals, and a H_2S smell.

4.3. Methods

The suspensions of mud samples were analyzed by X-ray diffraction. The < 2 μm grain-size fraction was separated by centrifuging the subsamples. After exchanging Mg with Ca using a $CaCl_2$ solution, the carbonate fraction was removed with 1N acetic acid buffered at pH=5 with Na-acetate. This process was performed while the suspension was kept constantly agitated to avoid irregular exposure to the acid. To eliminate the acetic acid, the samples were Ca-exchanged using a $CaCl_2$ solution; then the samples were rinsed. Subsequently 1 wt % of MoS_2 was added as an internal standard to the suspensions of the samples for the calibration of diffractograms and the quantification of mineral contents.

Oriented mounts were made on polished porous ceramic tiles by suctioning the suspensions. XRPD was carried out using a self built θ–θ goniometer equipped with a long-fine-focus X-ray tube (Cu*K*α radiation, 40 kV, 40 mA), variable divergence and anti-scatter slits, and a Kevex solid-state Si(Li) detector. The specimens were placed in an environmental chamber with Mylar^{TM} windows which were mounted on the goniometer. During measurements the chamber was constantly flushed with N_2 at a set relative humidity (RH) from a humidity generator. XRPD patterns were collected from 1° to 15º 2θ using the following settings: 20 mm irradiated specimen length, 0.2 mm receiving slit, 1 s/0.02º 2θ counting time.

The measurements were performed under controlled RH in order to identify the expanding clay minerals. This approach was preferred to the usual glycolation/heating method because it is gentler and better able to preserve the fragile clay minerals. Three measurements were performed: (a) first the still wet specimen which is regarded as having 100% RH was scanned immediately after preparation; and after drying at room temperature, two measurements were performed, respectively at (b) 50% RH and (c) 0% RH. Since expanding clay minerals show large shifts at the mentioned RH values, two specimen patterns were performed at small RH increments, namely, 0, 10, 30, 50, 70, 90, and 100% RH for a proper identification.

XRPD patterns were corrected for the Lorentz–polarization factor (McEwan *et al.* 1961) and for the diffracting specimen volume. Peak positions and widths were obtained by fitting Pearson-IV-functions (with computer program PEAKFIT 4.0, Jandell©).

Identification of the clay minerals from the XRPD patterns was done according to Brindley and Brown (1980). Clay minerals from the smectite group are identified by their characteristic swelling along the c-axis that is caused by hydration complexes of cations in

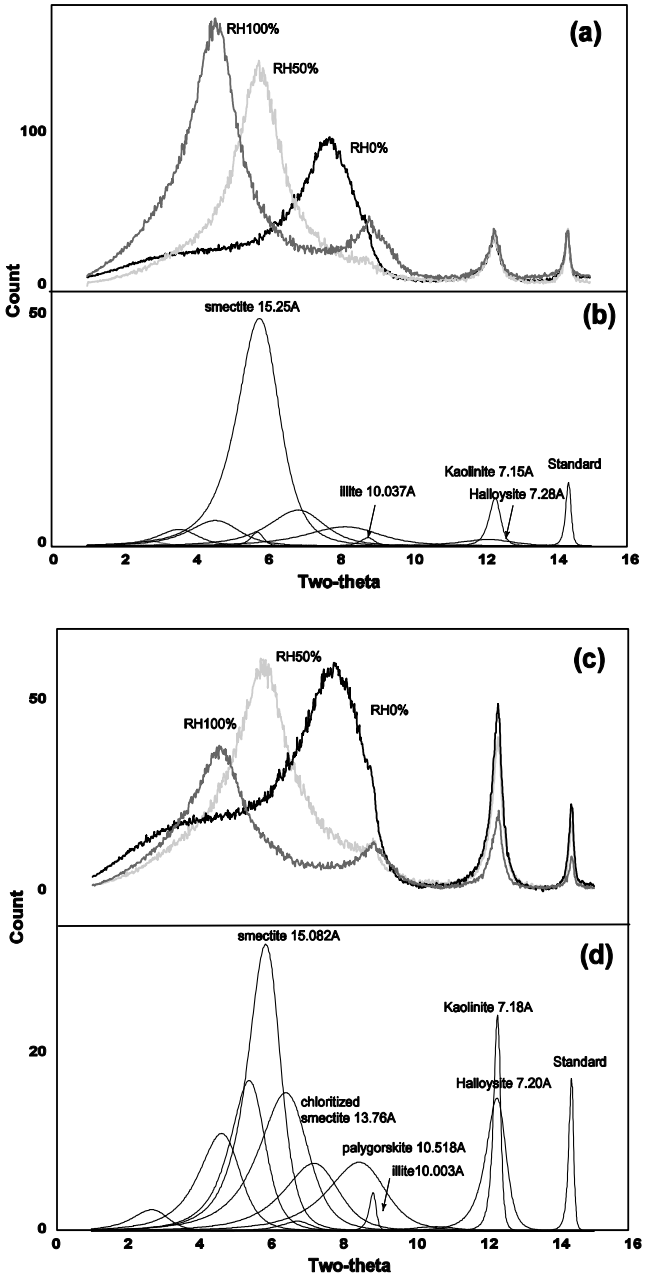

Figure 4.2: X-Ray patterns of the subsamples MNLBC1981 from Kazan MV (a) and MNLPC03_2 from Napoli MV (c) at different relative humidity percentages (RH of 100%, 50% and 0%), and their corresponding peak modelling, respectively (b) and (d), for RH of 50%.

their interlayer. This expansion of smectite is indicated by a shift of the (001) reflections from 11 Å at 0% RH, to 15 Å at 50% RH, and to 18-20 Å at 100% RH when water molecules are incorporated into the interlayer (Caroll 1969). "Chloritized" smectite is recognized from broad reflections centered on the chlorite spacing at 14 Å, whereas primary chlorite shows sharp peaks at these angles. Two minerals from the kaolin group are recognized: kaolinite with a basal spacing of 7.15 Å and dehydrated halloysite with a basal spacing of 7.2 Å, and broader reflections than kaolinite (Chamley 1989). Illite is used as a general term for minerals belonging to the mica group with basal spacing of 10 Å (Caroll 1969). Palygorskite is identified from a broad reflection at 10.5 Å. An example of typical XRPD patterns from this study is shown in Figure 4.2.

A truly quantitative evaluation of the amount of clays in the mixture is not possible through XRDP analysis because the intensity of X-ray peaks depends on many factors (e.g. the preferred orientation of the settling clay minerals, the crystallinity of the minerals, the thickness of the slide). Semi-quantitative analysis of the described clay minerals was carried out using the integrated peak area ratio of the clay minerals from 50 % RH patterns versus the internal standard from that pattern. The errors are estimated to 5 %.

4.4. Clay mineralogy of matrix

The results show a relatively similar clay assemblage in all the different areas of mud volcanism, largely dominated by the presence of smectite (64-90 %). The other clay minerals, with a significant presence in the sediment fraction less than 2 μm, are kaolinite (4-16 %), and palygorskite (2- 20 %); illite (1-6 %) and chlorite (< 2 %) are of less importance (Figure 4.3).

Previous clay mineralogy studies of the mud breccia matrix of mud volcanoes in the Olimpi field (Staffini *et al.* 1993; Akmanov *et al.* 1996; Robertson and Kopf 1998; Akmanov and Woodside 1998; Jurado-Rodriguez and Martinez-Ruiz 1998) also report the predominance of smectite-type clay minerals (Table 4.2). Illite content is usually small in the mud breccia matrix, but common in some clasts, such as mudstone fragments (Akmanov *et al.* 1996). Chlorite was only detected as traces in the clay fraction of Milano and Napoli (Jurado Rodriguez and Martinez-Ruiz 1998) but was reported as locally important in some of the other mud volcanoes (Staffini *et al.* 1993).

Smectite

Particulary high smectite values are found in the Anaximander Mountains area, in Amsterdam (average 89 %) and Kazan (85 %) mud volcanoes, and in the Florence Rise area (average 80 %). In the Olimpi Field, the average amount of smectite is 71 %, but part of the smectite may be "chloritized", i.e. the interlayer is blocked by Fe-hydroxides (and/or Mg-, Al-hydroxides). "Chloritized" smectite occurs within about 20 to 35 % of the total clay minerals, in sub-samples from Napoli and Moscow (Figure 4.3). In most of the samples, the lattice of the smectite collapses towards higher spacing than expected when dehydrated (e.g. 13 Å instead of 11 Å in the (001) direction). This could be caused by organic molecules within the smectite interlayer. Some authors (Ransom *et al.* 1998) indeed suggest that the sediment-linked organic

matter is associated with the clay fraction and that smectite-rich suites have distinctly higher organic carbon content than chlorite-rich suites

Kaolinite

Kaolinite group minerals are more abundant in the Olimpi field area (average 12 %) than in the Anaximander Mountains and Florence Rise area (average 7 %). The distribution of kaolinite with respect to halloysite, its hydrated form, also shows some difference from one area to another. The ratio kaolinite/halloysite is usually <1 in the Olimpi field, with a predominance of halloysite (average 7 %) over kaolinite (average 4.6 %). To the contrary, this ratio is >1 in the Anaximander and Florence rise area.

Palygorskite

The regional distribution of palygorskite shows a strong disparity between the different areas. It shows low amounts (from 2 to 7 %) in the Florence Rise and Anaximander areas, probably partly because of dilution by smectite. In the Olimpi field, it is a major component of the clay assemblage (from 12 to 19 %).

Illite

Clay minerals from the mica group (illite) show unusually low values (1 to 6 %) for the Mediterranean environment (Venkataratham and Ryan 1971, Chamley *et al.* 1978). Illite is more abundant in the Anaximander and Florence Rise area (average 4 %) than in the Olimpi field (average 1.5 %).

Primary Chlorite

Chlorite has been found in traces (<2 %) only in few samples and does not show any coherent distribution throughout the area.

	Smectite	Kaolinite	Illite	Chlorite
Staffini *et al*. 1993	29-66	27-57	1-18	0-17
Akmanov and Woodside 1998	44-66	17-30	14-30	-
Jurado-Rodriguez and Martinez-Ruiz1998	19-84	14-44	<5-50	traces
This study	64-90	4-15	1-6	traces

Table 4.2: Abundance of clay minerals (in %) in the mud breccia matrix of mud volcanoes from previous studies within the Olimpi field (Staffini et al.1993; Akmanov and Woodside 1998; Jurado-Rodriguez and Martinez-Ruiz 1998).

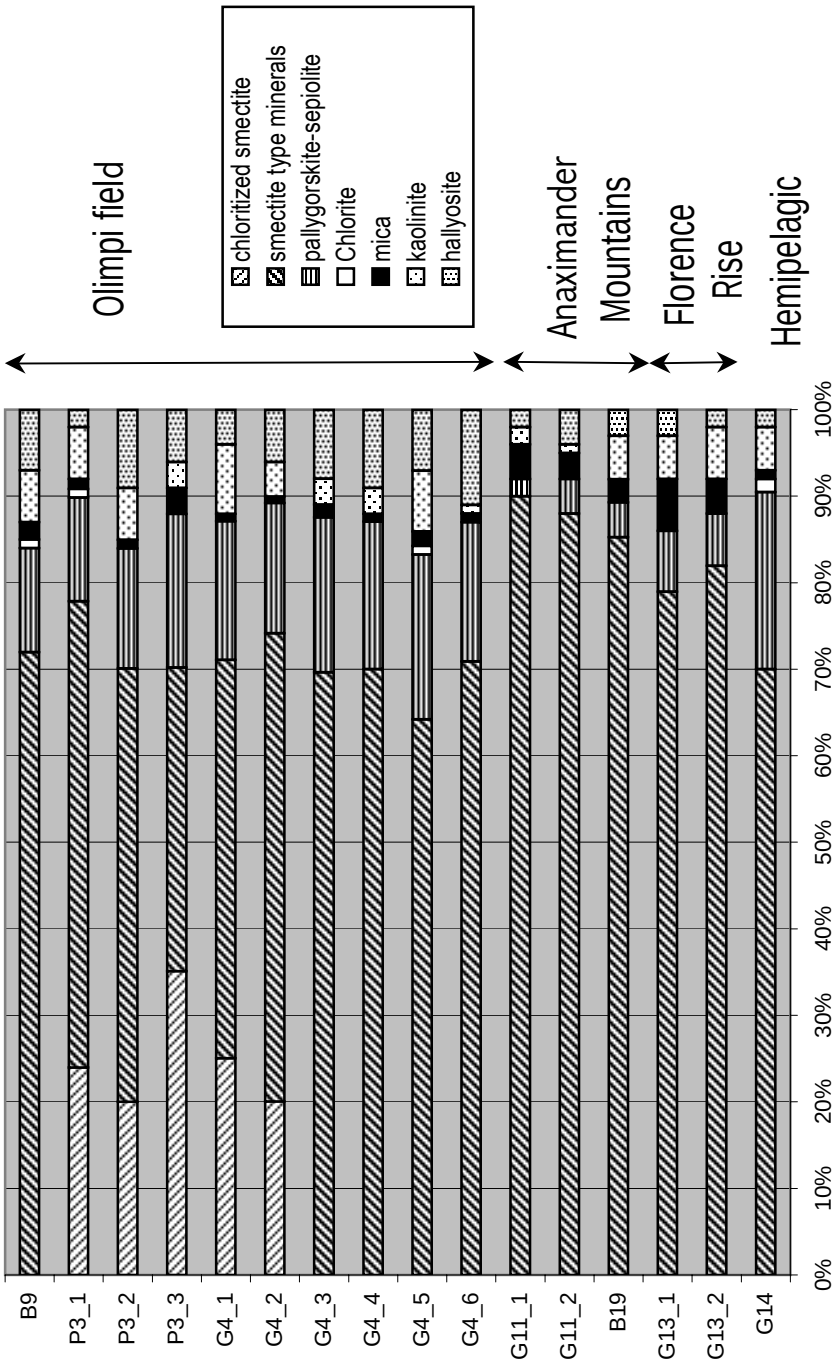

Figure 4.3: Relative abundance of clay minerals in the mud breccia matrix from mud volcano cores and in an hemipelagic core. Estimated errors are of 5% .

4.5. Provenance of clay minerals

To understand the provenance of clay mineral abundances in these mud volcanic deposits we can compare them with the present-day distribution patterns of Quaternary clay minerals in the Mediterranean Sea. Most of the clays present in Mediterranean assemblages are believed to derive from detrital input from the surrounding landmasses ultimately (Venkataratham and Ryan 1971; Chamley 1989). The major part of the detrital particles is supplied by fluvial processes through the major rivers: Nile River, Rhone River, Ebro River, Po river. Typically, smectite and kaolinite are of southerly origin (Nile-derived or from Saharian dusts), whereas illite and chlorite are of northerly origin (weathering of Alpine crystalline units), transported mainly by the Rhone and Po Rivers into the western Mediterranean Sea and Adriatic Sea (Figure 4.4). Palygorskite is of special interest, because the only significant source for this mineral is Paleogene deposits in Africa (Chamley 1989). Eolian supply from Saharian dusts being significant in eastern Mediterranean Sea (Chester *et al.* 1977; Tomadin and Lenaz 1989), the likely dispersal agent for palygorskite is wind transportation (Venkatharan and Ryan 1971; Mélières *et al.* 1998; Foucault and Mélières, 2000).

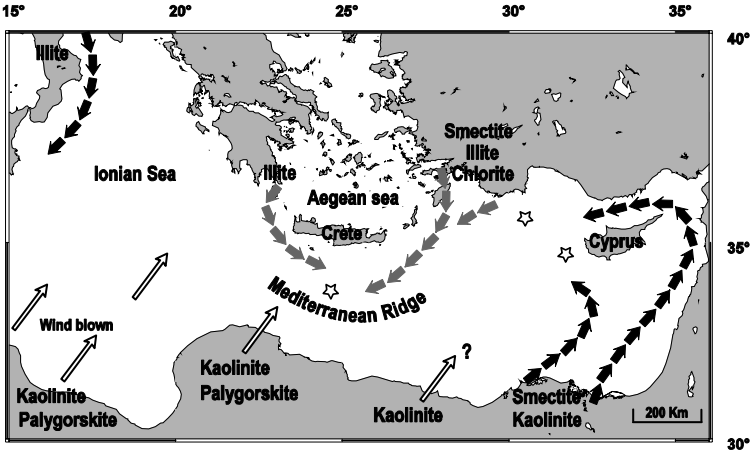

Figure 4.4: Present-day sources of clay minerals in the eastern Mediterranean Sea (modified from Venkatarathnam and Ryan 1971, Foucault and Melieres 2000). White arrows: eolian input, black arrows: fluvial input, grey arrows: dispersal by intermediate water. stars indicate the studied areas.

The eastern Mediterranean Sea sedimentary assemblages (Venkataratham and Ryan 1971, Maldonado and Stanley 1981) are controlled mainly by: (1) the terrigenous distribution of the Nile river (smectite and kaolinite-rich assemblage) dispersed by easterly-directed surface currents, (2) the dispersal by Levantine intermediate water of a smectite-chlorite-illite assemblage from the SE Aegean Sea toward the Mediterranean Ridge SE of Crete, (3) the eolian input of a kaolinite rich assemblage on the Mediterranean Ridge and the western Nile cone from northern Africa, probably in association with palygorskite (Chamley 1989; Foucault

and Mélières 2000), and (4) the dispersal by deep water of an illite rich assemblage restricted to the sediments of the Hellenic Trough (Figure 4.4).

To some extent, the enrichment in kaolinite and palygorskite in the Olimpi field, in contrast to the enrichment in smectite and illite in the Anaximander /Florence area (Figure 4.3), could reflect this geographical distribution. The Anaximander Mountains and Florence Rise area show an affiliation with Turkish and Cyprus units, with more illite and more smectite, possibly derived from the weathering of ophiolite units (Chamley 1989). Also the counterclockwise gyre along the Levant coast favours the dispersal of Nile-derived clays in these areas. On the Mediterranean Ridge (Olimpi Field), minerals with an African origin, and mainly transported by northerly winds, are more abundant (Figures 4.3 and 4.4), i.e. kaolinite and palygorskite (Venkatharan and Ryan 1971; Chester *et al.* 1977; Tomadin and Lenaz 1989).

However, the clay mineral assemblages show more similarities between the different geographical areas than expected from Quaternary sedimentation and may reflect earlier depositional history. Illite and chlorite, usually found in present-day Mediterranean sediments (Venkatharan and Ryan 1971), are observed in relatively small quantities, or only in traces in the mud volcano deposits brought up from deeper units.

4.6. Discussion and conclusions

4.6.1. Age of the remobilization unit

The high smectite percentages in the mud breccia matrix have some implications for matrix provenance. Such a simple assemblage with abundant smectite as an ubiquitous mineral is comparable to that of Messinian deposits throughout the circum-Mediterranean area (Chamley *et al.* 1978, Chamley and Robert, 1980). Data from Mediterranean basins (DSDP Leg 13 and 42A) and surrounding landmasses (Algeria, Spain, Italy, South of France) show general smectite enrichment in Messinian terrigeneous deposits (up to 95 % at DSDP site 375-376, west of Cyprus). Chamley and co-authors (Chamley *et al.* 1978; Chamley and Robert 1980) suggested that smectite enrichment in these types of deposits is related to the regional climatic conditions (Heimann and Mascle 1974; Gorsel and Troelstra 1980; Chamley and Robert 1980) that led to the development of poorly-drained smectitic soil in exposed coastal plains. Pedogenesis of smectite, favoured by an arid climate and strong contrast of rainfall periodicity (Paquet *et al.* 1969), could have taken place in low-relief areas exposed above the sea level drop, and been transferred in marine deposits through the increase of erosion and terrigeneous supply typical of Messinian time (Gorsel and Troelstra 1980). The smectite recognized in the ODP cores of the Napoli and Milano mud volcanoes were identified by TEM studies as Al-rich beidellites (Jurado-Rodriguez and Martinez-Ruiz 1998) suggesting a pedogenic origin (Chamley 1989).

Several observations already described in the literature (Robertson and Kopf 1998b; Kopf 2002) tend to support a Messinian origin for the mud matrix. Some authors (Kastens *et al.* 1987; Kopf *et al.* 2000) report similarities between the physical properties, colour and composition of the mud breccia matrix with Messinian ooze from the Tyrrhenian Sea. Schulz

and co-authors (1997) suggest, from the maturation of organic matter and the observation of fresh water fauna, that the matrix of Napoli mud breccia is derived from sedimentary strata deposited under terrigeneous, riverine or lacustrine influence, probably within the sub-aerial non-evaporite basins that developed in the Messinian circum-Mediterranean. Furthermore, on Napoli Mud Volcano, ODP drilling recovered some halite clasts (Emeis *et al.* 1996).

An open question is why material recovered from different volcanoes in the Olimpi field (Limonov *et al.* 1994, 1996) yielded nannofossils and pelagic foraminifers older than Miocene age, with some Oligocene, Early Eocene, and rare Cretaceous age (Premoli Silva *et al.* 1996), the latter especially found in Toronto MV. Cretaceous and Eocene microfossils were present in Napoli and Milano mud volcanoes, but ODP investigations have proved that these are reworked together with younger microfossils within the clasts (Emeis *et al.* 1996). In the same way, some earlier published ages of clasts may need to be reassessed in view of the possible role of reworking. One explanation to the presence of older microfossils in the clasts may be that the unit from which the mud matrix is derived is different from one mud volcano to another. It has already been proposed that the sources for the matrix and clasts of Toronto MV were different than those of other Olimpi field mud volcanoes (Akmanov 1996), because of the differences in clast ages and lithologies (Akmanov 1996), and in mud matrix composition (Staffini *et al.* 1993). Another explanation is that slices of older material (Eocene and Cretaceous units) are present above the Messinian source unit. In the accretionary wedge, the tectonono-stratigraphic position may be complicated by dense imbrication and deformation.

Although studies from different mud volcanoes are not statistically significant (with more studies on Napoli MV and Milano MV than on Toronto MV for example), the coherence of the matrix composition within this study and similar ones from the literature (Staffini *et al.* 1993; Akmanov 1996; Robertson and Kopf 1998; Akmanov and Woodside 1998; Jurado-Rodriguez et Martinez-Ruiz 1998) tend to demonstrate the uniqueness of the source of the mud throughout the different areas of mud volcanism in the eastern Mediterranean Sea: i.e the Olimpi Field, the Anaximander Mountains, and the Florence Rise area. In the Anaximander Mountains, however, older clasts are expected to be found in the mud volcanoes because basement rocks have been brought nearer the surface by the post-Miocene rifting and are directly overlained by Pliocene sediments. Cretaceous microfossils are indeed present in clasts from Kazan and Kula mud volcanoes (Woodside *et al.* 1997, Huguen *et al.* 2001a); yet this is coherent with a source of the mud rooting within sub-aerial deposits of Messinian age.

4.6.2. Depth of the mud remobilization

A deep origin of remobilization was inferred in the Olimpi field on the basis of (1) the presence of thermogenic gases, and (2) the geometry of the subducting plates (Camerlenghi *et al.* 1995), and was related to the décollement zone within the accretionary wedge, estimated to be 5300-7000 mbsf. Maturation of organic matter and vitrinite reflectance data for the Napoli Mud Volcano (Schulz *et al.* 1997) also suggest a similar depth range of remobilization (4900 to 7500 mbsf). However, a recent reevaluation of such a model by Kopf and co-authors (2000), with the same approach used for clasts and matrix of the Milano MV, is in favour of a shallower origin of both clasts and matrix, between 1.5 and 2 km. In a different model, based

on geometry modelling of the ascent of the mud, Kopf and Behrmann (2000) estimate a remobilization depth between 1640 and circa 1800 mbsf.

A shallow origin of the source is in agreement with the present mineralogical data that indicate that no diagenetic transformation has occurred, i.e. predominance of smectite and absence of mixed layers smectite/illite (Figures 4.2 and 4.3). Diagenetic transformations, such as the smectite-into-illite transformation, usually begin to occur at depths greater than 2 km (Chamley 1989). Assuming a normal geothermal gradient of 30°/km, the clay mineralogy will be significantly affected at depths beyond 2.5 to 3 km of burial, at about 80-100 °C (Millot 1964; Chamley 1989). Within the low-heat flow accretionary setting of the Mediterranean Ridge (25°/km; Camerlenghi *et al.* 1995), smectite might stay stable deeper (3.5 km), but not as deep as 5 to 7 km, which was proposed by several authors to be the depth of the mud reservoir (Camerlenghi *et al.* 1995; Schülz *et al.* 1997). Mixed layers smectite/illite were detected in Napoli and Milano dome (Akmanov and Woodside 1998; Jurado-Rodriguez and Martinez-Ruiz 1998), but illite layers in the smectite show low values and no significant variation downhole. Moreover, a shallow depth of the source is in agreement with new data concerning the geometry of the accretionary prism, showing that the mud volcanoes are located above the backstop, in the Olimpi Field (Huguen 2001), as well as on the western branch of the Mediterranean Ridge (Rabaute *et al.* 2003).

Smectite is a highly hydrated mineral. The interlayer water content of 15 Å and 18 Å phyllosilicate lies between 20 to 50 % of volume (Fitts and Brown 1999, Brown *et al.* 2001), and it has a very low density: 1.9-2.1 g/cc compared to 2.79-2.85 g/cc for anhydrous grains (Brown *et al.* 2001). Geochemical studies (Deyhle and Kopf 2001, Dählmann and de Lange 2003) proposed that the fluids have a deeper origin than the solid phase. It is thus probable that a smectite-rich unit is very easily remobilized into a mud diapir by some deeper fluids percolating through it.

4.6.3. Alteration processes

Mud volcanoes produce a distinctive geochemical environment, where the seeping of heavily mineralised fluids may cause authigenic mineral formation, such as carbonate cementation (Aloisi *et al.* 2000). A major difference between the surveyed mud volcanic fields (as already noted in Chapter 3), that may induce different mineralogical reactions, is the seeping in the Olimpi field of briny fluids, dissolved from the underlying Messinian layer (MEDINAUT/MEDINETH scientists 1999). Brines formed by the dissolution of late-stage evaporite minerals, such as bischofite ($MgCl_2.6H_2O$), are enriched in Mg^{2+} (Bernasconi 1999), e.g. in the Discovery Basin (Wallman *et al.* 2002) and may influence clay mineral alteration, especially palygorskite formation and “chloritization” of smectite (i.e. incorporation of Mg-hydroxide within the interlayer).

In the present-day Mediterranean Sea,some of the palygorskite originates from the erosion of authigenic deposits in the nearby arid region, transported as detrital particles by the wind (Chamley 1989, Foucault and Mélières 2000). However, the presence of palygorskite in very distal marine sediments (Bonatti and Joensuu 1968, Pletsch 1998) supposes that palygorskite can result from other genetic processes that need to be examined here. These

processes include the alteration of pre-existing sediments by hydrothermal or diagenetic fluids (Bonatti and Joensuu 1968; Pletsch 1998) in close contact with siliceous deposits (basalts or sepentines), the alteration of pre-existing sediments by salt brines (Gieskes *et al.* 1980), and the authigenic growth at the sediment surface from direct precipitation from Mg and Si-rich interstitial solutions in pore-fluids (Millot 1964; Pletsch 1998). The presence of brine lakes and brine seeps with high Mg and Si content (Wallman *et al.* 2002), associated with mud volcanism in the Olimpi field (in contrast to the Anaximander Mountains where these brines are absent) might result in the preferential formation of palygorskite in the Olimpi area. Robert and Chamley (1991) inferred that palygorskite formation must have taken place in shallow marine lagoons and evaporite basins; palygorskite in the Olimpi field can thus also be inherited from the underlying evaporite deposits.

In the same way “chloritized smectite” found only in the Olimpi field, could either reflect present-day alteration by brines, or be inherited from Messinian evaporite deposits in the deeper section, corrensite (mixed layer smectite/chlorite) being abundant in Messinian sediments (Chamley *et al.* 1978). Robertson and Kopf (1998) already proposed that the chlorite in the mud breccia matrix is a fingerprint of a diagenetic origin related to dessicating Messinian paleo-environments.

Part II

Tectonic control of mud volcanism: examples from the Anaximander Mountains at the junction between the Hellenic and the Cyprus Arcs

Chapter 5. The Anaximander Mountains: a clue to the tectonics of Southwest Anatolia

Abstract

The offshore Anaximander Mountains are an important link between the Hellenic and Cyprus Arcs. They were formed by southeastward rifting from Turkey in post-Miocene time. Gravity data have shown that the eastern part of the Anaximander Mountains is different from the western part; and multibeam mapping seems to confirm that the eastern Anaximander Mountains have affinity with the Florence Rise structure (western Cyprus Arc). Faulting along and across the latter feature is characterized in the seismic data by anastomosing faults and pop-up flower structures. It is likely that progressive adjustment to incipient collision developed into a broad zone of NW-SE transpressive wrenching extending towards south Turkey. In contrast, the western mountains are more directly related to the opening of the Rhodes basin and the Finike basin, as transtension may have dominated in southwest Turkey since the Pliocene. The connection with onshore Turkey is still unclear, but could be related to the Fethiye-Burdur fault zone that defines the western boundary of the complex Isparta Angle. The Anaximander Mountains and the Isparta Angle form together a tectonic accommodation zone between the active deformation in southwestern Turkey and the Aegean region and the tectonically quieter Cyprus region.

5.2. Introduction

Initial stages of continental collision in the eastern Mediterranean Sea dominate the tectonic interaction between Africa and Eurasia, represented by the westward extrusion of the Anatolian microplate. The plate boundary is well defined through the Hellenic Arc to the west and through the Cyprus Arc to the east. The junction between the two arcs, however, is rather enigmatic (Figure 5.1).

Subduction underneath the Hellenic Arc has been extensively studied during the last 30 years and is very well documented from marine investigations (Le Pichon and Angelier 1979; Ryan *et al.* 1982) and from tomography studies (Spakman *et al.*1988, Papazachos *et al.* 1995). It has resulted in the formation of the Mediterranean Ridge accretionary prism (Figure 5.1) of which both seabed and internal deformation has been well imaged through recent studies (Chaumillon *et al*. 1996; Huguen *et al*. 2001b). While the central branch of the Mediterranean Ridge is dominated by approximately orthogonal compressional stresses (Le Pichon *et al.* 1982b; Mascle *et al.* 1999), the western and eastern branches, i.e. the Matapan Trench to the west and the Pliny/Strabo trenches to the east (Figure 5.1), are undergoing transpressional deformation (Le Quellec and Mascle 1978; Le Pichon *et al.* 1979; Mascle *et al.* 1986; Huguen *et al*. 2001b). By contrast, the Cyprus Arc has not been studied extensively and our knowledge remains incomplete. It is important to note that most elements typical of a

This chapter is based on TAC Zitter, JM Woodside and J Mascle. 2003. The Anaximander Mountains: a clue to the tectonics of Southwest Anatolia. Geological Journal 38: 375-394. Reprinted with permissions of John Wiley & Sons, Ltd.

subduction zone are lacking in the Cyprus Arc (Ben-Avraham *et al.* 1995), such as: 1/ a raised accretionary prism, 2/ deep trenches along the subduction zone and 3/ a volcanic arc. Moreover, tectonic processes in the Cyprus region are complicated by the collision of the Eratosthenes Seamount with Cyprus (Robertson 1998a) and the westward lateral escape of Anatolia (McKenzie 1972; Le Pichon *et al*. 1995; Reilinger *et al.* 1997): processes that may exclude the existence of an actively subducting slab in this region.

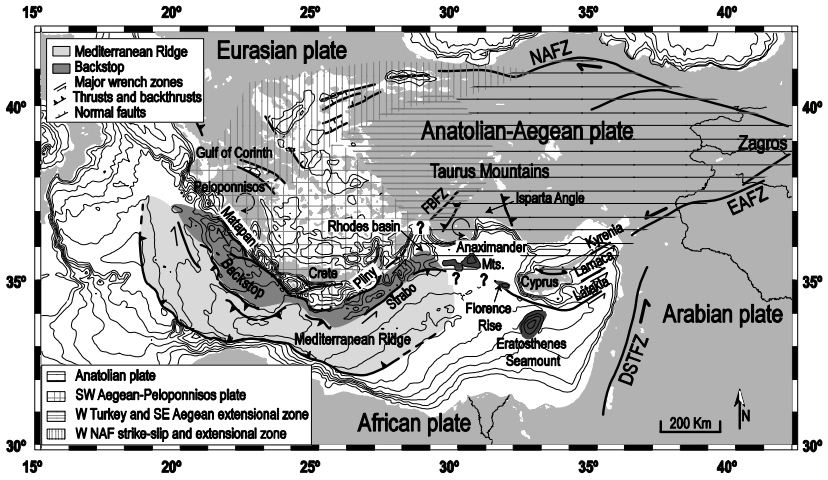

Figure 5.1: General tectonic context in the Eastern Mediterranean Sea with location of the main features cited in the text (modified after Mc Clusky *et al.* 2000, Huguen *et al.* 2001). Patterns indicate areas of coherent motion and zones of distributed deformation (see legend). Circular arrows indicate areas of possible rotation. Abbreviations are as follow, EAFZ: East Anatolian fault zone, NAFZ: North Anatolian fault zone, DSTFZ:Dead Sea transform fault zone, FBFZ:Fethiye-Burdur fault zone, Anaximander Mts.: Anaximander Mountains.

The blockage of the subduction process along the central and eastward segments of the Cyprus Arc were inferred by many authors (Ben Avraham *et al*. 1988, 1995; Kempler and Ben-Avraham 1987; Kempler and Garfunkel 1994) on the basis of seismic reflection data as well as seismicity observations. Recent studies have confirmed that the deformation from Cyprus to the Syrian coast is partitioned along strike-slip fault systems distributed over a wide zone, expressed in the bathymetry through the Kyrenia-Lanarca-Latakia Ridges (Ben Avraham *et al.* 1995; Vidal *et al.* 2000a, 2000b). On the other hand, the plate boundary along the western segment of the Cyprus Arc was usually referred to as a subduction zone, even though the exact locality of such a zone is unclear. This plate boundary is not defined seismically and has been proposed to follow the outline of the northern edge of the Mediterranean Ridge (Rotstein and Kafka 1982). Hence, it is often inferred to join the Florence Rise and the eastern extremity of the Strabo Trench, through the south of the Anaximander Mountains (Robertson 1998b).

The Anaximander Mountains, located offshore of southwest Turkey between Rhodes and Cyprus (Figure 5.1), appear in this context as an important link between both arcs. Their

formation, contemporaneous and probably linked with the formation of the Rhodes Basin, may be the result of their peculiar location where the two arcs interact. They are part of a broad zone of deformation accommodating the on-going collisional processes between Africa and Anatolia. Moreover, they appear to be related to the complex Isparta Angle (Blumenthal 1963), directly to the north, which separates areas of different relative plate motion in Turkey, from westward motion to the east of the Isparta Angle to more southwestward motion to the west (Barka and Reilinger 1997). This critical area needs to be considered as a whole as playing a major role in the neotectonic development of the eastern Mediterranean Sea.

The purpose of this paper is to address the origin and development of the Anaximander Mountains, and their reaction to the pronounced difference in tectonic activity between the Hellenic and Cyprus Arcs. From this, the relationship between deformation in the Anaximander Mountains and southwest Anatolia can be better understood. After briefly reviewing the geological background of the Anaximander Mountains as well as the surrounding areas, especially the Isparta Angle, the deformation style within the Anaximander Mountains and the Florence Rise to the south is discussed on the basis of multibeam mapping and seismic profiling data from the ANAXIPROBE 95 and PRISMED II 98 surveys. Two questions will be more specifically examined: (a) where is the Africa-Anatolian plate boundary between Rhodes, Cyprus and southwest Turkey? and (b) is there still a subduction zone below the western branch of the Cyprus Arc?

5.3. Background

5.3.1. Plate interactions in the eastern Mediterranean region

The eastern Mediterranean region marks a highly tectonically active region between the African and Eurasian plates and exhibits a large variety of tectonic processes (collision, subduction, back-arc extension, strike-slip faulting) within a relatively small geographical area.

The dominant stress field is governed by the convergence of the African and Arabian plates towards Eurasia, with northeastward and northward motion respectively. The difference in velocity between these two plates (18 $mm.y^{-1}$ in an Eurasia fixed reference frame for the Arabian plate (McClusky *et al.* 2000) against 6 $mm.y^{-1}$ for the African plate (McClusky *et al.* 2000)) induces major strike-slip faulting along the Dead Sea transform fault zone and causes the westward extrusion of the Anatolian-Aegean microplate, escaping away from the Zagros collision zone along both the East and North Anatolian Faults zones (Figure 5.1). The partitioning of plate movements in the Anatolian-Aegean region between the North Anatolian Fault (NAF) zone to the north, the Caucasus convergence, and the East Anatolian Fault (EAF) zone to the south, has been clarified and quantified using recent GPS data (Reilinger *et al.* 1997; McClusky *et al.* 2000). The westward motion of the Anatolian plate (central Turkey) can be described by a coherent counterclockwise rotation (with less than 2 $mm.y^{-1}$ internal deformation) around a pole of rotation located approximately NE of the Nile delta, with fault slip rates of 24 $mm.y^{-1}$ on the NAF and 9 $mm.y^{-1}$ on the EAF (McClusky *et al.* 2000). In contrast, the southwest Aegean-Peloponnisos plate is moving southwestward relative to Eurasia at 30 $mm.y^{-1}$ (McClusky *et al.* 2000), also in a coherent fashion with low internal

deformation (< 2 mm.y^{-1}), although the Peloponnisos undergoes clockwise rotation in an Aegean fixed framework (McClusky *et al.* 2000). In between these two plates is a zone of N-S extension that comprises western Turkey (Figure 5.1). Significant deviation occurs in the SE Aegean-SW Turkey-Rhodes area (McClusky *et al.* 2000) that undergoes a counterclockwise rotation moving toward the Hellenic trench (Figure 5.1). The Isparta Angle area, located in a region that could be consider as a triple junction between the Aegean, Anatolian and African plates (Figure 5.1), shows considerably slower motion in GPS data, about 10 mm.y $^{-1}$ relative to Eurasia (Barka and Reilinger 1997; McClusky *et al.* 2000).

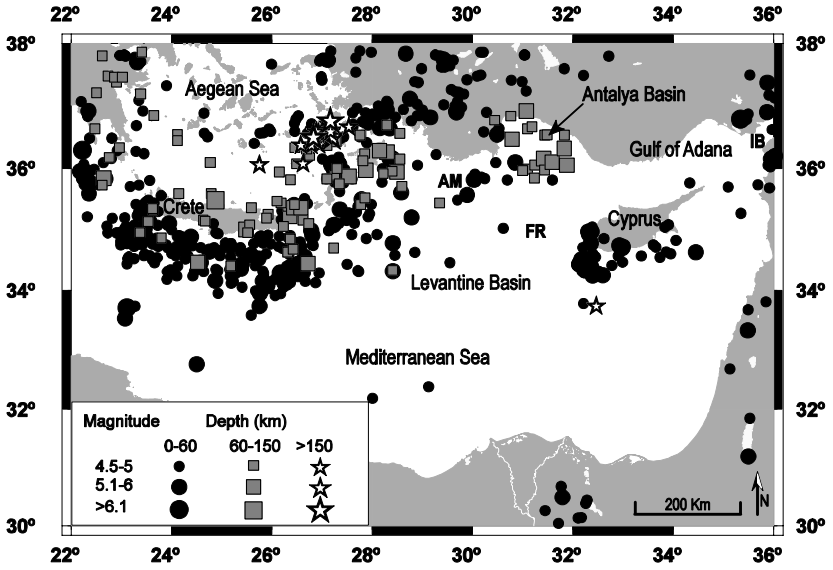

Figure 5.2: Seismicity of the southern boundary of Anatolian-Aegean plate and nearby areas for the period 1973-present. Data are from the USGS National Earthquake Information Center (NEIC), World Data Center for Seismology, Denver. Abbreviations are as follow, AM: Anaximander Mountains, FR: Florence Rise and IB: Iskenderum Bay.

Current knowledge of neotectonic processes in the eastern Mediterranean Sea is also inferred from its long history of seismicity. Historical records show that Turkey has experienced many major earthquakes that have seriously affected urban centres; some of them were afterwards abandoned or relocated (Waelkens *et al.* 2000). The highest activity is associated with faults along the margins of the Arabian and the Anatolian plates: along the collision zone between Turkey and Iran, along the Dead Sea Fault and along the North and East Anatolian Faults. Information on seismicity in the eastern Mediterranean Sea within the region bounded by longitudes 22° to 36° and latitudes 30° to 38° (Figure 5.2) is based on the USGS national earthquake information centre (NEIC) database covering the period 1973 to present. The magnitude values given in the figure are the body-wave magnitudes (mb). The precision of earthquake loci (and especially depth accuracy) is believed to be of satisfactory accuracy only for major events. Thus, Figure 5.2 only consider earthquakes with mb≥4.5. The

seismicity distribution for the Hellenic Arc is typical of subduction zones, with deeper events towards the back-arc region (Figure 5.2). Shallow earthquakes (from 0 to 60 km depth) are widespread along the Hellenic Arc, on the Greek and southwest Turkish mainland, over the island of Cyprus and in the offshore regions (Aegean Sea, Levantine Basin, Antalya Basin, Adana Basin and Iskenderun Bay). Events of intermediate depth (60 to 150 km) are mainly located in the inner part of the Hellenic arc and below the Aegean Sea, and in the region of the Antalya Basin along the Aksu thrust. Relatively low seismicity occurs below the southern Anaximander Mountains as well as below the Florence Rise, often assumed to be the African-Anatolian plate boundary.

5.3.2. Geological setting on land

The Isparta Angle (Blumenthal 1963) has been suggested to be a key link between the Hellenic subduction zone and the Cyprus Arc. It is a triangular region separating the western Taurus Mountains from the central Taurus Mountains and extending offshore into Antalya Bay (Monod 1976).

The Isparta Angle is bounded to the west by the northeast-southwest trending Fethiye-Burdur fault (Figure 5.3). Although this fault zone is seismically well defined, the style of deformation along this fault is still controversial. Some authors interpret this northeast-trending structure as a continuation of the northeast-trending left-lateral transform system of the Strabo and Pliny trenches on the basis of an en-echelon arrangement of the fault zone (Yağmurlu *et al.* 1997) and an inferred left-lateral sense of slip based on slickensides on normal fault planes (Dumont *et al.* 1979). On the other hand, the left-lateral motion has not been demonstrated by fault plane solutions of recent earthquakes (Taymaz and Price 1992), but it is consistent with GPS measurements in the area (Barka and Reilinger 1997; Kahle *et al.* 1999). The Lycian nappes and the Hoyran-Beyşehir nappes are thrusted over the Isparta Angle from the west and the east respectively (Figure 5.3). The eastern boundary of the Isparta angle is defined by what has been known as the Sultan Dağ thrust (Boray *et al.* 1985; Barka *et al.* 1995) but in recent works is considered to be a normal fault (Koçyiğit *et al.* 2000; Taymaz *et al.* 2002), and comprises two major structures, the late Miocene Aksu thrust and the Kirkkavak fault that experienced a phase of right-lateral displacement during Miocene time (Dumont and Kerey 1975) and developed into dominantly normal faulting during Pliocene-Recent time (Glover and Robertson 1998). The Isparta Angle itself consists of a number of Mesozoic carbonate platforms (Monod 1976; Poisson 1977, Robertson 1993), autochthonous relative to the overriding Antalya Nappes (Lefèvre 1967) or Antalya Complex (Robertson and Woodcock 1980), an assemblage of diverse Mesozoic sedimentary facies remnant of a passive continental margin, including ophiolite-derived sedimentary rocks. The autochthonous Susuz-Dağ and Bey-Dağları Massifs (respectively SZD and BD in Figure 5.3) constitute a wide anticline with relatively steep dipping margins and abut the coast west of Finike (Poisson 1977). Some east-west trending thrusts occur internal to the Bey-Dağları with southward vergence, towards the Mediterranean (Poisson 2001 Pers. Comm.). The Antalya Nappes Complex, in thrust contact with the eastern margin of the Bey-Dağları anticline (Figure 5.3), was formed from latest Cretaceous to early Miocene times by a combination of wrench and thrust tectonics (Woodcock and Robertson 1982, Hayward 1984), and extends from Finike to Antalya, forming

Cape Chelidonia. The main thrusts of the Antalya Nappes Complex were reactivated during the late Miocene Aksu phase (Gutnic *et al*. 1979; Woodcock and Robertson 1982). Several Neogene basins (from Miocene to Quaternary age) have developed forming the core of the angle (Flecker *et al.* 1998) (Figure 5.3).

The Isparta Angle records a Mesozoic to present history of compression, extension, and strike-slip motion (Poisson *et al*. 1984; Robertson 1993). During the Late Miocene, it underwent compression and transpression related to the final emplacement of the Lycian nappes (Collins and Robertson, 1998). The Lycian thrust sheets have been emplaced during three major phases (Collins and Robertson 1997, 1998): a late Cretaceous ophiolite emplacement, an Eocene phase associated with the development of a flexural foreland basin and a late Miocene southwestward translation of sheets over the Bey-Dağları, due to post-orogenic collapse of the Menderes Massif (Seyitoğlu *et al.* 1992; Collins and Robertson 1997, 1998). The evolution of the extensional systems in western Anatolia has been the object of various models (see Koçyiğit *et al.* 1999; Bozkhurt 2001). The formation of graben-horst systems in western Turkey has possibly developed in two-stages (Koçyiğit *et al.* 1999; Bozkurt and Oberhänsli 2001); extension was initially related to orogenic collapse in Early Miocene time (Seyitoğlu *et al.* 1992) followed later (Late Pliocene to Recent time) by extension throughout the Aegean-west Anatolian region, associated with the westward extrusion of Anatolia (Şengor *et al.* 1985**)**. This latest extensional phase, probably also related to the formation of Rhodes Basin (Woodside *et al.* 2000), led in the Isparta Angle to the formation of grabens and semi-grabens, as well as a series of N-S trending normal faults, such as the Kemer lineaments (Figure 5.3), overprinting pre-existing right-lateral Miocene-Early Pliocene strike-slip faults (Glover and Robertson 1998). The actual shape of the Isparta Angle was partially acquired by opposite rotations of both sides of the angle, i.e. a 30º anticlockwise rotation of the western limb during the Miocene (Kissel and Poisson 1986), shared with the coastal Kemer limestones (Morris and Robertson 1993), and a 40º clockwise rotation of the eastern limb since the Eocene (Kissel *et al*. 1990), whereas the core of the Isparta Angle does not indicate any detectable rotation (Kissel and Poisson 1986).

Similarly to southwest Turkey, the geology on the island of Cyprus records a history of compression, accretion and extension. Cyprus is composed of three distinct geological terranes: the Mamonia Complex, the Troodos Massif and the Kyrenia Range. The Troodos Massif in the centre of Cyprus is one of the best-preserved and most extensively studied ophiolite complexes (Gass 1968; Moores and Vine 1971 and many others). The Mamonia Complex of SW Cyprus (Figure 5.3), composed of sedimentary, igneous and metamorphic rocks, exhibits similarities with the Antalya Complex (Robertson and Woodcock 1979). This unit is allochthonous relatively to the Troodos ophiolite, and is the remnant of a passive margin (Robertson and Woodcock 1979). Western Cyprus also includes the major NNW-SSE trending Polis graben (Figure 5.3) as well as some Neogene to Pleistocene extensional basins (Payne and Robertson 1995). The Polis graben was formed during two extensional phase, in late Miocene times and in Plio-pleistocene times (Payne and Robertson 1995).

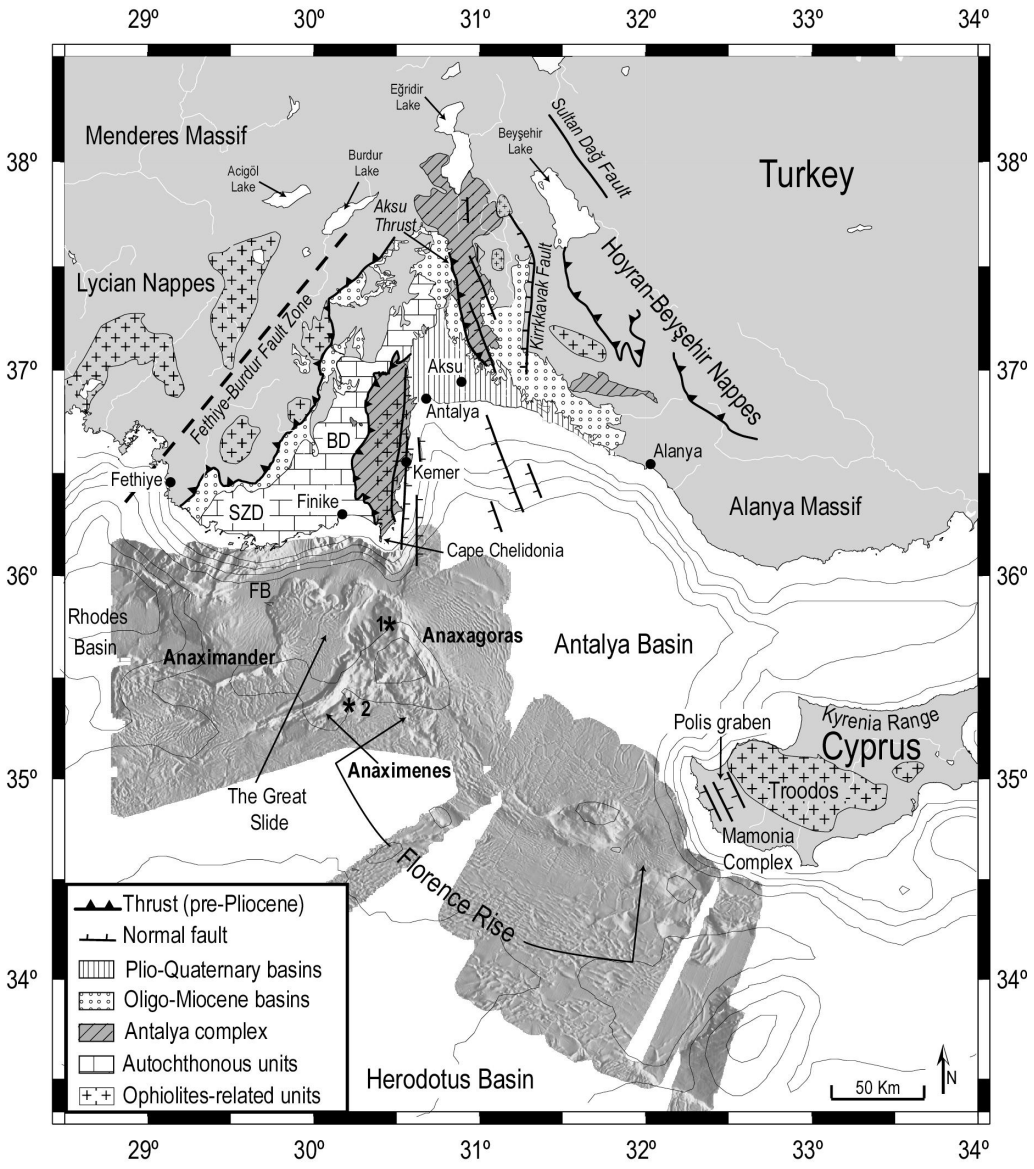

Figure 5.3: Outline geological map of the Isparta Angle, showing the main stratigraphic units and tectonic structures (modified after Gutnic et al. 1979; Hayward 1984; Payne and Robertson 1995; Collins and Robertson, 1998; Glover and Robertson 1998) combined with shaded bathymetry (illumination N090°) of the study area from ANAXIPROBE 95 and PRISMED II EM12D multibeam data with locations of the main features described in the text. Abbreviations are as follow, FB: Finike basin, SZD: Suzuz Dağ and BD: Bey Dağları. Asterisks indicate the location of 1: Kula Mud Volcano and 2: Amsterdam Mud Volcano.

5.3.3. Origin of the Anaximander Mountains

The first dedicated investigations of the Anaximander Mountains were made through the first Training Through Research cruise in 1991 (TTR1) on board the Russian R/V Gelendzhik. Prior to this cruise, several hypotheses were made concerning the origin of the Anaximander Mountains. As initially proposed by Ryan and co-authors (1970) and later by Woodside (1977), the Anaximander Mountains were first thought to be upthrusted blocks of the Neotethyan seafloor, caught up in the collisional process. Another hypothesis was that they were formed of continental lithosphere. Nesteroff *et al*. (1977), for example, speculated that they were part of southern Turkey separated from the Lycian promontory during a post-Miocene collapse of the area. On the other hand, Rotstein and Ben Avraham (1985) proposed that they were northward-colliding fragments of the African lithosphere that have migrated toward the subduction zone, causing a southward shift of the subduction front and break-up of the arc. This process was thought to be analogous to the situation for the Eratosthenes Seamount, which is a part of the African margin (Robertson 1998a) that migrated northward and is colliding with Cyprus since the early Pliocene time.

Results from TTR1, which provided echosounder, sparker seismic and OKEAN long range sidescan sonar data, as well as gravity and magnetic measurements along tracks, and several cores, gave the first evidence of the Anaximander Mountains being a foundered part of the southern Turkish microplate (Ivanov et al. 1992). According to this data set, most of the Anaximander Mountains seemed to be made up of a core of platform rocks possibly belonging to the Taurus Mountains. However, the situation was more complicated than anticipated and some parts of the Anaximander Mountains appeared to be completely different blocks, in terms of deformation stage, age, and composition.

Unequivocal proof of their origin, was then provided by the two expeditions of the Anaxiprobe project, one using the French R/V L'Atalante in 1995, and the other with the Russian R/V Gelendzhik in 1996 during the 6th Training Through Research cruise (TTR6). The Anaxiprobe 95 survey provided high resolution seismic profiling and 25000 square kilometres coverage of Simrad EM12D multibeam bathymetry and acoustic imagery. Detailed bathymetry in this area shows three main mountainous areas rising more than 1000 m above the surrounding seafloor, the two western mountains (Anaximander and Anaximenes) exhibiting typical tilted blocks with steep slopes (Figure 5.3). Seismic profiling across the northern part of the western mountain and across the Finike Basin shows evidence of tilting and subsidence of the Finike basin (Figure 5.4a). On this figure, the presence of an unconformable surface with onlapping of well-stratified Plio-Quaternary reflectors in the deep part of the Finike basin indicates the absence of Messinian evaporites. The same unconformable surface overlain by a restricted Plio-Quaternary sedimentary cover is observed on the top of the Anaximander Mountains themselves (Figure 5.4b). The absence of the Messinian evaporites in the Anaximander Mountains and in the deep basins bordering the Turkish margin, i.e. Rhodes Basin (>4 km deep) (Woodside *et al*. 2000) and Finike Basin (3 km deep), indicates that the southward rifting of the Anaximander Mountains occurred in post-Messinian time. In contrast, the Messinian evaporite formation is present to the east, in the Antalya Basin, and to the south and southwest of the mountains towards the Mediterranean Ridge and Herodotus Basin.

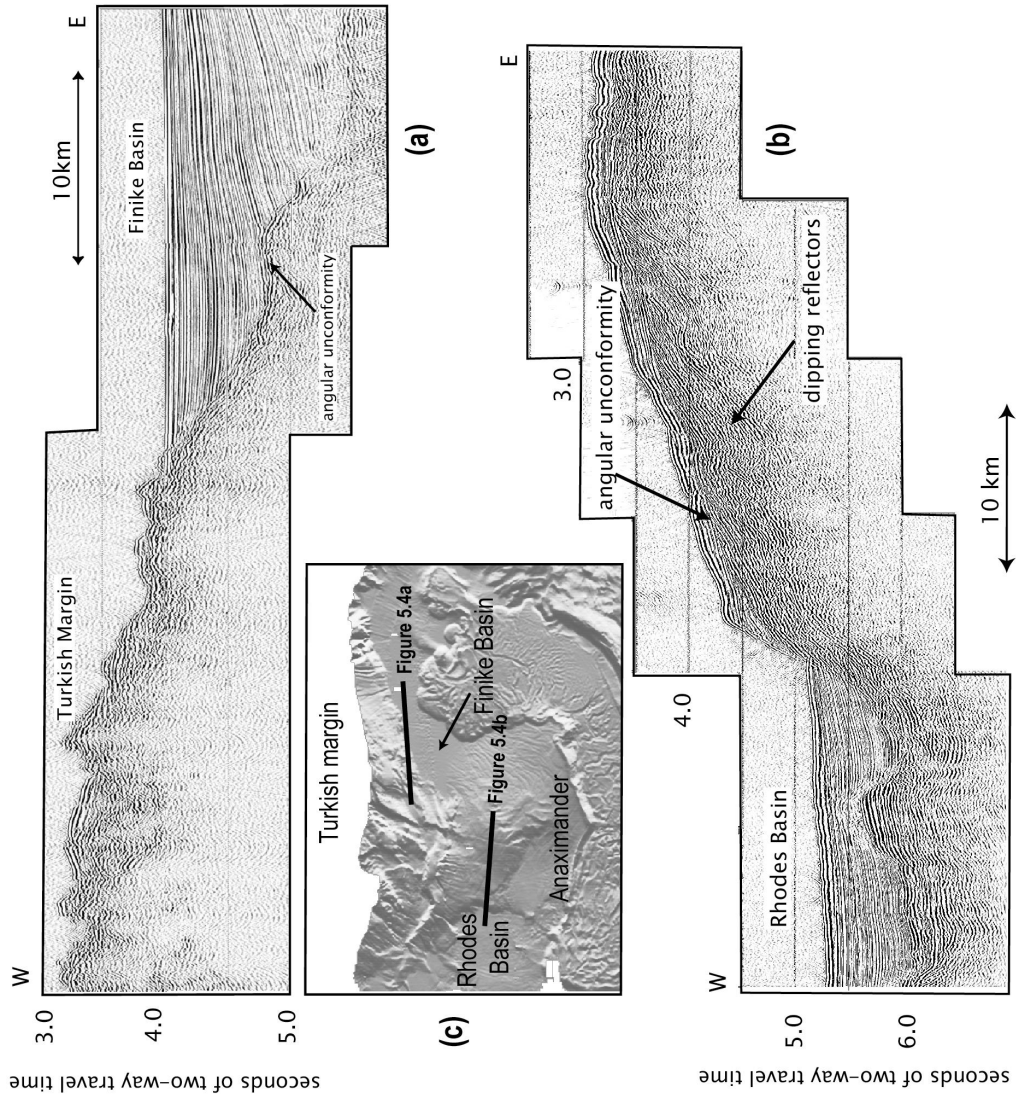

Figure 5.4: Seismic reflection profiles across (a) the Finike basin and (b) the northwestern part of Anaximander Seamount and Rhodes Basin, see inset (c) for location. Note the angular unconformity expressing the absence of Messinian salt in the deep parts of the basins and on top of the seamount. The westward dipping reflectors observed beneath Anaximander Seamount are inferred to be the Bey-Dağları formation similar to the westward dipping Bey-Dağları platform observed on the western side of the Isparta Angle (see text).

The TTR6 sampling results (dredging and coring) have demonstrated the similarities of the Anaximander Mountains with the Taurus Mountains (Woodside *et al.* 1997a). In the eastern part of the Anaximander Mountains (Anaxagoras, Figure 5.3), some ophiolitic material (i.e. fragments of serpentine and sepentinized peridodites), as well as Jurassic-Cretaceous sandstones and radolarian cherts (Woodside *et al.* 1997a), typical of the allochthonous unit have been recovered on the Turkish margin south of Cape Chelidonia and in the mud breccia of Kula Mud Volcano (Woodside *et al.* 1998) at the northern end of the Anaxagoras Seamount (Figure 5.3). The possibility of these clasts being reworked in flysch or molassic deposits before their incorporation in the mud breccia is thought unlikely because of the angular shape of the clasts. Their association with erupted mud volcanic material, which is generally from deep sources, rules out the possibility of these clasts being transported from Turkey. Thus, these clasts belonging to the allochthonous Antalya Nappes Complex are inferred to be in place below the Kula Mud Volcano, implying that the Antalya Nappes Complex extends southward as far as latitude N35° 30'. In contrast, the western part of the Anaximander Mountains (Anaximenes and Anaximander, Figure 5.3) shows affinity with the autochthonous unit that forms the onshore Bey-Dağları and Susuz-Dağ. Detrital limestones, green-gray siltstones and sandstones and black claystones and marlstones, attributed to a Middle Miocene flysch with the help of paleontological analysis, as well as Eocene rocks, have been identified from dredges and gravity cores south of Anaximenes, from the seamount slope, and from Amsterdam Mud Volcano, south of Anaximenes seamount (Figure 5.3) (Woodside *et al.* 1997a, 1998). The data suggest the occurrence of a geological province characterized by a Middle Miocene flysch overlying a neritic Eocene limestone, a succession typical of the Bey-Dağları Massif. This unit is inferred to extend as far south as N35° 10'. Thus, the lithology of the Anaximander Mountains is similar to that onshore, where the Bey-Dağları and Antalya complexes are juxtaposed west of the Isparta Angle.

5.4. Structure and tectonics of the Anaximander Mountains

5.4.1. Gravity anomalies within the Anaximander Mountains

The Bouguer gravity data (Figure 5.5) from the TTR1 expedition show important variations over the Anaximander Mountains. The western part of the Mountains is characterized by a strong positive anomaly up to 190 mgal assuming a Bouguer density of 2.67 $g.cm^{-3}$. The highest Bouguer values coincide with the depressions south of the Anaximander Mountains. The Anaximander and Anaximenes topographic highs are characterized by Bouguer values of 130-150 mgal (Figure 5.5), which imply that the western peaks are undercompensated crustal blocks. In contrast, the data show low positive Bouguer values over Anaxagoras seamount (down to 40 mgal). Also, the Bouguer anomaly over Anaxagoras trends NW-SE, which is similar to the seamount's relief (Figure 5.5). A dextral offset of the Bouguer anomaly lineations is observed at the latitude N35º 30', along a NE-SW trending scarp (Figure 5.5). The 150 mgal difference between the western mountains and eastern mountains is localized along a strong gravity gradient of about 2.5 mgal per km trending roughly N-S at the longitude of E30º. This strong gravity contrast can not be explained by lithological difference between the Anaximenes/Anaximander Mountains and Anaxagoras Mountain alone. Therefore

we interpret that there must be a major crustal discontinuity in the middle of the Anaximander Mountains.

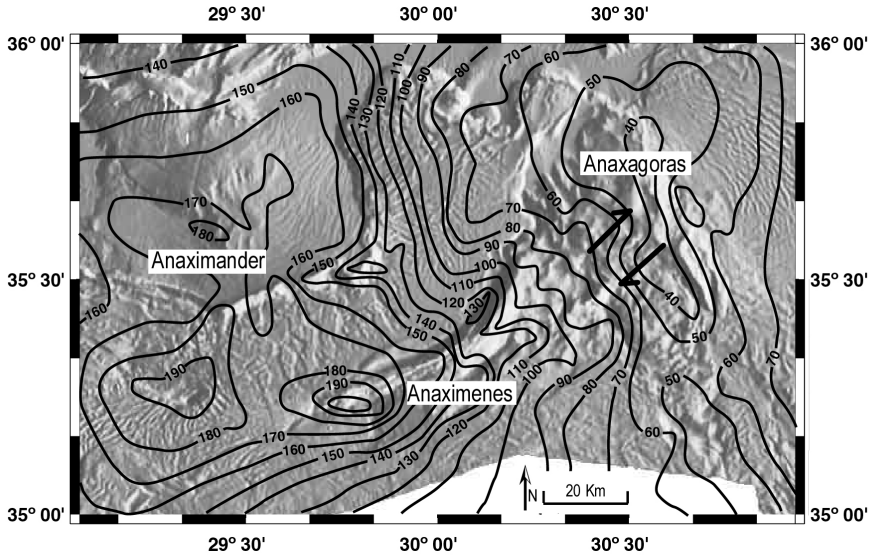

Figure 5: Bouguer gravity anomaly map computed assuming mean crustal density of 2.67 g.cm-3 (contour interval of 10 mgal) from TTR1 expedition shown on the multibeam shaded bathymetry (illumination N090°) of the Anaximander Mountains.

5.4.2. Deformation style within the Anaximander Mountains

The Anaximander Mountains are divided into different geological provinces on the basis of morphology and relief. Surficial deformation observed on the basis of the multibeam mapping (Figure 5.3) exhibits quite different styles between the western and eastern areas.

The Turkish margin, characterized by a steep continental slope with numerous gullies, canyons and mass flows, is bordered by several small deep basins, i.e. from west to east, the Rhodes Basin, the Finike Basin and the Antalya Basin. The Rhodes and Finike Basin are believed to have opened in post-Messinian time, as indicated previously. This occurred as a transtensional phase dominated the eastern Hellenic Arc and the southeast Turkey due to a kinematic change following the initiation of tectonic escape of the Anatolian plate in Mid to Late Miocene time. The Rhodes Basin may even have opened as a pull-apart basin along the eastward continuation of the Pliny-Strabo trench system (Woodside *et al.* 2000) in response to arc-normal tensional forces and retreat of the trench, combined with the progressive increase in curvature of the arc (ten Veen and Postma 1999). Ten Veen and Kleinspehn (2002) have also demonstrated the continuation of the Hellenic forearc structures from onshore Rhodes into the Rhodes Basin with the same N020° and N070° oriented fault network. Seismic profiling shows that the larger and older Antalya Basin has a different internal structure. It is a 2.5 km deep

actively northward subsiding basin, bounded in the NE and NW by high angle extensional faults (Glover and Robertson 1998), that contains a thick Messinian salt layer.

As previously discussed, the two westernmost mountains are inferred to be tilted blocks rifted from southern Turkey. The Anaximander Mountain (Figure 5.3) represents a sharply asymmetrical seafloor high reaching 1250 m water depth with its summit forming an elongated ESE-WNW ridge along its southern margin. The southern and southeastern slopes of the mountain are steep escarpments (trending ESE-WNW and ENE-WSW respectively) with up to 15º dip and are bounded by faults. The northern slope dipping up to 4° towards the Turkish margin, is cut by shallow erosional valleys and gullies directed downslope. The Plio-Quaternary sedimentary cover on the top of the mountain passes gradually to heavy turbiditic sedimentation within the Finike basin that separates the Anaximander Mountains from the Turkish margin. The Anaximenes Mountain (Figure 5.3) has a similar asymmetrical shape but with higher relief, with water depths varying from about 2500 m to 680 m. It also has steeper northern and southern slopes, the northwest facing slope dipping up to 24º and the southeast slope up to 16°. In between Anaximander and Anaximenes, a large flow-like mass of sediments with almost semicircular lobes at the front has been referred to as the "Great Slide" (Figure 5.3). Its origin has already been discussed by Woodside *et al.* (1998), who inferred it to be made up of Pliocene to Recent sediments that collapsed from between the two mountains and flowed out mainly toward the Finike Basin, possibly triggered by the disassociation of gas hydrates.

In the southwestern part of the area, at about latitude N35º 10', lie a series of E-W elongated depressions (south of Rhodes Basin, southwest of Anaximander, and south of Anaximenes) that show gentle folds with highly variable trends. These depressions, which were in the past described as trenches (Rotstein and Kafka 1982), outline the boundary of the salt-bearing northern edge of the Mediterranean Ridge and Herodotus Basin. They may be associated with thrusting especially south of the Rhodes Basin (Woodside *et al*. 2000) and are probably related to superficial sediment motion.

Contrasting sharply with the pattern of deformation of the two western mountains, the Anaxagoras Mountain exhibits a very rough topography with a rather flat summit (Figure 5.6a). Its losangic shape suggests it is controlled by major faults. The relatively steep eastern flank, separating the summit plateau region of about 1200 m water depth from the Antalya Basin 1 km below, is rather linear with a NW-SE trend and is roughly parallel to the western flank. From north to south, the seamount can be subdivided into three main blocks, bounded by NE-SW scarps with a southward step-like decrease of relief. The northern part has the greatest relief rising up to 930 m water depth in the north-central part of the plateau. It is bounded to the south by a ridge extending southwestward towards Anaximenes. This ridge has a pronounced bathymetric expression with a vertical scarp of about 500m. It has been called the "Faulted Ridge" (Figure 5.6a and 5.6b; see also Figure 6.9) and was the subject of a Nautile dive during MEDINAUT(MEDINAUT/MEDINETH shipboard scientists 2000). Both southern parts of the seamount show slightly greater relief in their eastern region, bounded by NW-SE extending ridges. The southwestern part of the seamount merges with the Florence Rise further south.

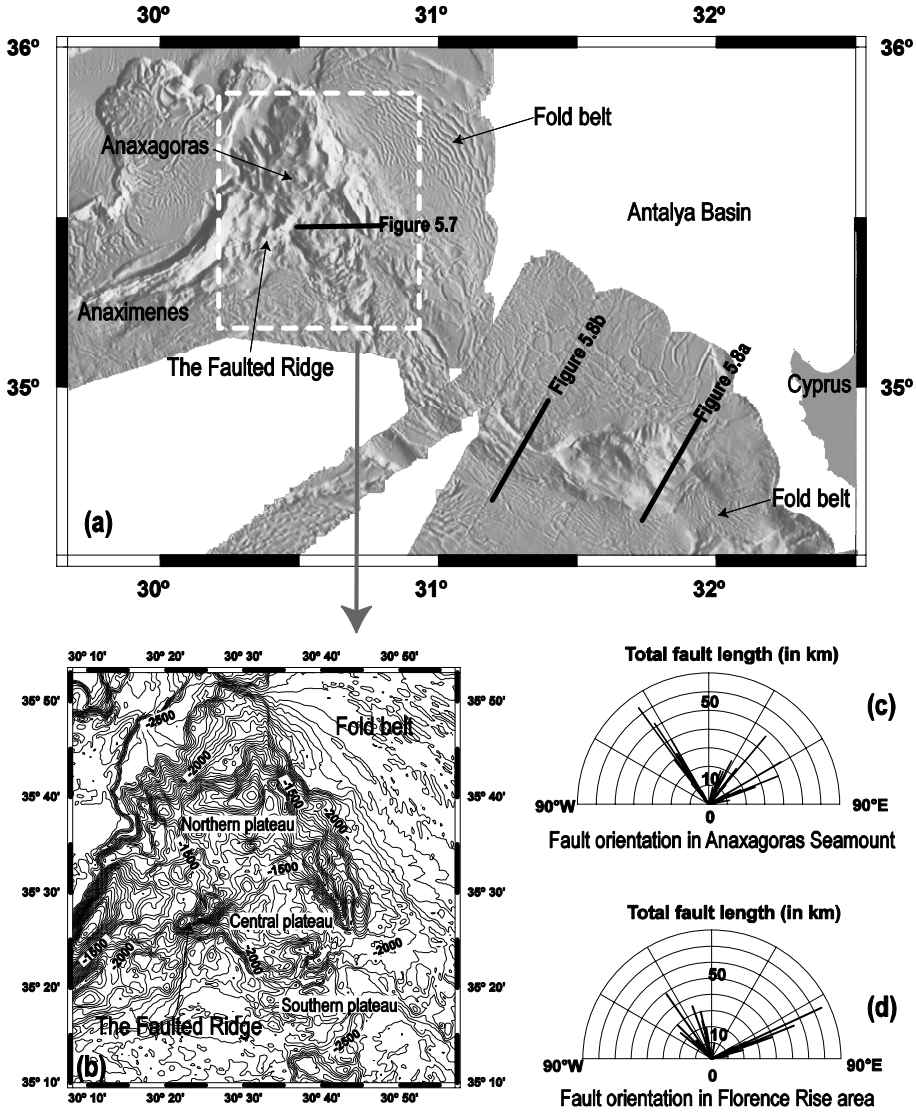

Figure 5.6: (a) Multibeam shaded bathymetry of the western branch of the Cyprus Arc (illumination N090°) from ANAXIPROBE 95 and PRISMED II data, illustrating the important fault network along the arc and the fold belt systems. See text for further explanation. (b) Detailed bathymetric map of the Anaxagoras Seamount (contour interval of 50 m) showing its peculiar angular form with NW-SE and NE-SW elongated ridges and scarps. These NW-SE scarps separate the seamount in three plateau-like areas with increase of the elevation northwards. (c) Rose diagram of fault trends in the Anaxagoras Seamount. (d) Rose diagram of fault trends in the Florence Rise area.

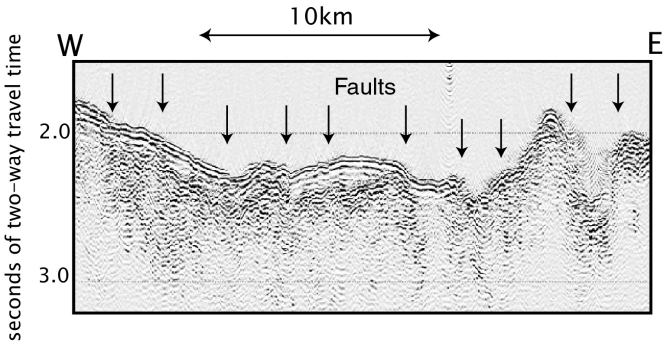

Figure 7: Seismic section across the Anaxagoras Seamount illustrating the high density of subvertical faulting. For location, see Figure 5.6.

The numerous linear ridges and scarps described over Anaxagoras indicate that the area is crosscut by a very dense network of faults which fall into two main families, one trending NW-SE and the other NE-SW (Figure 5.6c). A seismic section across Anaxagoras (Figure 5.7) attests to the high density of subvertical faulting. Although some of these faults display significant vertical offset, they are inferred, on the basis of both their seafloor expression on the multibeam mapping and their seismic expression, to be the result of dominant strike-slip faulting. In length, the faults with an orientation ranging from N140° to N150° are dominant and correspond to the general elongation of Anaxagoras (Figure 5.6b and 5.6c). The other main family of faults cuts across the seamount with a N060° to N070° orientation (Figure 5.6c). They appear to be the youngest ones since they are cut across the other features, especially the N140° faults family. These faults also show some continuity from Anaxagoras to Anaximenes, as in the case of Faulted Ridge, in spite of the different origin of the two seamounts, i.e. Bey-Dağları unit for Anaximenes and the Antalya nappes complex for Anaxagoras. Such lineament trends have also been observed in southwest Turkey cross-cutting the onshore boundary between the Bey-Dağları and Antalya complexes (Gutnic *et al.* 1979). N020° to N030° trending faults are also largely represented (Figure 5.6c), especially in the northwestern part of Anaxagoras seamount (see also Chapter 6). They may be the continuation of features recognized on-land, such as the Kemer lineaments, as well as offshore in the northern Antalya Basin (Glover and Robertson 1998). Within the Isparta Angle, N020° trending Pliocene extensional faults have been recognized (Glover and Robertson 1998) and such faults may be here reactivated in the strike-slip system. N040° trending faults also occur in this area (Figure 5.6c).

A regular arcuate fold belt in the Antalya Basin (Figure 5.6a), convex towards the northeast, indicates a limited amount of NE-SW compression. The wavelength and amplitude of the folds increase towards the northeast into the deeper part of the basin. The stress field is similar to that expected from a rigid block indenting plastic sedimentary material, i.e. the more rigid backstop of the Anaxagoras seamount indenting the Antalya Basin sediments, and suggests the northeast lateral motion of the Anaxagoras Seamount along the N070° faults.

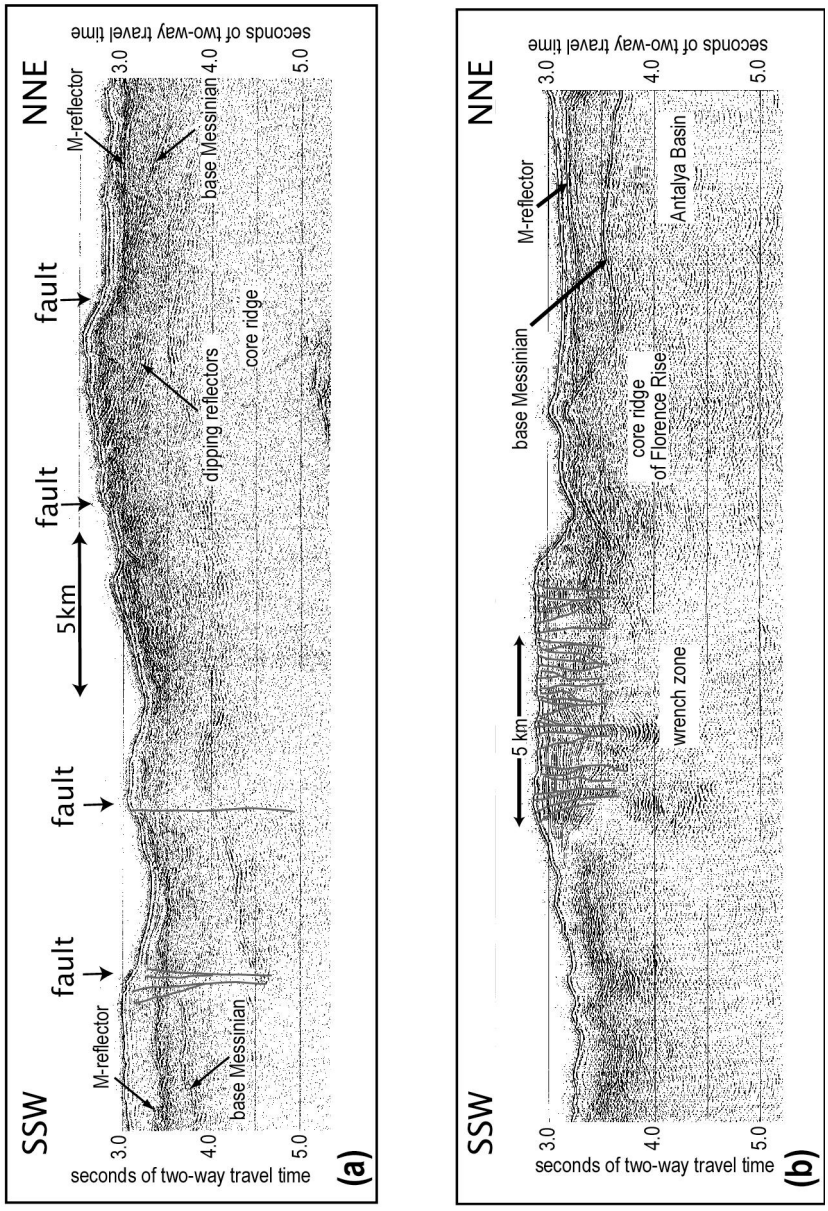

Figure 5.8: Seismic sections across (a) the eastern Florence Rise and (b) the western Florence Rise, see Figure 5.6 for location. These seismic sections illustrate the deepening westward of the core ridge of the Florence Rise, almost buried in its western part, and the pinching out of the Messinian evaporites to the north and the south of the Florence Rise. Subvertical faults mark the lineations observed on the multibeam map (see Figure 5.6) at the eastern end of the Rise and a typical transpressive flower structure can be observed on (b) corresponding to an area of high seafloor deformation (see Figure 5.6).

5.5. The western limb of the Cyprus Arc

Multibeam mapping of the western part of the Cyprus Arc, from both the 1995 ANAXIPROBE and 1998 PRISMED II expeditions, reveals that the Florence Rise structure and its associated deformation continue northwards in the eastern Anaximander Mountains, with the Anaxagoras Seamount forming its northwestern end. The structural continuity from Cyprus to Turkey is shown by the seafloor fabric as well as by the network of faulting (Figure 5.6a; see also Figure 6.1).

The Florence Rise consists of an arcuate feature with no real bathymetric expression except at its southeastern end where a structural block with an angular shape rises from Antalya Basin by about 600m (Figure 5.6a). This block shows a rhombohedral shape delimited by two major trends, roughly N130° and N070°. Figure 5.8a shows a seismic section crossing its inferred N130° faulted boundaries. These boundaries are near-vertical faults with a relief expression on the seafloor of about 0.2 s two-way travel time, or approximately 150 m, and are characterized by a complete loss of lateral continuity of the reflectors from the surface towards the deepest visible part of the section. They are inferred from the characteristics observed in the seismic profiles (e.g. flower structures) to be presently active shear faults. Directly south of the Florence Rise, seafloor deformation observed on multibeam maps displays a short wavelength arc-parallel linear fabric with the highest degree of surface deformation. On seismic sections (Figure 5.8b), this area displays subvertical faulting with anastomosing fault branches and positive flower structures affecting post-Messinian sediments (Woodside *et al.* 2002), and is believed to be the most active area of the region. This typical transpressive deformation is responsible for the construction of the relief (about 200 m) of the central part of the rise (between E30° 40' and E31° 20'). In contrast, the core of the rise (Figure 5.8) displays relatively low relief and appears on the seismic images as deepening towards the northwest. On the side of this core ridge, the Messinian evaporites pinch out (Figure 5.8), which implies that the Florence Rise was an existing positive topographic feature during Messinian time. The whole rise is now subsiding northward together with the Antalya Basin. The salt distribution indicates that the Florence Rise may have always been better expressed topographically near Cyprus.

Below the highest part of the rise some reflectors can be observed dipping northward on many profiles (Figure 5.8a), in some places slightly folded. Sage and Letouzey (1990) interpreted them as allochthonous ophiolitic nappes. However the relatively featureless magnetic anomalies suggest that there is no ophiolitic material below the Florence Rise. These structures could still be related to or similar to either the Mamonia Complex on Cyprus or the Antalya Nappes Complex, but without the ophiolite component. Another interpretation would be that they are part of the old buried accretionary prism (Robertson 1998b; Woodside *et al.* 2002). However, if thrusting has occurred in this area, it is limited to pre-Pliocene age rocks and is now crosscut by transcurrent faults.

The highest frequency of faulting observed along the Florence Rise is for the N070° trending faults (Figure 5.6d), recognized also within the Anaxagoras area, which show a well-defined orientation between N065° and N070°. A convex southwestward fold belt develops near the southeast end of the rise between the latitudes N34º 30' and N34º 40' (Figure 5.6a)

suggesting that some lateral motion occurs along this NE-SW direction. The NW-SE arc-parallel faulting is also widely represented (Figure 5.6) along the southeast Florence Rise; but, in contrast to further north, this trend shows more deviation, with the orientation ranging between N130° and N145° (Figure 5.6d). This could indicate counterclockwise rotation of the Florence Rise area with respect to the Anaxagoras seamount. Generally, the orientation of these arc-parallel faults tends to shift towards the southeastern part of the rise (towards Cyprus) from a roughly NW-SE direction to more E-W direction. This fault deviation could be due to the proximity of the rigid block formed by Cyprus and may denote the influence of the collision of Eratosthenes Seamount with Cyprus acting as an indenter. Secondary faulting can also be observed, such as N155°-N170° trending faults (Figure 5.6d), which may be related to the normal faults along the eastern side of the inner Isparta Angle and their continuation into the Antalya Basin i.e. the Çandır-Pınargözü-Ovacık trends (Glover and Robertson 1998) and/or to the faults bounding the Polis Graben on Cyprus (Payne and Robertson 1995) (Figure 5.3). N010°-N020° trending faults which are also present (Figure 5.6d) are best observed on the top of the highest part of the rise.

5.6. Discussion and conclusions

The tectonics of the eastern Mediterranean Sea changed drastically in Middle to Late Miocene time as relative plate motion between Africa and Eurasia shifted from N-S to more NE-SW (Le Pichon and Angelier 1979). This kinematic change followed the collision of the Arabian and African plates in eastern Turkey and in the Caucasus, which initiated the westward extrusion of the Anatolian-Aegean plate along the North Anatolian Fault, which probably formed in Late Miocene-Early Pliocene (~5 Ma) (Şengör *et al* 1985; Bozkurt 2001), and the East Anatolian Fault, also of Pliocene age (Şengör *et al* 1985; Bozkurt 2001). As a result, the Cyprus-Hellenic subduction zone evolved more distinctly into two separate arcs and extensional tectonics increased in the Aegean and western Turkey. The geometrical configuration of two highly arcuate subduction zones in the eastern Mediterranean Sea results in difficulties in accounting for plate convergence in the area between the two arcs.

The Hellenic and Cyprus Arcs are thus generally assumed to be connected through a cusp (McKenzie 1972; Nur and Ben Avraham 1978). But the plate geometry of this region is more complicated. As stressed in this paper as well as in previous studies (Rotstein and Kafka 1982), the continuity between the two arcs in the centre of the Levantine Basin is in disagreement with the low and scattered seismicity of this area. In contrast, the pattern of seismicity indicates continuity of the eastern branch of the Hellenic Arc into mainland Turkey along the Rhodes basin and the Burdur fault, where strong shallow earthquakes occur. This observation by itself is an evidence of the connection of both features, even though a left-lateral motion has not been proved along the Fethiye-Burdur fault. To the east, the Antalya basin, and the eastern boundary of the Isparta Angle are considerably more seismically active than the Levantine Basin.

Due to the lack of a seismically defined plate boundary in the Levantine Basin, some authors (Rotstein and Kafka 1982; Anastasakis and Kelling 1991) delimited it using morphological elements, following the northern outline of the Mediterranean Ridge i.e. from

west to east, the supposed continuation of the Strabo Trench through the southern part of the Rhodes Basin, small depressions southwest and south of the Anaximander Mountains, and along the Florence Rise. This interpretation was commonly accepted up to now, mainly as it shows some consistency with the delimitation of the plate boundary along the eastern Hellenic Arc, which is indeed outlined by the edge of the Mediterranean Ridge, along the Strabo/Pliny trenches and the Strabo Mountains. However, although the Strabo Mountains show some similarities with the Anaximander Mountains, this interpretation is not supported by our observations. The crustal discontinuity indicated by the gravity data, as well as the continuation of the Florence Rise structure within the eastern Anaximander Mountains towards Turkey, argue against the connection of the Strabo/Pliny trenches with the Florence Rise along the southern side of the Anaximander Mountains.

The small depressions observed south of the Anaximander Mountains are inferred to be related to the creeping of the Mediterranean Ridge sediments above the Messinian evaporite-bearing decollement (Chaumillon *et al.* 1996; Woodside *et al.* 2000) rather than reflecting present-day deep-seated tectonic processes. In that sense, they are the last remaining parts of a deep basin here which is in the process of being filled by the migrating Pliocene to recent sediments. In contrast, the Rhodes Basin is a rather new basin of post-Miocene age (Woodside *et al.* 2000); however, thrusting occurring at its southern boundary (Woodside *et al.* 2000) illustrates the gliding of these sedimentary nappes, probably facilitated by the contrast of rheology between areas where the Messinian evaporites are present and areas where they are absent.

Deep seismic events in the Gulf of Antalya and beneath Turkey have prompted some authors (McKenzie 1972; Ben Avraham *et al.* 1988) to suggest that a zone of subduction with a marked Benioff zone exists on the western branch of the Cyprus Arc. Still, deep events do not occur as expected, orthogonal to the supposed subduction zone but rather much further north. Moreover, fault plane solutions in the Antalya Basin indicate northward compression (Rotstein and Kafka 1982; Papazachos and Papaioannou 1999) instead of the northeast motion expected. Rotstein and Kafka (1982) underlined the complexity of the seismicity pattern in this area by identifying two sections with down-going seismic zones across the Antalya Bay: a SW-NE from offshore Cape Chelidonia to offshore Alanya and a NS section. A section orthogonal to the Florence Rise further south (e.g. 35°N) would show no deep seismicity. In addition, fault plane solutions for a cluster of earthquakes, including the M6.8 Cyprus earthquake on 9 October 1996, just west of Cyprus (Ardvisson *et al.* 1998; Papazachos and Papaioannou 1999) show unequivocally strike-slip motion. It is thus doubtful whether the northward dipping slab observed beneath the Antalya basin, could be associated with any supposed subduction below the western Cyprean Arc, at least not in its southern region.

The present study sheds light on two main questions posed at the beginning: about the style of deformation along the western branch of the Cyprus Arc and the location of the plate boundary at the junction between both Arcs. The present data show that no evidence of present-day thrusting is observed along the Anaxagoras-Florence Rise section. To the contrary most of deformation is interpreted to be the result of strike-slip faulting with a small amount of shortening (Figure 5.9). Rather than developing new faults, this on-going deformation could have reactivated existing thrusts, e.g. prior thrusts of the Florence Rise and normal faults, e.g.

the Kemer lineaments extending from the Isparta Angle seaward into the northeastern part of Anaxagoras Seamount, as predominantly strike-slip faults. This may make it difficult to fit the observed fault network into one single tectonic framework.

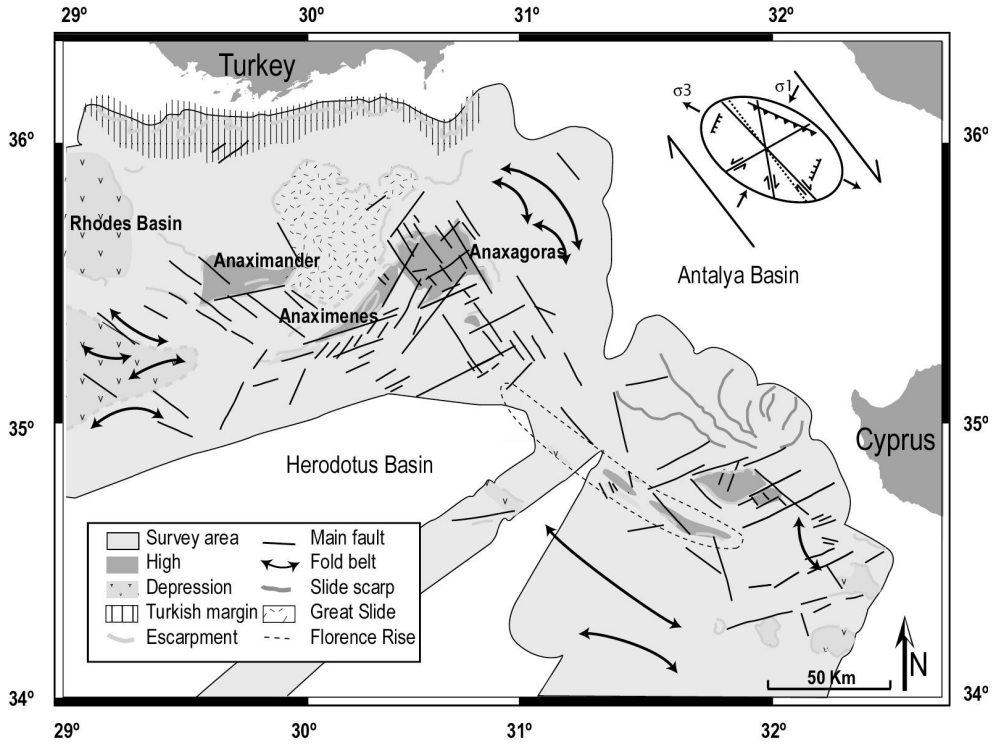

Figure 5.9: Simplified structural scheme of the study area, interpreted from multibeam bathymetry (Figure 5.3), backscatter and seismic profiling. The fault network along the western branch of the Cyprus Arc is inferred to be representative of a dextral wrenching along the arc, see text for further discussion.

An attempt has been made to describe this deformation as a northwest-southeast dextral wrench (Woodside *et al.* 2002). This interpretation is appealing since the assumed stress field would explain the main faulting observed as well as the secondary faulting, such as NS normal faulting (Figure 5.9). Moreover, as the Cyprus Arc is commonly believed to be an analogue of the Hellenic Arc (Rotstein and Kafka 1982), this would make the similarity between them more remarkable, with sinistral faulting along their eastern branches i.e. Strabo/Pliny versus Kyrenia/Larnaca/Latakia ridges (Ben Avraham *et al.* 1995; Vidal *et al.* 2000a, 2000b) and dextral faulting along their western branches. Some problems remain yet: the dextral shearing is inconsistent both with the dextral offset observed in the gravity data along the NE-SW faults (e.g. a sinistral offset is predicted by the model of Woodside *et al.* (2002) and with the fault plane solutions of the Cyprus earthquakes (Papazachos and Papaioannou 1999). However, Papazachos and Papaioannou (1999) did not know clearly the orientation of the fault and inferred a NNE-SSW fault (named by the authors the Paphos Fault)

on the basis of the alignment of earthquakes. Such a trend is not clear from the new multibeam data presented here and the same fault plane solution may accommodate a slip on another fault or zone of faulting, such as N130° trending faults recognized in the area.

A noteworthy point is that in this junction area it is plausible that the stress fields from both the eastern branch of the Hellenic Arc (sinistral wrenching) and the western branch of the Cyprus Arc (inferred dextral wrenching) interact (Figure 5.10) or have been dominant at different times in turn, thus causing this complex shear zone to comprise faults with opposite or mixed shear sense. Moreover, the fairly minor present-day relative motion along this zone, as implied by a pole of rotation located nearby to the south (NE of the Nile fan; Le Pichon *et al.* 1995) makes determination of the sense difficult, especially as it may change along strike (ten Veen *et al*. 2003) Understanding the onshore-offshore relationship may help to determine the deformation style in the area.

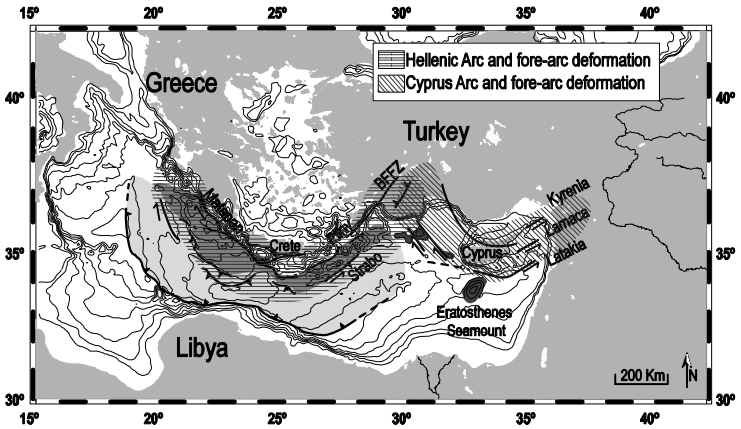

Figure 5.10: Synthesis and interpretation of the tectonics at the junction of Hellenic and Cyprus Arc. Tectonic symbols and abbreviations are as in figure 5.1.

Whether the sense of the shearing is dextral or sinistral, it is evident that plate interaction has widened into a broad zone of deformation dominated by strike-slip in the same fashion as the eastern branch of the Cyprus Arc (Figure 5.10). It is likely that subduction in the area slowed down or stopped as a result of the collision of the Eratosthenes Seamount with Cyprus (Robertson 1998a, 1998b). The Eratosthenes Seamount could have arrived at the Cyprus margin by the late Miocene time and forceful collision is dated from Late Pliocene time (Robertson 1998a). The resulting blockage of the subduction, coupled with the initiation of lateral escape of Anatolia in Late Miocene-Early Pliocene time, may have forced the Cyprean Arc to evolve from compression to a transpressive wrenching system along the arc to the west and east (Figure 5.9). The end of active subduction in the area may be coeval with the Late Miocene compressional Aksu phase and the remaining and likely detached slab, as proposed by Rotstein and Kafka (1982), is hanging beneath the Antalya Bay, eventually displaced northward by the strike-slip faulting. The continuous shearing deformation along the western branch of the Cyprus Arc and across it, with the later developed transverse NE-SW faulting, suggests strong coupling between both sides of the Arc (Figure 5.9). In that view, the plate

boundary between SW Anatolia and Africa is more or less sutured. As the incipient collision occurs, coupling of tectonic process off and onshore increases, and the plate boundary eventually penetrates into Turkey.

An important result is that the connection between the Hellenic Arc and the Cyprus Arc does not occur in the Anaximander Mountains but inland in southwest Turkey, and thus the Isparta Angle is a full component of the Cyprus Arc deformation.

Acknowledgments

This paper is based on a presentation at the 4th International Symposium on Eastern Mediterranean Sea Geology in Isparta (Turkey) and benefits from the numerous discussions that took place there. We are grateful to the Ifremer/Genavir crew and technical team of the R/V L'Atalante for their involvement during the ANAXIPROBE and PRISMED II expeditions and to the crew and technical team of R/V Gelendzhik for their involvement during the Training Through Research expeditions. J.H. ten Veen provided constructive comments that contributed to improvement of an early version of this paper. We thank the referees, as well as A.H.F. Robertson, for their critical and helpful reviews. Financial support was obtained through NWO 750.195.02 and 809.63.011 projects, respectively ANAXIPROBE and MEDISED. This paper is contribution number 20020203 of the Netherlands Research School of Sedimentary Geology (NSG) and contribution number 426 of Géosciences-Azur CNRS UMR N° 6526.

Chapter 6. Tectonic control on mud volcanoes and fluid seeps in the Anaximander Mountains

6.1. Introduction

In the eastern Mediterranean Sea, the Anaximander Mountains are pronounced topographic seamounts lying offshore southern Turkey, between the Rhodes Basin and the Antalya Basin (Figure 3.2). Their location, at the intersection of the Hellenic and Cyprus Arcs, suggests them to be a product of complicated tectonic interaction in the Eastern Mediterranean Sea, as described in Chapter 5. In this specific area, as well as many other areas of the eastern Mediterranean Sea, the intense tectonic activity appears to be closely associated with the mobilization of recent sediments, mud volcanism, release of methane and the development of chemosynthetic benthic communities, in association with authigenic carbonate crusts (Camerlenghi *et al*. 1995; Woodside *et al*. 1998; Huguen 2001).

Tectonic control on mud volcanism has been often discussed in the literature (Barber *et al*. 1986; Brown and Westbrook 1988; Reed *et al*. 1990; Hieke *et al*. 1996; Faugères *et al*. 1997; Robertson *et al*. 1998; and many others). Mud volcanoes are mainly composed of material originating from stratigraphic units older than their depositional environment and therefore need conduits to rise from deeper levels to the seafloor. The best candidates for facilitating mud emplacement and expulsion of fluids are thus deep-seated faults and fractures. However, the relationship between different types of faulting and mechanisms of mud extrusion and the distribution of mud volcanoes is not clearly established. In the compressive context, e.g. accretionary prism, it is inferred that the principal mechanism responsible for mud volcanoes is lateral shortening (Limonov *et al*. 1996), and that they are therefore linked with thrusts and backthrusts. Tectonic models of the Mediterranean Ridge involve the emplacement of the mud along backthrusts, either extruded from the decollement level (Camerlenghi *et al*. 1995), or squeezed from higher levels in the accretionary wedge (Robertson and Kopf 1998b). The significance of extension and strike-slip for the extrusion of mud within compressive environments is less well known but was discussed with respect to mud volcanoes in Indonesia (Barber *et al*. 1986), Barbados (Faugeres *et al*. 1997; Sumner and Westbrook 2001), the Carribean Colombian margin (Vernette *et al*. 1992), and the Alboran Sea (Perez-Belzuz *et al*. 1997).

This Chapter examines the interaction of mud volcanism with structural elements in the Anaximander Mountains. The regional structural pattern is observed in the EM12D multibeam imagery and bathymetry data, in combination with seismic profiles. In this area, the interplay of compression, shearing, and extension is an ideal target of studies to evaluate the extrusion mechanisms of mud volcanoes. The importance of the different types of faults is determined through a directional analysis based on high-resolution sidescan sonar observations and interpreted in the light of the structural analysis conducted by ten Veen and co-authors (2003), summarised hereafter. Seafloor evidence for a clear connection between tectonic features and seeping areas is also investigated using sidescan sonar and submersible

observations. These observations are focused on several mud volcanoes (MV) and cold seeps of the Anaximander Mountains and nearby areas (Florence Rise): Amsterdam MV, Kazan MV, Kula MV, Saint Ouen l'Aumône MV, Tuzlukush MV, Texel MV, and seeps along and through a fault escarpment named the Faulted Ridge.

6.2. Structural framework

The Anaximander Mountains are a complex of three distinct seamounts (i.e. Anaximander in the west, Anaximenes in the south and Anaxagoras in the east; Figure 3.2) rising more than 2000 m above the surrounding sea floor. They form a zone of tectonic accommodation between the active deformation in southwestern Turkey and the Aegean, and the tectonically quieter Cyprus and Florence Rise region (Zitter *et al.* 2003). Sampling and dredging from the joint ANAXIPROBE-TTR6 expedition have proved the mountains to be crustal blocks rifted away from southern Turkey (Woodside *et al.* 1997a), with samples from basement rocks showing an affinity with the Taurus Mountains. The two westernmost mountains (Anaximander and Anaximenes) are related to the Bey Dağlari and Susuz-Dağ carbonate platforms, that form a wide anticline structure onshore (Poisson 1977; Gutnic *et al*. 1979), whereas Anaxagoras is related to the Antalya nappes Complex (Gutnic *et al.* 1979; Robertson and Woodcock 1980; Woodside *et al.* 1997a; ten Veen *et al.* 2003). The contrasting geology of the different seamounts is partly responsible for their strong morphological differences (Figure 3.2).

Recent multibeam swath mapping and seismic profiling have provided essential new information about the prevailing strain pattern in the Anaximander Mountains (Figures 3.2 and 6.1) and along the western branch of the Cyprus Arc (Woodside *et al.* 2002; Zitter *et al.* 2003; ten Veen *et al*. 2003; see Chapter 5). The Anaximander Mountains area has been undergoing complex multiphase deformation (ten Veen *et al*. 2003) in its neotectonic development. Active faults have been recognized from their expression in imagery and bathymetry (linear features with contrasting backscatter and offsetting of the bathymetric contours) as well as their extension in the deeper section observed from seismic profiling (see Chapter 5).

During the Late Miocene, crustal extension created N120°-oriented grabens which developed into a vast subaerial to shallow marine area comprising the southern Aegean (ten Veen and Postma 1999), Rhodes (ten Veen and Kleinspehn 2002) and the present-day Anaximander Mountains (ten Veen *et al.* 2003). In the northwestern part of the Anaximander Mountains, these N120° faults are now structuring the Turkish continental slope (ten Veen *et al.* 2003). The Miocene-Pliocene transition marked a kinematic change within the southern Aegean region partly related to the lateral extrusion of Anatolia (McKenzie 1972; Le Pichon *et al*. 1995). Subsequently, the Anaximander Mountains area as well as the adjacent Rhodes Basin was affected by strong post-Miocene differential subsidence (Woodside *et al.* 2000; ten Veen *et al*. 2003; Zitter *et al*. 2003), as proved by the absence of Messinian evaporites throughout the area, and the unconformably overlying Pliocene sediments.

From Pliocene to present, a second phase of deformation has been active, which raised transtensional stresses in the western Anaximander Mountains but more transpressional tectonics in the eastern Anaximander Mountains (ten Veen *et al.* 2003). Since Late Pliocene,

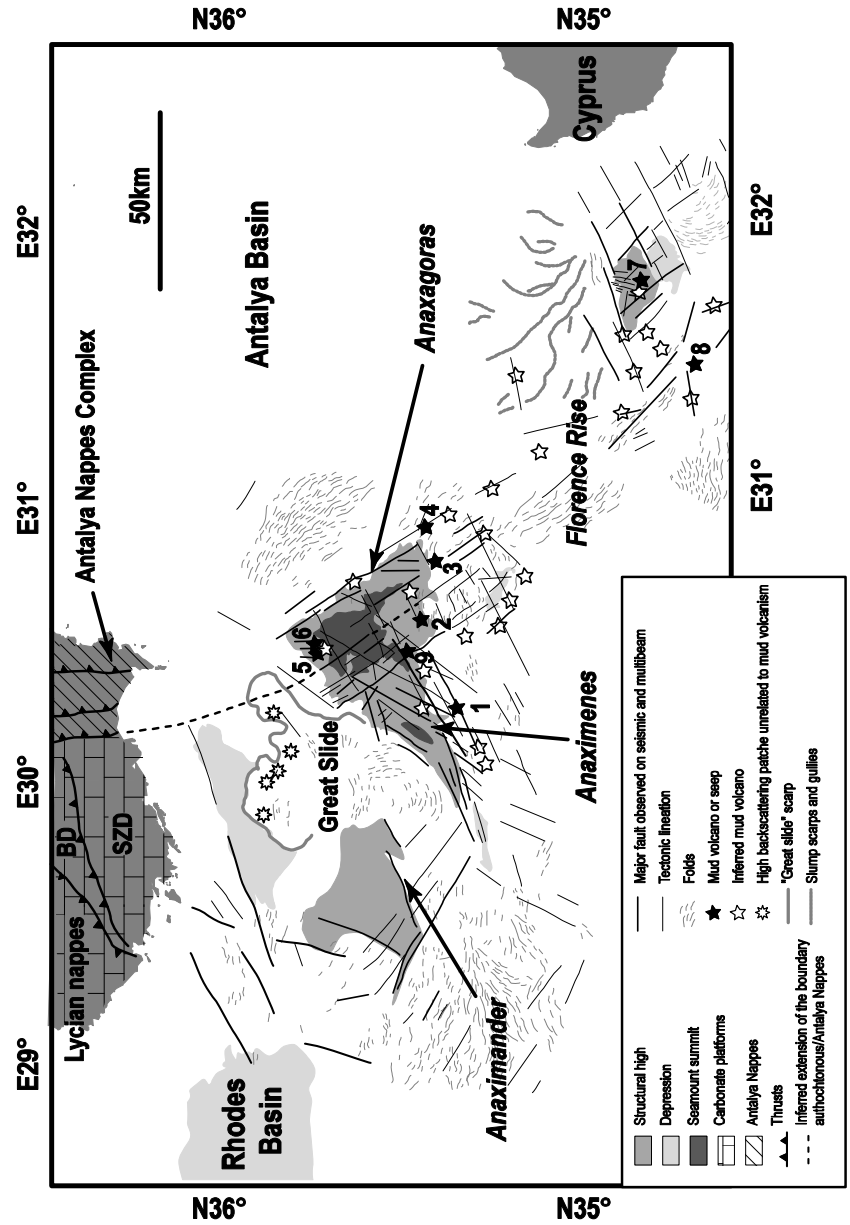

Figure 6.1: Structural scheme of the study area, interpreted from multibeam bathymetry, imagery, and seismic profiling, showing the main faulting, the mud volcanoes and cold seep areas (1: Amsterdam MV, 2: Kazan MV, 3: Tuzlukush MV, 4: St Ouen l'Aumône MV, 5: Kula MV, 6: San Remo MV, 7: Texel MV, 8: Harderwijk MV, 9: Faulted Ridge) and the high backscatter patches inferred to relate to mud volcanism activity (white stars).

this deformation phase is dominated by the development of N070°-trending sinistral strike-slip fault zones along the western branch of the Hellenic Arc, in the Rhodes Basin and in the western Anaximander Mountains (ten Veen *et al.* 2003). In the western part of the Anaximander Mountains, the onset of the N070° shear was marked by large N020° normal faulting in early Pliocene, and is followed by N120° dextral strike-slip in late Pliocene (ten Veen *et al.* 2003). To the contrary, the eastern part of the Anaximander Mountains is characterized by normal and/or normal oblique at reactivated N150° thrusts (Zitter *et al.* 2003, ten Veen *et al.* 2003). Although the N070° strike-slip faults unquestionably penetrate largely into the Anaxagoras domain (eastern Anaximander), their lateral slip appears to diminish eastward (ten Veen *et al.* 2003). Large-scale N020° extension-related structures are absent in the eastern domain but short N-S extensional faults occur segmented by N150° faults and are probably associated with them (ten Veen *et al.* 2003).

From a morphological point of view, the Anaxagoras Seamount forms the continuation of the Florence Rise, which together form the western limb of the Cyprus Arc (Woodside *et al.* 2002; Zitter *et al.* 2003; see Chapter 5). The Cyprus Arc is an arcuate feature strongly dominated, bounded, and transected by active N150° and N070° faults (Figure 6.1). Increasing relief northwestward in steps defined by the N070° fault scarps suggest normal component along these faults. Along the Florence Rise structure, N150° faults are characterized on the seismic profiles by anastomosing sub-vertical patterns and pop-up structures, indicating shear stresses (Woodside *et al.* 2002; Zitter *et al.* 2003).

6.3. Distribution of mud volcanoes deposits

6.3.1. Structural distribution

The mud volcanoes are identified on the EM12D multibeam acoustic data as high backscattering patches (Volgin and Woodside 1996; see also Chapter 3), associated with subcircular positive relief in the multibeam bathymetry (Figure 6.2). From these data, more than 30 mud volcanoes were inferred (Figure 6.1) over the Anaximander Mountains and its southeastern continuation, the Florence Rise. They are especially concentrated over the Anaxagoras Seamount and south of Anaximenes (Figure 6.1). Many of them appear lineated along either the N150° faults or the N070° crosscutting faults, or are located at the intersection of several faults.

Six mud volcanoes (numbered 1 to 6 in Figure 6.1) were the targets for numerous surveys (see Chapter 3). The largest, Amsterdam MV, is up to 3 km across (see Chapter 3) with high backscattering mud flows to the south covering an area of more than 50 km^2. It is located on the southeastern flank of Anaximenes Seamount, along a N070°-trending fault zone (Figure 6.1). This fault zone has a pronounced morphological expression in the multibeam bathymetry and merges to the northeast with one of the major scarps shaping the Anaxagoras Seamount (Figure 6.2). This scarp, named the Faulted Ridge (Woodside *et al*. 1997a), has a vertical offset of more than 500 m. On the basis of high backscattering in the sonar imagery and acoustic wipeout, it was identified as a potential dredging target during ANAXIPROBE because of the

likely presence of outcropping basement rocks. Dredging there during the TTR6-ANAXIPROBE cruise actually recovered basement rocks as well as some tubeworms and a Nautile dive confirmed the existence of numerous seeps along this scarp (number 9 in Figure 6.1). Eastwards, the mud volcanoes of the southeastern part of Anaxagoras, i.e. Kazan MV, Tuzlukush MV and Saint Ouen l'Aumône MV,are located at the intersection of the major N150° and N070° strike-slip faults. To the north, Kula MV and San Remo MV are sited at the northern end of the Anaxagoras Seamount, in an area dominated by short N-S oriented normal faults. Several small domes are clustered on a small plateau there (Figure 6.2)

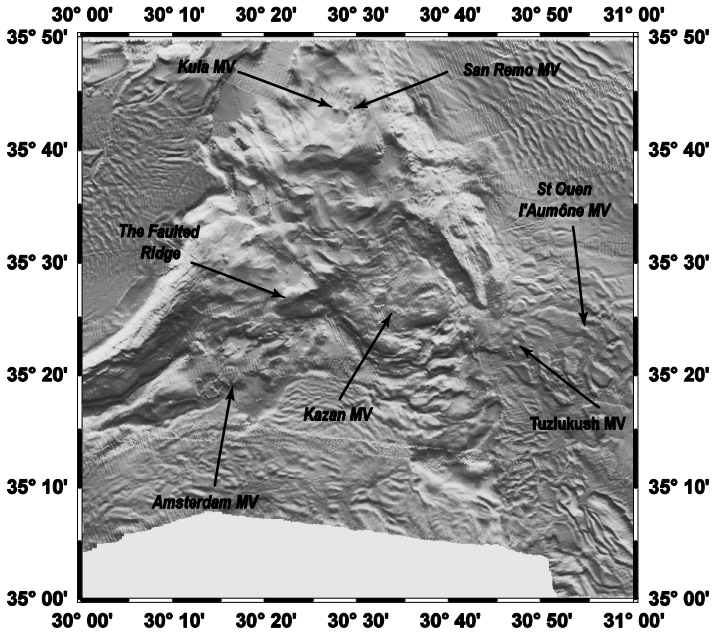

Figure 6.2: Multibeam shaded bathymetry of the Anaxagoras Seamount (Illumination N090°) with the location of the mud volcanoes.

Within the Florence Rise area, the mud volcanoes appear also associated with the main transcurrent system (Figure 6.1). Two of them were sampled on the Florence Rise during the MEDINETH cruise in 1999 (numbers 7 and 8 in Figure 6.1). Texel MV is situated on a plateau at the top of the highest part of the Florence Rise, together with one other small rounded dome inferred to be a mud volcano. This high is an angular block bounded by N150° and N070° faults, referred to as the DSDP block (Woodside *et al*. 2002), because of DSDP drillholes there (Hsü *et al*. 1978). However, Texel MV appears to be more closely related to short N-S normal faults transecting the summit of the block, in a similar fashion to Kula MV and San Remo MV in Anaxagoras Seamount. Harderwijk MV is situated in a small depression at the interaction of two strike-slip faults trending N070°and N135°.

No mud volcanoes have been found in the western domain of the Anaximander Mountains. The Anaximander Seamount and the Anaximenes Seamount are also strongly

tectonized blocks rifted from south Turkey but structural pattern and the inferred stress field there are completely different compared to the eastern domain (ten Veen *et al*. 2003; see Chapter 5).

6.3.2. Geological distribution

Geological units exposed in southern Turkey are inferred to extend seaward buried under the hemipelagic Plio-Quaternary cover. From the observation of seismic facies combined with sampling and dredging results, the continuation of the boundary between the Antalya Nappes Complex and the autochthonous limestones (Susuz-Dağ and Bey Dağları) can be followed southward through the Anaxagoras Seamount (ten Veen *et al*. 2003; Figure 6.1). The variation of clast lithologies within the mud breccia of the Anaximander Mountains mud volcanoes indicates that the erupted material is going through different lithological units during the mud ascension. Kula and San Remo MVs are situated above the extension of the Antalya Nappes Complex, because their erupted mud breccia contains some ophiolitic-derived clasts, gathered during mud ascension through the ophiolite bearing allochthonous units. In Kula mud breccia, some limestones, sandstones, cherts, serpentines and serpentinized peridotite were recovered (Woodside *et al.* 1997a). There, some clasts exhibit a dense network of fractures with calcite recrystallisation, and are dated as Campanian from nannofossils analysis (Huguen *et al*. 2001a). Cross-cutting veinlets and calcite joints observed on the surface of the clasts are inferred to indicate the hydrofracturing that formed with the release of pressure during mud volcanic eruption (Robertson and Kopf 1998a). In San Remo mud breccia, red and green cherts were recovered as well (Woodside *et al.* 1997a). In contrast, the clasts from Amsterdam and Kazan mud breccia show an affinity with the typical succession of the Bey-Dağları Massif (Woodside *et al.* 1997a). Amsterdam clasts include detrital limestones, siltstones and sandstones and black claystones and marlstones, attributed to a Middle Miocene (Serravalian) flysch and Eocene neritic limestones (Woodside *et al.* 1997a, 1998). Clasts from Kazan MV show similar lithologies but with ages as old as Maastrichtien (Huguen *et al*. 2001a). Dredging on the Faulted Ridge also recovered similar lithologies with the predominance of dark marlstones (Woodside *et al*. 1997a). Tuzlukush and Saint Ouen l'Aumône mud flows contain clasts of limestones, sandstones, siltstones, claystones and specific rocks described as volcanic rock fragments (Woodside *et al.* 1997a); thus it is still unclear whether the Antalya Nappes Complex extend as far south as these mud volcanoes.

6.4. Morpho-tectonic analysis from deep-tow sidescan records

On deep-tow sidescan records, many linear features can be detected, often associated with shadows that reflect small-scale relief on seafloor or enhanced backscatter indicating scarps or inhomogenities of the insonified surface (Figures 6.3 and 6.11b). The enhanced backscatter could also be caused by the cementation of sediments by Mg-calcite within cracks and fractures (Hieke *et al.* 1996). The features may show a morphological expression on the seafloor, with scarps and small steps, associated with a hyperbolic acoustic facies on the subbottom profiler (SBP). Although the SBP cannot resolve the continuation of these features at depth, they can be interpreted as an expression of fault deformation on the basis of analogy

with features seen on both EM12D acoustic imagery and seismic profiles, and because they show a good correlation with the main regional fault directions.

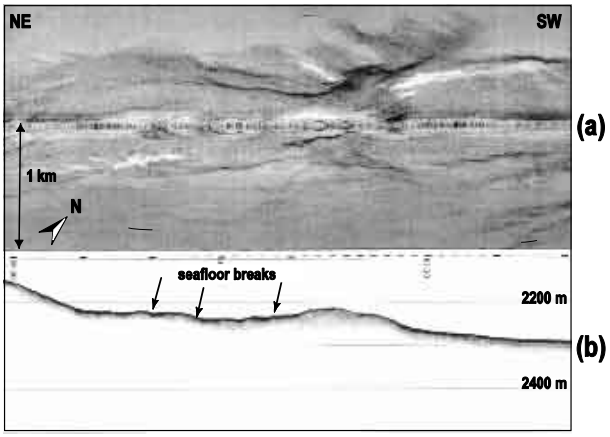

Figure 6.3: Sidescan sonar image (a) and subbottom profiler record (b) of a section of line MNLDT06 south of Anaximenes Seamount illustrating the signature of the faults on sonar records.

The lineaments observed on the sidescan sonar records were mapped in the vicinity of, and across the different mud volcanoes. Across Amsterdam MV, they were mapped on a section of line MAK46 and along the O.R.E.Tech sonar lines MNLDT04, and MNLDT06, respectively running to the north and to the west of the mud volcano (Figure 3.4). They were mapped along line MNLDT05 for Kula MV. For Kazan MV, Saint Ouen l'Aumône MV and Tuzlukush MV, they were also mapped from sections of line MAK46. The lengths of all the mapped lineaments trending in the same direction (+/-1°) for each mud volcano are summed and plotted on rose diagrams (Figure 6.4).

From the deep-tow sonar records running across Amsterdam Mud Volcano, the largest diversity of faults is observed (Figures 6.4a and 6.5). However, three groups of azimuths appear to be prevalent: around N060°, between N120° and N150° and between N020° and N050° (Figure 6.4a). The area surrounding Kazan MV also shows a large spread of fault azimuths (Figure 6.4b). This probably arises from the position of Amsterdam and Kazan at the intersection of major faulting between the Anaximenes and the Anaxagoras seamounts. For Kazan MV, the most important fault-trend corresponds to one of the large-scale regional fault directions observed in the multibeam analysis, namely N070°. Additionally, several other trends are significant: N050-060°, N090°, N110-120°, and N150°. Around Saint Ouen l'Aumône MV, the dominant N060-N070° trend is observed for faults cutting right through the summit of the dome (Figures 6.4d and 6.6). Another family of faults, trending N135°, delimite a zone of surficial folding on the southeastern side of the volcano. N110-120° faults have been mapped as well. The area surrounding Tuzlukush MV also presents the two fault directions already recognized in most sidescan sonar records: N050-070° and N120-130° (Figures 6.4c and 6.7). Along O.R.E.Tech line MNLDT05, the N-S to N010°-trending faults are often observed at Kula MV, (Figure 6.4e). Such faults are associated with vertical displacements of a

MV	Faults observed on EM12D	Sonar line	Fault observed on sonar	Signification into regional tectonics (ten Veen *et al.* 2003)
Amsterdam	N070° N020°-030°	MNLDT04 MNLDT06 MAK1-46	N060-070º N120º N020-030º N140-150º N040-055º N-S N090º	▪ N070° sinistral strike-slip ▪ N120° dextral transtensiona ▪ N020° normal faults ▪ N150° oblique faults ▪ N050° synthetic shear
Kazan	N070°	MAK1-46	N050-060º N070º N110-120º N150º N090º	▪ N050° synthetic shear ▪ N070° sinistral strike-slip ▪ N120° dextral transtensional ▪ N150° oblique faults
Tuzuklush	N070° N150°	MAK1-46	N070º N050-060º N120-130º	▪ N070° sinistral strike-slip ▪ N050° synthetic shear
Saint Ouen l'Aumône	N150° N070°	MAK1-46	N060-070º N110-120º N135-150º	▪ N070° sinistral strike-slip ▪ N120° dextral transtensional ▪ N150° oblique faults
Kula	N-S	MNLDT05	N-S N040-060º N090º N150°	▪ N-S normal faults ▪ N050° synthetic shear

Table 6.1**:** Fault directions mapped along the sonar lines in the surroundings of the different mud structures.

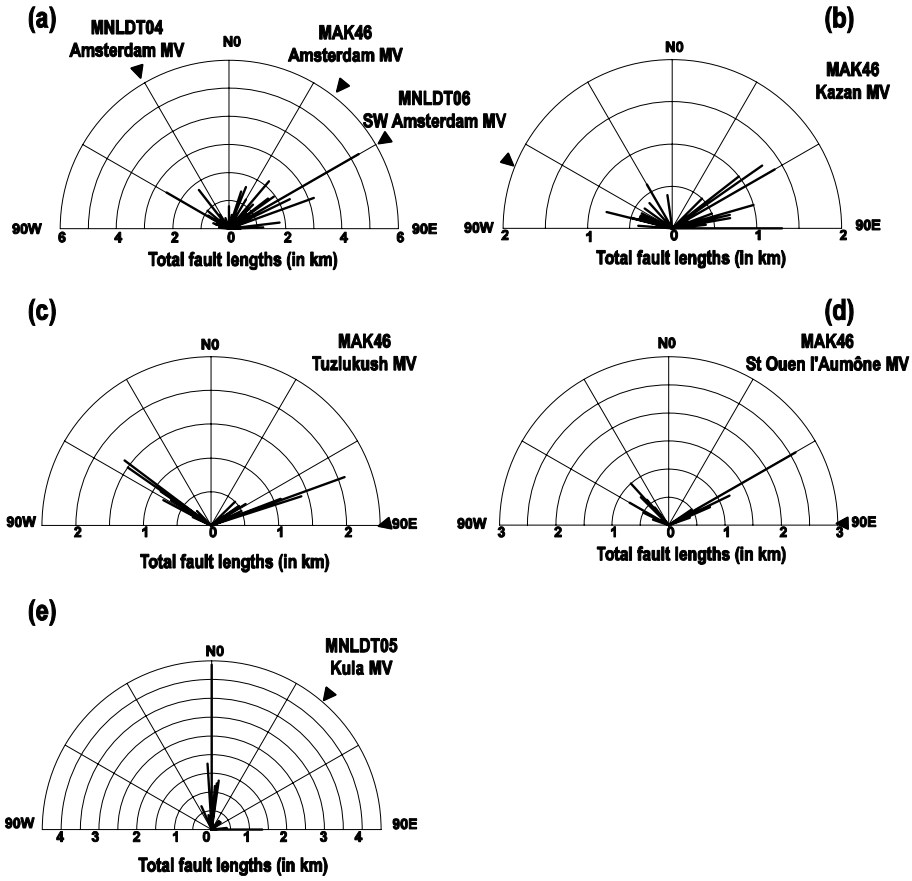

Figure 6.4: Directional analysis of the lineaments observed (a) across and in the vicinity of Amsterdam MV from O.R.E.Tech sonar line MNLDT04, O.R.E.Tech sonar line MNLDT06, and MAK1 line 46; along sections of MAK line 46 across (b) Kazan MV, (c) Tuzlukush MV, and (d) St Ouen l'Aumône MV; and (e) along O.R.E.Tech sonar line MNLDT05 crossing Kula MV. The black triangles indicate the orientation of the sonar lines.

few meters (up to 8 m) on the profiler record (Figure 6.8). The N040-N060° faults occur less significantly, apparently restricted to small lineaments in the area close to Kula MV. Some E-W trending faults have also been mapped all along this profile.

In the next section, we try to fit the morphotectonic directions into the larger regional tectonic setting (ten Veen *et al.* 2003; Zitter *et al.* 2003; Table 6.1):

(1) The most important trend observed in connection with the mud volcanoes is related to the N060-070° sinistral strike-slip faults. They were recognized on all the deep-tow

records, even though not always with the same significance (Figure 6.3), and appear thus as the preferential path for mud extrusion.

(2) Another important family of faults observed in relationship with mud volcanism trends N120°. They are best expressed in the southern part of the Anaxagoras seamount, especially at the junction of Anaxagoras with Anaximenes and therefore could relate to the major dextral transtensional faults that develop in the western part of the Anaximander Mountains and penetrates eastward. The large variety of trends associated with mud volcanoes in this area, mainly Amsterdam MV and Kazan MV (Figure 6.4a and 6.4b), suggests a complex deformation at the intersection of the different western and eastern stress fields.

(3) A third trend, often observed in connection with the mud volcanoes, is N040-050°; these faults could correspond to synthetic faults (R-shear) associated with the inferred N070° sinistral strike-slip faults.

(4) The N150° faults are less often observed on the deep tow records, as seen along line MNLDT05 running across Kula MV, or SW of Amsterdam MV, on line MNLDT06. They may be more difficult to see, as they relate to prior thrusting, i.e. the last emplacement phase of the Antalya Nappes Complex (Poisson 1977; ten Veen *et al.* 2003). However, these faults are presently reactivated as normal/transcurrent faults, and have a clear expression in both the multibeam bathymetry and imagery (Figure 6.2). At a regional scale, they appear determinant for the occurrence of mud volcanoes in the area.

(5) N-S to N010°-oriented faults are of less importance with respect to all the mud volcanoes, but they are worth noting because they are the dominant faults associated to the emplacement of Kula MV in the north of Anaxagoras. They show significant normal offset on the SBP, and are inferred to be secondary faults related to the N150° oblique faulting.

(6) Large-scale N020° normal faults, occurring in the western Anaximander domain, are only observed in connection with Amsterdam MV.

(7) Although thrust tectonics is inferred to occur in the area, thrusts do not seem to be linked with mud volcanoes and may only be restricted to the small N090° faults observed in connection with some of the mud domes (e.g. Kazan, Kula MVs).

6.5. Seafloor evidence for tectonic control on mud volcanoes

6.5.1. Mud flows

Mud flows are often emplaced along tectonic lineaments (Mascle *et al*. 1999; Kopf *et al.* 2001). The mud breccia may fill the faults and fractures, and the resulting backscatter enhancement makes them easier to distinguish on sidescan sonar data. Kula MV is the best example of such tectonically driven mud emplacement (Figure 6.8) because a network of crosscutting high backscatter lineaments can be observed on the deep-tow record on the top of this mud volcano. These lineaments, associated with small steps on the seafloor, are inferred to be faults. They control the repartition of the high backscattering patches, and are thus inferred to channel the extrusion and flow of the mud breccia. They act as pathways for mud ejection as

well as for the release of fluids and gases. The injected mud flows along faults can also be observed on Texel MV, e.g. near the western termination of a high backscattering tongue-shape mud flow, a 1 km-long narrow high backscattering lineament suggests that the mud breccia is filling up a fault (Figure 6.9). On Saint Ouen l'Aumône MV, several high backscattering spots are lineated along a N085° direction suggesting tectonic emplacement of the mud flows as well (Figure 6.6).

Tectonic control on mud flow emplacement is best observed on mud volcanoes displaying weak and/or limited areas of backscattering. It is probable that massive and recently extruded mud flows have the tendency to cover and attenuate the visibility of deep-seated faults. However, some relationship between faults and mud flows can be observed around Amstredam MV (Figure 6.4). On the southeastern side of the mud volcano, the direction of the mud flow inferred from the small lineaments mapped at the surface of the flow (②on Figure 6.5) is controlled by the slope which in turn is structured by N150° faults (① in Figure 6.5).

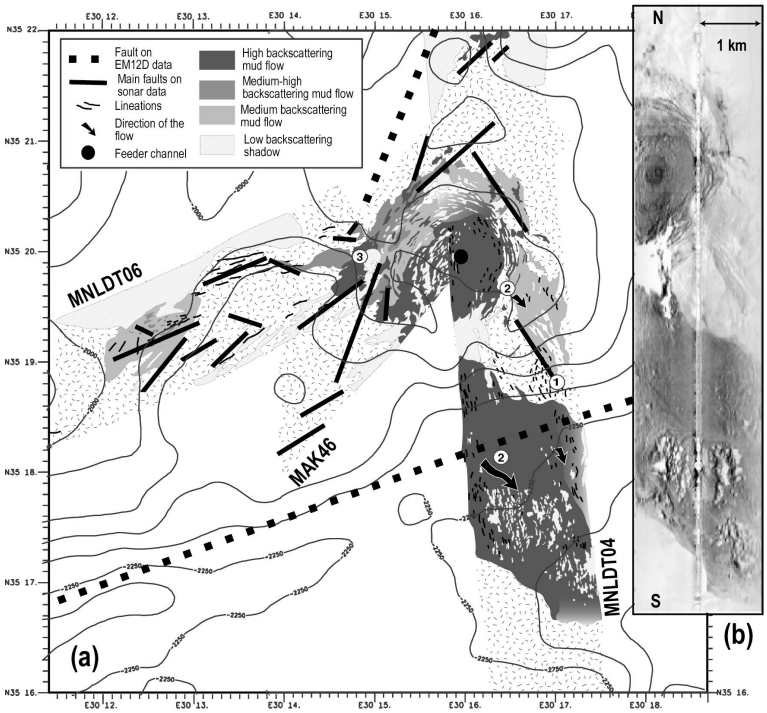

Figure 6.5: (a) Map of Amsterdam MV and its surroundings, with the interpreted mud flows and tectonic lineations observed from the sidescan sonar, superimposed on multibeam bathymetry with the major regional faults mapped from EM12D data. Note the relationship between the faults ①, the mud flows and the structuration of the slope ②, or the tectonically controlled eruptive parasitic centre ③. (b) Sidescan sonar record of part of ORETech line MNLDT04 showing the mud flow and the eastern side of the summit of Amsterdam MV. Note the very high backscattering dark patch of the feeder channel.

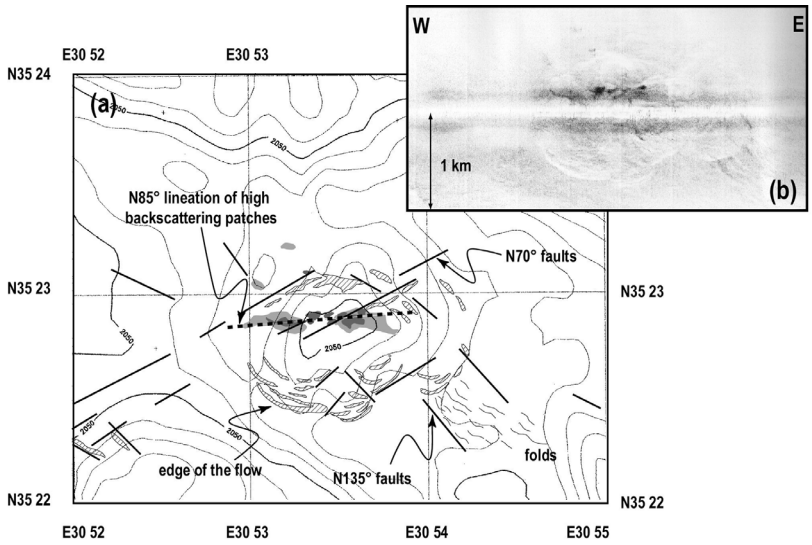

Figure 6.6: (a) Multibeam bathymetric map of Saint Ouen l'Aumône Mud Volcano with interpreted faults (lines), folds, high backscattering patches (grey scale) and acoustic shadows (hatches) outlining the edge of the old mud flows. For legend, see Figure 6.5. (b) Corresponding sidescan record.

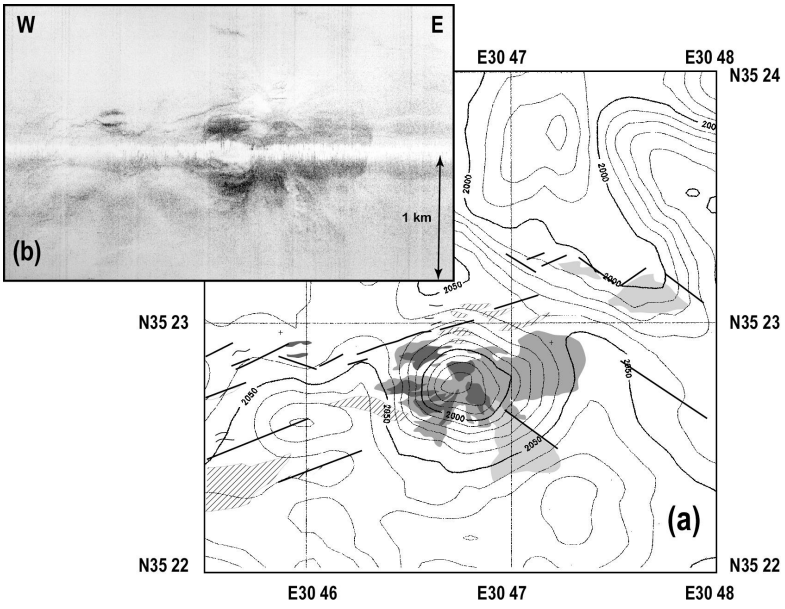

Figure 6.7: (a) Multibeam bathymetric map of Tuzlukush Mud Volcano with the interpretation from the sidescan sonar record (b). The line represent tectonic lineations, and the different patterns indicate different mud flows (grey scale) and acoustic shadows (hatch). For legend, see Figure 6.5.

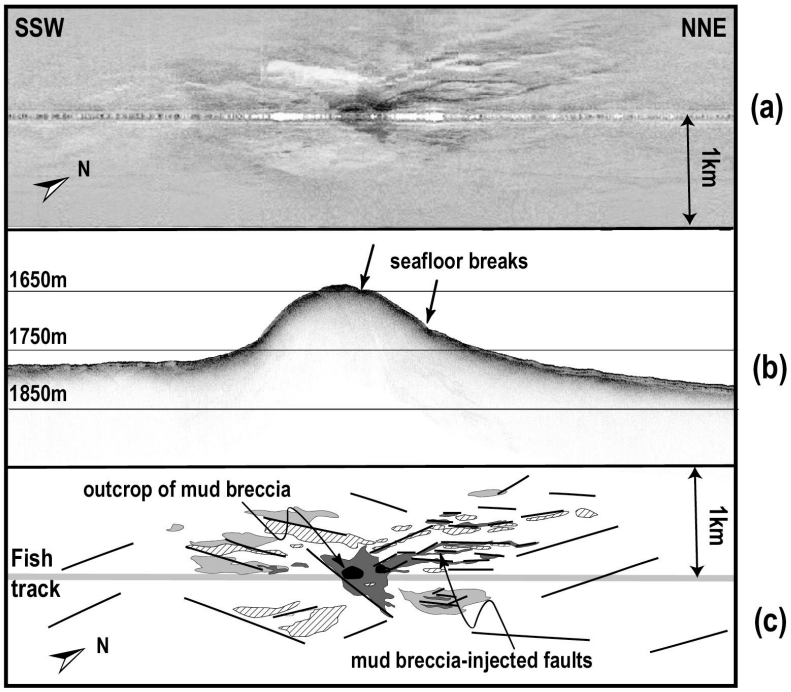

Figure 6.8: Sidescan sonar image (a) and subbottom profiler record (b) of Kula Mud Volcano with the interpretation (c).The different patterns indicate different mud flows (grey scale) and acoustic shadows (hatch). For legend, see Figure 6.5.

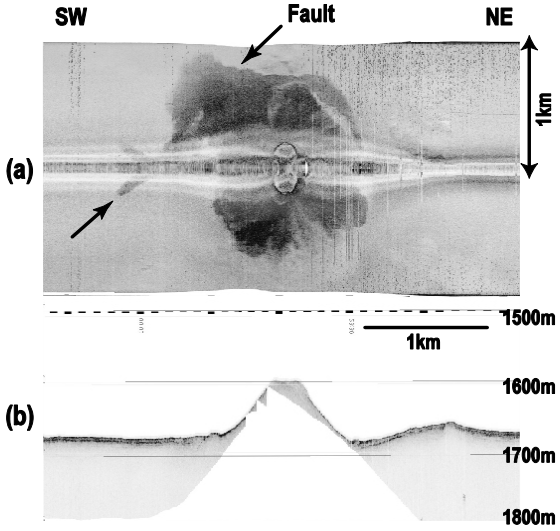

Figure 6.9: Sidescan sonar image (a) and subbottom profiler record (b) of Texel Mud Volcano, modified after Woodside et al. (2002).

6.5.2. Seeps and scarps

Scarps observed during the Nautile dives attest to the intense tectonic activity. The largest one is the Faulted Ridge explored between 1760 and 1280 m water depth (Figure 6.10). Different parts of the scarps observed during the dive include: (1) steep slopes with large pieces of fallen rocks, often associated with shells and debris of tubeworms, (2) scarps with outcropping stratified rocks, disrupted by fractures and dusted by hemipelagic sediments and (3) actual cliffs or walls, up to 100 m high, displaying intensively fractured layered dark rocks. Fluid seeping through the scarp is indicated by patches of concentrated chemosynthetic-based fauna. Shells are observed in several different places, but particullarly concentrated at the base of the cliffs. More intensive fluid emissions are inferred to occur in two places (Figure 6.10): (1) between 1660 and 1560 m water depth, along a cliff displaying tubeworms and active seeps characterized by purple reduced sediments and bacterial mats, and (2) at 1440 m water depth, on a wall where the greatest abundance of living vestimentiferans can be observed. The tubeworms are often located within the fractures or along the bedding planes, suggesting that fluid is seeping along them. In some places, vestimentiferans are organised into bunches of hundreds of living individuals settling along fractures (Figure 6.10).

On a smaller scale, many scarps from a few tens of centimeters to a few meters were observed. On Kazan MV, at least two linear N055°-trending scarps disrupt the seafloor with about 20 and 50 cm offset (Figure 6.11), showing the present-day activity of the faults. The importance of the tectonics on this mud volcano is also indicate by numerous ridges on the seafloor, mainly corresponding to the regional tectonic direction: N120° and N050-70°. Kula MV also reveals some scarps and surface deformation that correlate with the fault directions observed on the sidescan sonar record (see Chapter 3, Figure 3.10).

The majority of the scarps result from regional faulting, but some of them are related to local deformation within the mud volcanoes and the implicated mass flows. Mass wasting processes are found commonly in association with mud volcanoes (Vogt *et al*. 1999). The dive observations indeed reveal scarps or faults developing from mass destabilisation in response to the volume change of the mud volcano and/or due to the creeping on the steep flanks of the mud volcanoes (MEDINAUT/MEDINETH shipboard scientists 2001, see Chapter 3). This destabilisation process is well imaged on Amsterdam MV with the numerous concentric ridges and crevasses developing in the outer part of the summit (Figure 3.4). Although not related to deep-seated tectonic but superficial tectonic, the folding and crevassing induced by the mud movment within the mud volcano control the local seep distribution. Active seeps with massive carbonate crusts and tubeworms were frequently observed on top of the ridges developing around Amsterdam MV (see Chapter 3, Figure 3.6). These ridges located in the inner part of the alternating high and low backscatter ring surrounding the summit are probably built initially as eruptive ridges but the faulting related to peripheral collapse structures might also facilitate the focussing of superficial fluid flow. However, active seeps are not observed in the external part of the mud volcano in relationship with the outermost crevasses, except on a parasitic eruptive cone, associated with the interaction of N020° and N050° regional faults (③ in Figure 6.5).

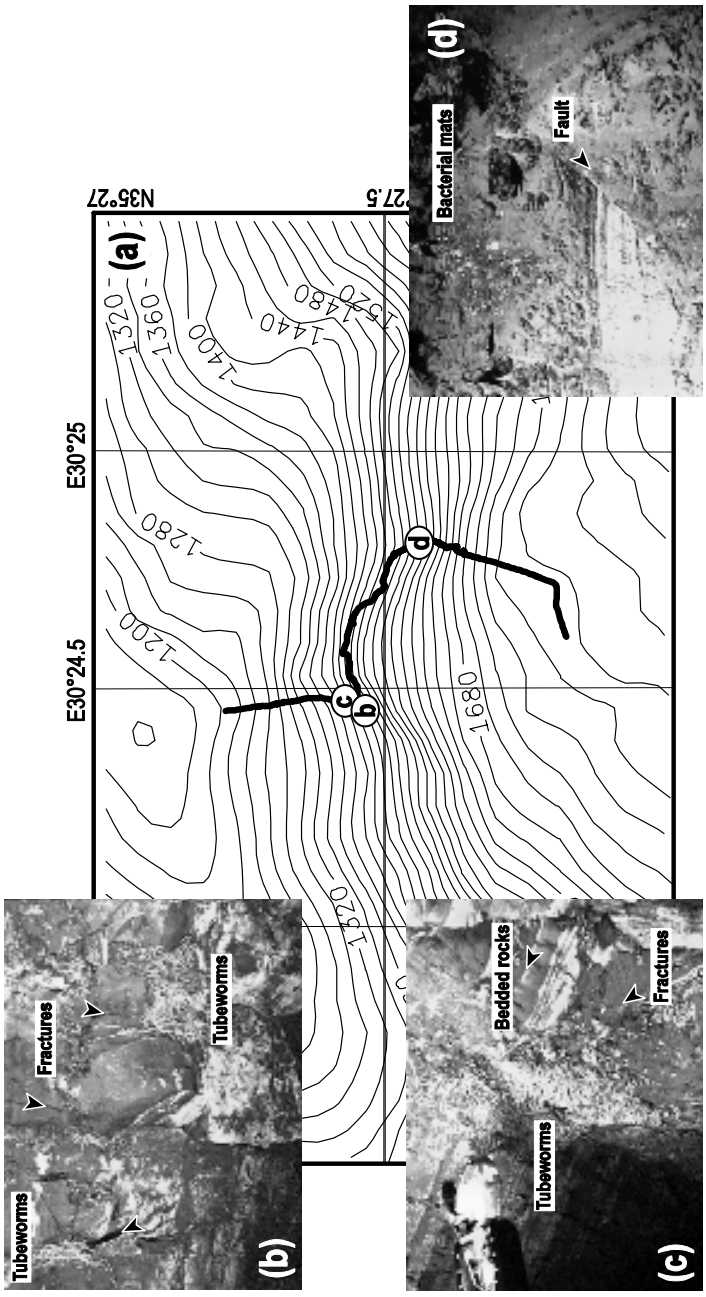

Figure 6.10: (a) Multibeam bathymetry map of the "Faulted Ridge" with the track of the Nautile dive and the location of the seafloor image showing: (b) the cliff and the tubeworms located within the fractures; (c) bunch of living tubeworms, at the intersection of fractures and beddings; (d) bacterial mats on the cliff.

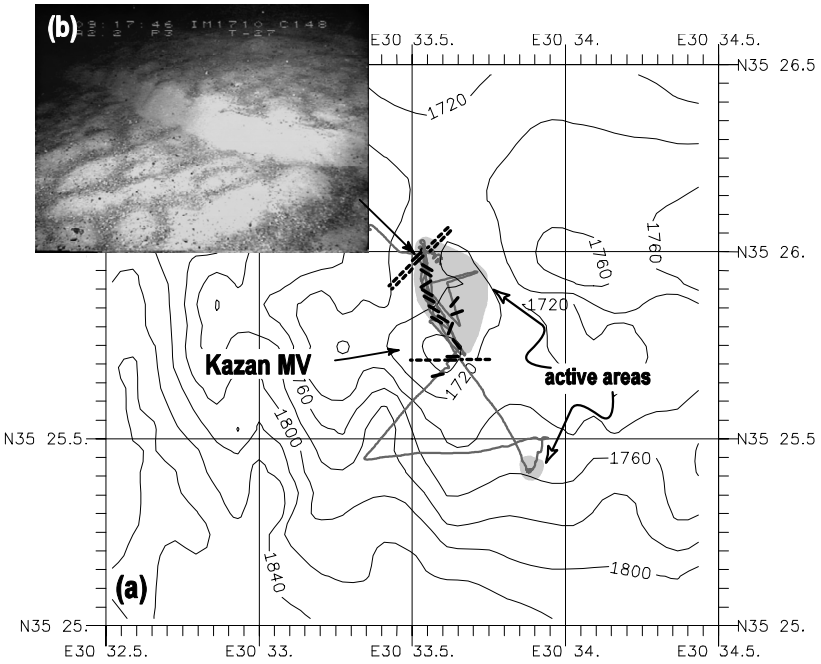

Figure 6.11: (a) Multibeam bathymetry map of Kazan MV with the direction of ridges (small lines) and scarps (dashed lines). (b) Seafloor image during dive 11 on Kazan MV, showing a fresh scarp of about 20 cm.

6.6. Discussion

6.6.1. Tectonic control on distribution of mud volcano deposits

In the Anaximander Mountains, mud volcanism occur in the strongly tectonized eastern domain, along a former thrust belt (along the Cyprus Arc). Compression appears as an important parameter for overpressuring sediments at depth. However this thrust belt is Pliocene-Recent reactivated as a normal/ transcurrent system (ten Veen *et al*. 2003, Zitter *et al*. 2003). In addition, most of the surveyed mud volcanoes of the Anaximander Mountains show a close relationship with strike-slip and normal faults (Table 6.1). With the exception of the N070° active sinistral strike-slip faults that are associated to all mud volcanoes, they are generally not associated with the same type of faults.

In the southern part of Anaxagoras, the faults observed are related to the interaction of both western and eastern Anaximander tectonic regimes, and the complex deformation resulting from this interaction. It involves mainly N120° dextral strike-slip, N150° oblique faults and N050° synthetic shears. On the other hand, the Kula MV in the northern part of Anaxagoras is associated with short N-S extensional faults related to the N150° oblique faulting. This indicates that overpressured fluids and mud use the pre-existing faults to reach

the surface and suggests that mud volcanoes are not only linked with major faults but also with minor associated faults or fractures, which may be under less compression, acting as a better conduit for mud extrusion.

The N070°-oriented strike-slip faults appear most significant in controlling the occurrence of mud volcanoes probably because they are the most active faults of the area. In the first place, they have a strong topographic expression in the multibeam bathymetry (e.g. the "Faulted Ridge" bathymetric offset), and secondly they are inferred to be the youngest faults because they are observed crosscutting the other faults. Although the precipitation of authigenic carbonates from circulating fluids will tend to reduce the permeability within fault zones, fault activity will obviate this and create or rejuvenate such conduits for fluid flow. Therefore, active faults are important to control mud and fluid expulsion. Also, the active strike-slip faults are steep to vertical and thus likely to be deep-seated faults able to reach the mud source (about 2 km deep; see Chapter 4). Finally the N070° transtensive faults probably facilitate the extrusion of the mud, when compared to thrusts which are tighter because of the compression across the fault. Compression alone is thus insufficient for the occurrence of mud volcanoes; a good plumbing system must exist as well.

The interaction between the faults is also an important factor to localise the extrusion of the mud. In the Anaximander Mountains, mud volcanoes are frequently located at the interplay of strike-slip and extensional faults. Active fracturing occurs where the stresses, especially tensile stresses, are more concentrated (Scholz *et al*. 1993). These regions of concentrated stresses, also called the breakdown regions, are found: (1) at the termination of the fault, (2) at the interaction area between two or more faults, where the fault terminations are in close proximity or overlap (e.g. zones of relay) (3) at the intersection of several faults, or (4) along the fault trace, because friction during slip can form localized fracturing along the fault zone (Scholz *et al*. 1993; Curewitz and Karson 1997). According to Curewitz and Karson (1997), fluid flow occurs preferentially within an interaction zone such that the three first structural settings are more permeable for focusing the fluid flow than the fracturing along the fault zone. Recent studies on the central domain of the Mediterranean Ridge (Huguen 2001) as well as within its western branch (Rabaute *et al*. 2003) also emphasize the importance of the zones of relay between the strike-slip faults for the localization of mud volcanism.

6.6.2. Tectonic control on the nature of fluid emissions and mud volcanism

A wide diversity of mud volcano morphologies is represented in many areas around the world (see Higgins and Saunders 1974). For example, on the Barbados prism, several main types of mud structures observed are: (1) active circular mud volcanoes that show extruded mud flows, (2) concentric flat-topped "mud pies" settled below the seafloor within subsiding basins, (3) piercing mud diapirs or mud mounds and (4) up to 18 km long mud ridges extruded from thrust faults and anticlinal crests (Brown and Westbrook 1988; Le Pichon *et al*. 1990; Henry *et al*. 1990). We can thus ask ourselves what the parameters that control such diversity are and how much the tectonic style can influence the nature of fluid emissions, and the morphology of mud volcanoes. On the Mediterranean Ridge (MR), the mud volcanoes also occur as highly variable structures, e.g. 2-8 km circular dome-like structures (Napoli MV,

Milano MV, Maidstone MV), ridges (Moscow MV), large low-relief structures with strong backscatter mud flows (Gelendzhik MV), wide flat extrusions of low backscatter mud flows ("pies" of the eastern MR branch; Huguen *et al*. 2001b; Kopf *et al*. 2001). Viscosity and density of the mud probably largely controls the geometry of the mud volcanoes (Brown 1990). However, it is inferred that tectonics partly controls these morphological varieties (Huguen 2001; Kopf *et al.* 2001).

In the Anaximander Mountains, mud volcanoes are morphologically less differentiated although they also present differences in activity, morphologies, and geophysical characteristics (see chapter 3). Amsterdam MV stands out with its particular size (up to 3 km across) and "mud pie" shape. It is also the only mud volcano linked with large-scale deep-seated N020° normal faulting. It is probable that due to the extensive context, the conduit for the mud ascent is wider. From theoretical calculations based on fluid dynamics (Kopf and Berhmann, 2000), it appears that the size and volume of the mud features are a function of the size of the feeder channel, and that large features generally relate to wider conduits. Texel MV and Kula MV also relate to normal faults, but probably more small-scale extensive tectonics, linked to the development of large-scale N150° transpressive faults. These two mud volcanoes are similar conical mounds with injected mud flows, however it is not statistically reliable to relate their morphology to their specific tectonic context.

The evidence for the activity of the Anaximander Mountains mud volcanoes (see Chapter 3) based on their geology (Zitter *et al*. 2003), associated chemo-synthetic fauna (Olu *et al*. 2003), and amount of degassing CH_4 (Charlou *et al*. 2003), indicate that the intensity of fluid emissions is highly variable. Fluid emissions appear very active in western Anaxagoras, at the intersection with Anaximenes Seamount, at Amsterdam and Kazan MVs, as well as on the Faulted Ridge. On the other hand, Tuzlukush, Saint Ouen l'Aumône and Kula MVs appear less active or even dormant. Two parameters might constrain this difference in the nature of seeping: firstly, the complex deformation at the interaction between the western Anaximander transtensive regime and eastern Anaximander transpressive regime, second, the difference of lithology of the underlying units. Autochthonous limestones or such brittle rocks take longer time to get sealed by fluid precipitates,thus facilitating fluid seeps compared to ductile units.

6.7. Conclusion

The Anaximander Mountains area displays evidence of active mud volcanism in a transpressive tectonic context, along the dominant structural trend of the western branch of the Cyprus Arc. The relationship between mud volcanism and neotectonic structures is observed from multibeam data and deep-tow sidescan sonar, as well as dive observations. Numerous faults or fissures are observed in connection with the mud volcanoes, acting as conduits for mud ejection and the release of fluids. Seafloor observations reveal the major role of both major (N060-070°, N120°, N150°) and secondary (N-S, N040-050°, N90°) faulting in mud volcanism. Not all the mud volcanoes are characterized by the same type of faults; however, mud volcanoes appear to be associated predominantly with the interplay of the dominant N060-070° sinistral shearing and some major and/or minor extensional/transtensional faulting (N150°, N120° and/or N-S to N020°).

Acknowledgements

This research was partially funded by the Netherlands Organisation for Scientific Research (NWO) through the Medised project (809.63.011), the ANAXIPROBE project (750.195.02) and the MEDINAUT/MEDINETH project (750.199.01). It was carried out partly using ADELIE and CARAIBES software from IFREMER. We are grateful to the IFREMER/Genavir crew and technical team of the R/V "Nadir" and the submersible 3Nautile" for their involvement during the MEDINAUT cruise and to the captains and crews of both R/V "Gelendzhik" and R/V"Professor Logachev" for their involvement during the TTR6-ANAXIPROBE and MEDINETH surveys respectively. We greatly acknowledge Jean-Marie Augustin for his help in reprocessing the sonar data. ten Veen acknowledge financial support from NOW-PULS project (831.48.009).

Chapter 7. Synthesis

The main objective of this research was to gain an integrated understanding of mechanisms of mud extrusion and fluid emissions at the seafloor. In Chapter 3, I reviewed bio-geological characteristics of mud volcanism and fluid emissions. Chapter 4 investigated the source of mud volcanic sediments, and Chapter 5 and 6 addressed the tectonic setting of mud volcanoes and how it controls their activity. In this synthesis, I will summarize the main results from the previous chapters and I will integrate results from (bio)geochemical and (micro)biological studies obtained within the MEDINAUT and MEDMUD groups.

7.1. Nature of mud volcanism

7.1.1. Activity of a mud volcano

It is awkward to define when a mud volcano is active, inactive, dormant or extinct, because it depends on which type of phenomenon is considered (e.g. fluid emissions, mud eruptions, biological activity). From the observations in Chapter 3, two features appear to characterise the activity of a mud volcano: the existence or not of a recent (see 7.1.2 below) mud eruption, and the amount of emitted methane, features that are not always fully coupled. Although the eruption of a mud volcano releases large volumes of methane-rich sediments (as noted in Chapter 3), gas and fluids are not only expelled during eruptive events, but also through continuous processes. On the other hand, recently extruded mud flows can mask evidences of methane seeps (e.g. centre of Amsterdam MV). Active areas are then identified by biogeochemical characteristics of methane emission (e.g. diversity and density of chemosynthetic fauna, mainly bivalve fields, bacterial mats, authigenic carbonate crusts, anoxic sediments, see 7.4.3 below) and/or geological characteristics of fresh mud flow (see 7.1.2 below). Thus, mud volcanoes are active when they display numerous mud eruptions outcropping on the seafloor, and/ or when they exhibit evidence of fluid emissions such as active seeps and degassing structures, even if young mud flows are absent (e.g. Napoli MV). Different levels of activity might also be distinguished depending on the density of the biological population, density of seeps, measured methane emission, age of the mud flows (see 7.1.2 below), and geographical extent of the active areas. In contrast, topographic structures that do not present any fresh mud flows at the surface (smooth seafloor, no exposed clasts), nor any evidence for fluid emissions (carbonate crust, chemosynthetic communities, gas bubble) might be dormant or dead, depending on later potential reactivation.

7.1.2. Evolution of the mud flows

Visual observations of the surface of a submarine mud volcano (Chapter 3) reveal a relationship between the age of the mud flow, the quantity of visible clasts on the seafloor, the

distribution of the benthic fauna, the presence of carbonate crusts, and the small scale relief of the seafloor. With time, the seafloor will exhibit fewer exposed clasts and more and more authigenic crusts. Bivalve fields and bacterial mats are characteristic of active seepage, whereas thick crusts dusted with hemipelagic sediments indicate extinct or dormant seeps. The evolution of a given mud flow through time can be described as follows (Table 3.1):

(1) At the time of the extrusion, the fresh mud flow shows a very rough surface (centimetre to metre scale) with numerous clasts exposed on the seafloor. Lots of gas and turbid fluids (water and sediments) are expelled from the mud flow through chimneys (e.g. in the centre of Amsterdam). The seafloor is quickly colonized by chemosynthetic-based benthic fauna, mainly dispersed bivalves. No authigenic carbonate crust has developped yet. If any localized seeps were previously occurring in the area, they have been covered up by the mud and are thus not present because they have not yet developed pathways through the new mud flow to seafloor.

(2) The colonization by benthic fauna (bivalves and tubeworms) develops scattered related to general degassing of the mudflow, and some concentrated fields of bivalves appear. The seafloor is rough (metre scale) with some clasts exposed on seafloor. The mud flow is still releasing large volumes of methane but less turbid fluids. Localized active seeps characterized by typical purple-grey reduced sediments also appear sometimes associated with bacterial mats. Brine pools and brine rivers (Woodside and Volgin 1996; MEDINAUT/MEDINETH shipboard scientists 1999; Huguen 2001) occur in areas where the fluids may dissolve underlying Messinian salt, as in the Olimpi area (e.g. Napoli). Thin crusts develop in places.

(3) The seafloor becomes smoother and dusted with hemipelagic sediments. Long-term seeps, which have been re-established through the mud flow, are identified by the presence of thick carbonate crusts with bushes of tubeworms (e.g. Kazan). Both active and dormant seeps might occur within the same area. Benthic fauna are distributed in concentrated fields (clusters of bivalves and bushes of tubeworms). The pavement of carbonate crust that covers a major part of the seafloor may be broken in some places due to the mud motion.

(4) The fractures from stage (3) develop into large crevasses (e.g. outer part of Amsterdam). Thick carbonate crusts occur isolated on the otherwise hemipelagic sediments; they reflect past occurrences of long-term seeps. Few living chemosynthetic-based benthic fauna, (shells, clusters of dead tubeworms) but the seafloor is intensively bioturbated.

7.1.3. Spatial distribution of activity

Mud volcanism activity usually shows a concentric organization around the centre of the mud volcanoes (Chapter 3). The youngest mud flows are often observed right on top of the mud volcanoes (e.g Amsterdam, Kula) and the oldest in external parts. However, parasitic

eruptive centres might focus part of the active fluid emissions within the peripheral areas. Sometimes spatial distribution is less predictable such as on Kazan MV were the central part of the mud volcano is less active than the northern and southern areas. Pathways for fluid to reach the seafloor are possibly easier to develop at the margin of the mud volcano because of thinner overlying mud flow and faulting related to peripheral collapse structures.

7.1.4. Episodicity/duration

Localized seeps might have a short-term (< 1 year) periodicity. Within a nine months period –in between the Nautile dives (December 1998) and deep-tow video (August 1999) over the top of Napoli MV– some previously active brine lakes have been observed empty (MEDINAUT/MEDINETH shipboard scientists 2000). Dormant seeps can be seen within young areas, coexisting with active seeps. On the other hand, some seeps might be active for much longer periods (several hundreds of years), because the continuous gas discharge permits the growth of more than 1 m high carbonate crusts (assuming a growth rate of 0.15 cm/y; Liebetrau *et al.* 2003).

Mud eruption periodicity is difficult to assess for marine mud volcanoes (Kopf and Behrmann 2000). Within some cores, the alteration of part of the mud flow at depth (Chapter 4) indicates episodes of oxidation, i.e. the mud flow was in contact with seawater (but not long enough to be covered by hemipelagic sediments), giving evidence of different eruptive events. The interfingering of mud flows with hemipelagic sediments indicates long periods of inactivity between episodic eruptions (multiple eruptive events with longer periodicity); e.g. approximately 50 kyrs of inactivity for Saint Ouen l'Aumône MV assuming a sedimentation rate of 5 cm/kyrs (Emeis *et al*. 1996) for the 2.2 m of hemipelagic sediments on top of the mud flow (Woodside *et al*. 1997a). On land, mud eruption periodicity is better known, due to well-documented historical records: in Azerbaijan, Dashgil MV had one eruption every 6-32 years (Hovland *et al*. 1997) in between 1882 and 1958. In Trinidad, Piparo MV had major eruptions in 1953, 1968, 1969 (Higgins and Saunders 1974) and the last mud eruption of this mud volcano dates from 22nd february 1997 (CDERA, 2003).

Napoli and Milano mud volcanoes have been active for over one million years as demonstrated by ODP Leg 160 investigations (Robertson and Kopf 1998b). However, there is no evidence that the Anaximander Mountains mud volcanoes are of the same age.

7.2. Origin of the mud

7.2.1. Origin of the matrix of the mud breccia

The clay mineral analysis of the matrix of the mud flows (Chapter 4) reveals a very similar mineral assemblage for every mud volcano studied, which is dominated by the presence of smectite. In the Mediterranean Sea stratigraphic sequence, this clay assemblage shows affinity with smectite-rich terrigeneous deposits (marls, sandstones, mud stones, limestones) of Messinian age (Chamley *et al*. 1978; Chamley and Robert 1980). From this research a

Messinian derivation of the mud matrix is proposed, also supported by the following arguments:

- The mud contains algae and foraminifer (*Ammonium Becarii*) characteristic of a brackish environment typical of the "Lago Mare setting" (Schulz *et al*. 1997; Spezzaferri *et al*. 1998).
- A Messinian age was inferred from a study using the Lopatin method to estimate the maturation of the organic matter within the mud (Schulz *et al*. 1997).
- Chemical composition of smectite within the clay fraction corresponds to Al-Fe bedeilites (Jurado-Rodriguez and Martinez-Ruiz 1998) abundant in Messinian deposits (Chamley and Robert 1980).
- The mud matrix shows lithological resemblance with Messinian ooze from the Tyrrhenian Sea (Kastens *et al*. 1987; Kopf *et al*. 1998).

It is possible that the matrix came from different sources in different mud volcanoes. However, the coherence between the results for different mud volcanoes of the Olimpi field, Anaximander Mountains, and Florence Rise areas tends to indicate an unique source for most of the mud volcanoes in the Mediterranena Sea.

7.2.2. Depth of origin of the matrix

Two alternate hypotheses have been proposed in the literature: (1) a very deep origin (5 to 7 km deep) from the décollement level within the accretionary prism (Camerlenghi *et al*. 1995; Schulz *et al*. 1997; Robertson and Kopf 1998); (2) a shallower (< 2 km) depth of remobilization (Jurado-Rodriguez and Martinez-Ruiz 1998; Kopf *et al*. 2001). This research favours the latter proposition as the clay mineralogy analysis is inconsistent with the occurrence of diagenetic transformations (see Chapter 4) that would be expected from deep burial.

7.2.3. Mechanism of extrusion

Because smectite is a highly hydrated low density mineral (Grim 1968; Brown *et al*. 2001), the smectite-rich Messinian terrigeneous unit is thus more likely to become undercompacted during early stages of compaction and to be less dense than overlying sediments. This unit will therefore be easily remobilized by fluids percolating through it. This implies that the fluids are coming from deeper within the sedimentary section, a hypothesis that seems to be supported by geochemical analysis (see 7.4.2 below).

7.3. Relationship with tectonics

As already discussed in Chapter 1, mud volcanism occurs when a light fined-grained undercompacted layer becomes overpressured at depth (Brown 1990). In some areas, hydrocarbon generation might be sufficient to initiate mud volcanism but most of the time additional processes are required to induce overpressuring. These processes comprise: (1)

sediment loading (high sedimentation rate) and (2) tectonic loading (lateral pressuring by compression, overthrusting).

In the eastern Mediterranean Sea, the global compressive tectonic context appears thus as important to the occurrence of mud volcanism. However, mud volcanoes also need a good plumbing system for the extrusion of the mud. A relationship between faults and mud volcanoes has been evidenced from multiscale analysis within the Mediterranean Ridge (Huguen *et al*. 2001b) and in the Anaximander Mountains (Chapter 6), indicating that faults act as pathways for mud and fluids. Furthermore, the link with strike-slip tectonic features is clearly observed within mud volcano areas (Huguen *et al*. 2001b; Rabaute *et al.* 2003; see Chapter 6).

The central part of the Mediterranean Ridge is inferred to undergo frontal collision, involving folding and faulting. Within this context, controlled by compressive stresses (Mascle *et al*. 1999), mud volcanoes are thought to be emplaced along thrusts and backthrusts (Robertson *et al*. 1996, Robertson and Kopf 1998b). The relationship between mud volcanoes of the Olimpi field and high-dipping thrust planes has been clearly observed (Huguen 2001). However, for the first time in this area, a clear connection is also noted between mud extrusion and secondary faulting, related to right lateral strike-slip movements along regional fractures affecting the sedimentary cover (Huguen *et al.* 2003).

The deformation style in the Anaximander Mountains/ Florence Rise area is complicated by the tectonic interaction between the Hellenic and Cyprus arcs. The western branch of the Cyprus arc (eastern Anaximander Mountains and Florence Rise) is affected by large transpressive system (i.e. longitudinal normal/oblique faults oriented N150° and crosscutting sinistral strike slip faults trending N070°) accommodating pre-collisional deformation (Chapter 5; ten Veen *et al*. 2003). In contrast, the western Anxaximander Mountains show a more transtensive stress pattern (ten Veen *et al*. 2003). Mud volcanism, occurring along the structural trend of the western branch of the Cyprus Arc, is then related to more deep-seated transcurrent tectonics. Mud volcanoes appear predominantly associated with the interplay of faults, mainly strike-slip and extensional faults (see Chapter 6), that might be more active or under less compression, thus facilitating mud extrusion.

This research reveals the major role of both major and secondary faults related to the transcurrent stress field. The extensive constraints generated by transpressive or transtensive faulting appear thus as one of the major conditions for mud extrusion.

7.4. Results from MEDINAUT/MEDMUD

As noted in Chapter 1, this research is part of two multidisciplinary research programmes (MEDINAUT and MEDMUD) in which integration of the different results is an essential condition for understanding mud volcanism processes. A number of results are already published elsewhere. I will present here the major outcomes of these programmes related to petrological, geochemical, and micro-biological issues, and discuss their significance in respect to this study.

7.4.1. Origin of the clasts

Clasts from the MEDINAUT survey have been evaluated for paleoenvironmental conditions of deposition and subsequent developments (Huguen *et al*. 2001a). Clasts from the Olimpi field, mainly comprising marls and calcareous sandstones, have been interpreted as deposited under deep marine conditions in a distal deep-sea-fan environment. Clasts from the Anaximander Mountains area are dominated by sandstone facies indicating basement geology with an affinity to continental margin conditions. This difference in petrology confirms the different tectonic and geological settings between the Olimpi area and the Anaximander Mountains. Control of clast shape by sets of early microfractures before extrusion on the seafloor indicates a pre-fracturating (Huguen *et al*. 2001a), probably related to overpressuring at depth (Robertson and Kopf, 1998). In the easternmost part of the Anaximander Mountains, where clasts are derived from the underlying Antalya Nappes Complex (see Chapter 6), this pre-fracturating might be inherited from the emplacement of the ENE-dipping stack of nappes (Lefèvre 1967; Robertson and Woodcock 1980). Thrusts separating the nappe sheets might provide a basis for later faulting and fluid pathways.

7.4.2. Origin of the fluids

At depth, fluid-sediment interactions affect the fluid chemistry, thus the geochemistry of pore fluids within mud volcano sediments reflects the source of these fluids. At the equilibrium between fluids and rocks, formation water temperatures ranging from 80°C to 150°C have been estimated in the Anaximander Mountains area (Haese *et al*. 2003; Werne *et al*. 2003), indicating a deep source for the fluids, between 2 and 4 km under normal geothermal gradient (30-35°/km; Erickson 1970).

Pore fluid geochemistry at eastern Mediterranean mud volcanoes often shows a decrease in salinity at depth (low chlorinity), also called “pore water freshening”, interpreted as an artifact due to gas hydrate dissociation during core recovery (De Lange and Brumsack 1998), and thus indicating *in situ* gas hydrates within the subsurface. Recent studies have reassessed the significance of this chlorinity variation (Haese *et al*. 2003; Dählmann and De Lange 2003), together with pore water isotopic composition ($^{18}\delta O$ and δD), showing that this pore water signature might be better interpreted as the signature of clay mineral dehydration (Brown *et al*. 2001). That would also imply a deep source for these fluids (more than 2 km deep).

Comparison of these results with clay mineralogy results (section 7.2 above) indicates probable multiple sources for the expelled material, with a deep source for the fluid (and gaseous?) phase of the mud breccia and a shallower source for the solid phase of the mud breccia.

7.4.3. Role of methane gas

Anaerobic oxydation of methane is a dominant biogeochemical process in the subsurface of mud volcanic sediments (Pancost *et al*. 2000). This process associated with sulfate reduction and sulfide oxidation can be inferred from organic chemistry studies (lipid

analysis), microbial analysis (phylogenetic investigations), isotopic analysis, as well as pore water geochemistry (Aloisi *et al*. 2002; Werne *et al*. 2003). Biomarkers of archea and bacteria depleted in $^{13}\delta C$, present both in mud breccia sediments and in authigenic carbonate crusts of eastern Mediterranean mud volcanoes, indicate methane consumption through a consortium of micro-organisms (Pancost *et al*. 2000, 2001). Pore water concentrations of sulfate, sulfide, dissolved organic carbon (DIC) and its isotopic signature $^{13}\delta C_{DIC}$ also all imply that anaerobic oxidation of methane is occurring in eastern Mediterranean mud volcano sediments (Haese *et al*. 2003).

Four types of authigenic carbonate crusts were observed by Aloisi and co-authors (2001): Type A/ massive lithified mud breccia, Type B/ massive lithified pelagites, Type C/ thin lithified mud breccia and Type D/ nodules. Types A, B and C are composed of a calcite/aragonite mixture and their $^{13}\delta C$ values (e.g. 3 to -45 $^{o}/_{oo}$ PDB) show they are related to methane consumption. The occurrence of type B crust indicates that mud flows covered by hemipelagic sediments might still release enough methane for crust precipitation. Carbonate crusts are thus a sink for methane carbon migrating from depth to the seafloor (Aloisi *et al*. 2000, 2002).

An important quantity of the emitted methane is therefore consumed before reaching the surface, through this anaerobic methane oxidation process (Werne *et al*. 2003), however, the methane oxidation is not complete. Huge amounts of methane (e.g. up to 2000 nmol/kg for Amsterdam MV) are injected into seawater to form plumes of 100 to 200 m high (Charlou *et al*. 2003). The amount of methane in bottom seawater over mud volcanoes is highly variable, and usually shows a maximum in the centre of the mud volcanoes, attesting to the concentric organization of activity (see section 7.1.3 above). High turbidity is also observed in some cases (e.g. Amsterdam MV), attesting to the very recent emplacement of the mud flows (see section 7.1.2 above) or/and the intense venting.

Symbiotic macro-fauna also participate in methane consumption. The eastern Mediterranean Sea shows a high richness in chemosynthetic species (Olu *et al*. 2003), more diversified than in other cold seeps in the Atlantic and Pacific Seas (8 chemosynthetic species at eastern Mediterranean mud volcanoes versus 4 to 6 species at comparable depth in Louisiana, Oregon, Barbados and Nankai mud volcanoes; Olu *et al*. 2003). The spatial distribution of benthic fauna varies with the intensity of fluid seepage (see 7.1.2 above). Amsterdam mud volcano present the largest area covered by shells (Olu *et al*. 2003) but the densest coverage of active areas with shells is observed on Kazan (40% of active areas, in comparison with 20% on Amsterdam and 10% on Napoli).

7.4.4. Importance of gas hydrates

As previously discussed (see section 7.4.2 above), a decrease in the salinity of pore fluids at depth might not always be interpreted as a sign of the presence of gas hydrates within the sediments. Pore water freshening has been observed in all the eastern Mediterranean mud volcanoes, leading to the supposition that gas hydrates were of widespread occurrence there. Until now, gas hydrates were not recovered from the Olimpi field mud volcanoes, but were found on most active mud volcanoes of the Anaximander Mountains, i.e. Kula (during the

TTR6-ANAXIPROBE cruise in 1996 (Woodside *et al*. 1997a) and during the MEDINETH cruise in 1999), Amsterdam (during the MEDINETH cruise in 1999) and Kazan (during the recent ANAXIMANDER cruise in 2003; Lykousis *et al*. 2003). Amsterdam is a very active mud volcano (recently extruded mud flows and evidence of high methane emission; see Chapter 3, and above), so the finding of gas hydrates there refutes the previous hypothesis that a cap of gas hydrates develops only during dormancy periods (Robertson and Kopf 1998). Sampling tends to indicate that gas hydrates are common in the Anaximander Mountains but may be absent from the Olimpi field mud volcanoes. Several hypotheses may explain this disparity: a) the higher salinity in the Olimpi field due to the seeping of briny fluids may reduce the gas hydrate stability zone within this area (see Figure 7.1); (b) the type of hydrocarbons, which, if proven to contain relatively higher percentages of heavier hydrocarbons in the Anaximander Mountains (Stadnitskaia Pers. Comm. 2003), can also increase the thickness of the gas hydrate stability zone there (Figure 7.1); (c) the amount of methane is higher in the Anaximander Mountains; (d) the different sedimentology of the underlying units between both fields (basement rocks in the Anaximander Mountains versus more hemipelagic sediments on the Mediterranean Ridge).

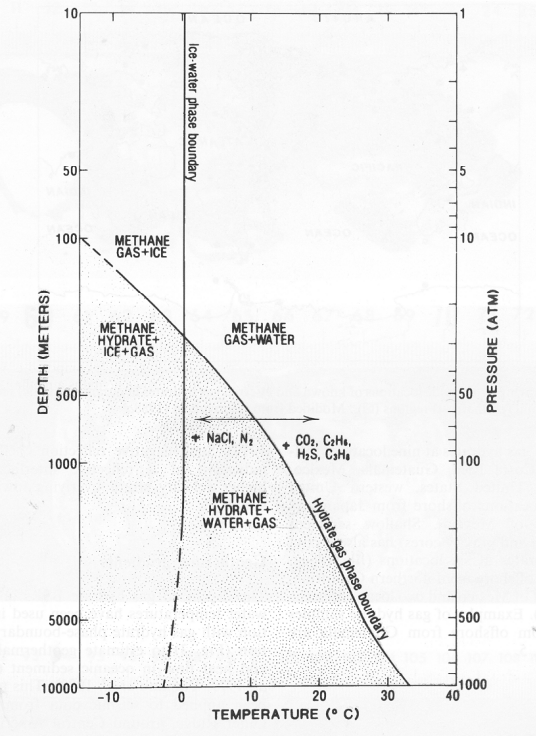

Figure 7.1: Phase diagram showing the boundary between free methane gas (no pattern) and methane hydrate (pattern) for a pure water and pure methane system, from Kvendolden (1998). Addition of NaCl shifts the curve to the left, whereas addition of heavier hydrocarborn shifts the boundary to the right and thus increase the area of hydrate stability field.

7.5. Future research

An integrated multidisciplinary approach to investigate tectonic, sedimentological, and biogeochemical processes related to gas within marine sediments in eastern Mediterranean basins has been essential to widen our conception of mud volcanism phenomenon. The increasing importance of mud volcanism at convergent zones revealed with the advanced seafloor mapping techniques has profound implications for the geochemical cycles within the subduction factory. Although methane anaerobic oxidation occurring within the subsurface sediments plays a significant role in regulating the methane flux into Mediterranean bottom seawater, mud volcanoes may be a significant natural source for emitted atmospheric methane, thus having a real impact on the climate change issue. Future mud volcano studies should focus on integrated studies, especially quantifying the different processes contributing to this phenomenon, i.e. quantifying levels of mud volcanism activity, assessing their role on a global scale, evaluating their potential gas hydrates reservoirs, long-term monitoring of gas and fluid flux. Quantification and calibration of the acoustic response of mud volcanoes and seafloor characterization studies would improve detection of mud volcanoes and related activity (carbonate crusts, seeps and pockmarks, gas hydrates) with high-resolution seafloor mapping surveys. Finally, comparison of mud volcanoes within different settings (e.g. in the Eastern Mediterranean Sea comparison of mud volcanoes in convergent zones with those on the Nile deep-sea fan) would bring useful additional information on mud volcanism processes.

References

Aharon P, Schwarcz HP and Roberts HH. 1997. Radiometric dating of submarine hydrocarbon seeps in the Gulf of Mexico. Geological Society of America Bulletin, 109: 568-579

Akmanov G. 1996. Lithology of mud breccia clasts from the Mediterranean Ridge. Marine Geology, 132: 151-164.

Akmanov GG and Woodside JM. 1998. Mud volcanic samples in the context of the Mediterranean Ridge mud diapiric belt. In: Robertson AHF, Emeis KC, Richter C, and Camerlenghi A (eds.), Proceedings of the ODP, Scientific Results, 160: College station, TX (Ocean Drilling Program), 597-605.

Aloisi G. 2000. La diagenèse carbonatée liée à l'hydrothermalisme froid et à l'activité microbienne sur les volcans de boue sous-marin. Thèse, Université Paris 6, Paris.

Aloisi G, Pierre C, Rouchy J-M, Foucher J-P and Woodside JM. 2000. Methane-related authigenic carbonates of eastern Mediterranean Sea mud volcanoes and their possible relation to gas hydrate destabilisation. Earth and Planetary Science Letters, 184: 321-338.

Aloisi G, Bouloubassi A, Heijs SK, Pancost RD, Pierre C, Sinninghe Damsté JS, Gottschal JC, Forney LJ and Rouchy J-M. 2002. CH_4-Consuming microorganisms and the formation of carbonate crusts at cold seeps. Earth and Planetary Science Letters, 203: 195-203.

Anastasakis G, Kelling G. 1991. Tectonic connection of the Hellenic and Cyprus Arc and related geotectonic elements. Marine Geology 97: 261-267.

Ardvisson R, Ben-Avraham Z, Ekstrom G, Wdowinski S. 1998. Plate tectonic framework for the October 9, 1996, Cyprus Earthquake. Geophysical Research Letters 25/12: 2241-2244.

Barber AJ, Tjokrosapoetro S, Charlton TR. 1986. Mud volcanoes, shale diapirs, wrench fault and melanges in accretionary complexes, eastern Indonesia. Bulletin of the American Association of Petroleum Geologists 70: 1729–1741.

Barka A, Reilinger R. 1997. Active tectonics of the eastern Mediterranean region: deduced from GPS, neotectonic and seismicity data. Annali di Geofisica 40/3: 587-610.

Barka AA, Reilinger RE, Saroğlu F, Şengor, AMC. 1995. Isparta Angle: its importance in the neotectonics of the Eastern Mediterranean Region. In: Piskin D, Ergun M, Savascin MY, Tarcan G (eds.), International Earth Science Colloquium on the Aegean Region Proceedings: 3-18.

Bellaiche G, Loncke L, Gaullier V, Mascle J, Courp T, Moreau A, Radan S, Sardou O. 2001. Le cône sous-marin du Nil et son réseau de chenaux profonds; nouveaux résultats (campagne Fanil). Comptes Rendus de l'Academie des Sciences, Serie II. Sciences de la Terre et des Planètes 333/7 : 399-404.

Ben-Avraham Z, Kempler D, Ginzburg A. 1988. Plate tectonics in the Cyprus Arc. Tectonophysics 146: 231-240.

Ben-Avraham Z, Tibor G, Limonov AF, Leybov MB, Ivanov MK, Yu Tokarev M., Woodside JM. 1995. Structure and tectonics of the eastern Cyprean Arc. Marine and Petroleum Geology 12/3: 263-271

Bernasconi SM. 1999. Interstitial water chemistry in the Western Mediterranean: results from leg 161. In: Zahn R, Comas MC, and Klaus A (eds.) Proceedings of the Ocean Drilling Program, Scientific Results, 161: College station, TX (Ocean Drilling Program), 423-432.

Blumenthal M. 1963. Le système structural du Taurus Sud Anatolien. In Livre à la mémoire du Professeur Paul Fallot. Mémoires hors-série de la Société Géologique de France, Paris II: 611-652.

Bonatti E and Joensuu O. 1968. Palygorskite from Atlantic deep sea sediments. The American Mineralogist 53: 975-982.

Boray A, Saroğlu F, Emre O. 1985. Isparta Buklumunun kuzey kesiminde D-B daralma icin bazi veriler [Evidence for E-W shortening in the north of Isparta Angle]. Jeoloji Muhendisligi 23: 9-20 [in Turkish with English abstract].

Bozkurt E, Oberhaensli R. 2001. Menderes Massif (western Turkey): structural, metamorphic and magmatic evolution – a synthesis. International Journal of Earth Sciences 89: 679-708.

Bozkurt E. 2001. Neotectonics of Turkey - a synthesis. Geodinamica Acta 14/1-3: 3-30.

Brindley GW and Brown G. 1980. Crystal structures of clay minerals and their X-ray identification. Mineralogical Society Monograph, 5, Mineralogical Society, London.

Brönner M and Makris J. 2000. Crustal structure of the Libyan Margin. CIESM Workshop series 13: 63-66.

Brown KM. 1990. The nature and hydrogeologic significance of mud diapers and diatremes for accretionary systems. Journal of Geophysical Research 95/B6: 8969-8982.

Brown KM and Westbrook GK. 1988. Mud diapirism and subcretion in the Barbados Ridge Complex: The role of fluids in accretionary processes. Tectonics 7: 613-640.

Brown KM, Saffer DM, and Bekins BA. 2001. Smectite diagenesis, pore-water freshening, and fluid flow at the toe of the Nankai wedge. Earth and Planetary Science Letters 194: 97-109.

Camerlenghi A, Cita MB, Hieke W and Ricchiuto T. 1992. Geological evidence for mud diapirism on the Mediterranean Ridge accretionary complex. Earth Planetary Science Letters 109: 493-504.

Camerlenghi A, Cita MB, Della Vedova B, Fusi N, Mirabile GL and Pellis G. 1995. Geophysical evidence of mud diapirism on the Mediterranean Ridge accretionary complex. Marine Geophysical Researches 17: 115-141.

Caroll D. 1969. Clay minerals: a guide to their X-ray identification. The Geological Society of America Special Paper 126: 1-80.

CDERA (the Carribean Disaster Emergency Response Agency). 2003. Situation report on the mud volcano eruption in Piparo, Trinidad and Tobago. WWW page, http://www.cdera.org/Archive/Situation_Reports/sr110397.htm

Chamley H. 1989. Clay sedimentology. Springer-Verlag, Berlin: 623 pp.

Chamley H and Robert C. 1980. Sédimentation argileuse au Tertiaire supérieur dans le domaine méditerranéen. Géologie Méditerranéenne VII/ 1 : 25-34

Chamley H, Dunoyer de Segonzac G and Mélières F. 1978. Clay minerals in Messinian sediments of the Mediterranean area. In: Hsü, K.J., Montadert, L.C. et al. (eds.), Initial reports DSDP, 42A, Washington (U.S. Gov. Print. Off.): 389-394.

Chamot-Rooke N, Lallemant SJ, Le Pichon X, Henry P, Sibuet M, Boulègue J, Foucher J-P, Furuta T, Gamo T, Glaçon G, Kobayashi K, Kuramoto S, Ogawa Y, Schultheiss P, Segawa, J, Takeuchi A, Tarits P and Tokuyama H. 1992. Tectonic context of fluid venting at the toe of the eastern Nankai accretionary prism: Evidence for a shallow detachment fault. Earth and Planetary Science Letters 109: 319-332.

Charlou JL, Donval JP, Zitter T, Roy N, Jean-Baptiste P, Foucher JP, Woodside J and MEDINAUT Scientific Party. 2003. Evidence of methane venting and geochemestry of brines on mud volcanoes of the eastern Mediterranean Sea. Deep Sea Research I, *in press*.

Chaumillon E and Mascle J. 1995. Variation latérale des fronts de déformation de la Ride méditerranéenne (Méditerranée orientale). Bulletin de la Société Géologique de France 5 : 463-478.

Chaumillon E, Mascle J and Hoffmann HJ. 1996. Deformation of the western Mediterranean Ridge: Importance of Messinian evaporites formations. Tectonophysics 263: 163-190.

Chester R, Baxter GG, Behairy AKA, Connor K, Cross D, Elderfield H, and Padgham, RC. 1977. Soil-sized eolian dusts from the lower Troposphere of the Eastern Mediterranean Sea. Marine geology 24: 201-217.

Cita MB and Wright R (eitors). 1979. Geo- and biodynamic effects of the Messinian salinity crisis in the Mediterranean. Paleogeography, Paleoclimatology, Paleoecology 59: 368 pp.

Cita MB and Camerlenghi A. 1990. The Mediterranean Ridge as an accretionary prism in collisional context. Memorie della Società Geoogica Italiana 45: 463- 480.

Cita MB, Ryan WBF and Paggi L. 1981. Prometheus mud breccia. An example of shale diapirism in the Western Mediterrranean Ridge. Annales Géologiques des Pays Hélléniques 30 : 543-569.

Cita MB, Camerlenghi A, Erba E, McCoy FW, Castadrori D, Cazzani A, Guasti G, Gambastiani M, Lucchi R, Nolli V, Pezzi, G, Redaelli M, Rizzi E, Torricelli S and Violanti D. 1989. Discovery of Mud diapirism on Mediterranean Ridge. A preliminary report. Bolletino della Società Geologica Italiana 108: 537-543.

Collins AS, Robertson AHF. 1997. Lycian melange, southwestern Turkey: An emplaced Late Cretaceous accretionary complex. Geology 25: 255-258.

Collins AS, Robertson AHF. 1998. Processs of Late Cretaceous to Late Miocene episodic thrust-sheet translation in the Lycian Taurides, SW Turkey. Journal of the Geological Society London 155: 759-772.

Curewitz D and Karson JA. 1997. Structural settings of hydrothermal outflow: fracture permeability maintained by fault propagation and interaction. Journal of Volcanology and Geothermal Research 79: 149-168.

Dählmann A and De Lange GJ. 2003. Fluid–sediment interactions at Eastern Mediterranean mud volcanoes: a stable isotope study from ODP Leg 160, Earth and Planetary Science Letter 212: 377-391.

De Lange GJ and Brumsack. 1998. The occurence of gas hydrates in Eastern Mediterranean mud dome structures as indicated by pore-water composition. In: Henriet JP, Mienert J (eds.), Gas hydrates: relevance to world margin stability and climate change, Geological Society, London, Special Publications 137: 167-175.

Dercourt J, Ricou LE and Vrielynck B (editors). 1993. Atlas Tethys Paleoenvironments maps. 14 maps, 1 plate. Gauthier-Villars: Paris

De Voogd B, Truffert C, Chamot-Rooke N, Huchon P, Lallemant S and Le Pichon X. 1992. Two-ship deep seismic sounding in the basins of the Eastern Mediterranean Sea (Pasiphae Cruise). Geophysical Journal International 109:536-552.

Dewey JF, Pitman WCIII, Ryan WBF and Bonnin J. 1973. Plate tectonics and the evolution of the Alpine system. Geological Society of America Bulletin 84: 3137-3180.

Deyhle A and Kopf A. 2001. Deep fluids and ancient pore waters at the backstop: stable isotope systematics (B, C, O) of mud volcano deposits on the Mediterranean Ridge accretioary wedge. Geology 29/11: 1031-1034.

Dimitrov LI. 2002. Mud volcanoes ─ the most important pathway for degassing deeply buried sediments. Earth-Science Reviews 59: 49-76

Dumont J-F and Kerey E. 1975. L'accident de Kirkkavak: un décrochement important dans la chaîne taurique occidentale. Bulletin de la Société Géologique de France XVIII /2: 429.

Dumont J-F, Poisson A, Sahinci A. 1979. Sur l'existence des coulissements sénestres récents à l'extrémité orientale de l'arc égéen (sud-ouest de la Turquie). Comptes Rendus de l'Académie des Sciences de Paris, série D 289/3: 261-264.

Emeis KC, Robertson, AHF *et al.* 1996. Proceedings of the Ocean Drilling Program, Initial Reports, Mediterranean I, 160: College Station, TX (Ocean Drilling Program), 972pp.

Erickson AJ. 1970. The measurement and interpretation of heat flow in the Mediterranean and Black Sea. Unpublished Ph.D thesis (M.I.T.): 272pp.

Faugères JC, Gonthier E, Bobier C and Griboulard R. 1997. Tectonic control on sedimentary processes in the southern termination of the Barbados Prism. Marine Geology 140: 177-140.

Foucault A and Mélières F. 2000. Paleoclimatic cyclicity in central Mediterranean Pliocene sediments: the mineralogical signal. Paleogeography, Paleoclimatology, Paleoecology 158: 311-323.

Fitts TG and BrownKM. 1999. Stress-induced smectite dehydration: ramifications for patterns of freshening and fluid expulsionin the N Barbados accretionary wedge. Earth and Planetary Science Letters 172: 179-197.

Flecker R, Ellam RM, Müller C, Poisson A, Robertson AHF, Turner J. 1998. Application of Sr isotope and sedimentary analysis to the origin and evolution of the Neogene basins in the Isparta Angle, southern Turkey. Tectonophysics 298/ 1-3: 83-101.

Fowler SR, Midenhall J, Zalova S, Riley G, Elsley G, Desplanques A and Guliyev F. 2000. Mud volcanoes and structural development on Shah Deniz. Journal of Petroleum Science and Engineering 28: 189-206.

Fusi N and Kenyon NH. 1996. Distribution of mud diapirism and other geological structures from long-range sidescan sonar (GLORIA) data, in the Eastern Mediterranean Sea. Marine Geology 132: 21-38.

Gass IG. 1968. Is the Troodos massif of Cyprus a fragment of Mesozoic seafloor? Nature 220: 39-42

Gieskes JM, Graham D, and Ellis R. 1980. Interstitial-water studies, Deep Sea Drilling Project Sites 415 and 416. In: Lancelot Y, Winterer EL et al. (eds.) Initial Reports DSDP, 50, Washington (U.S. Govt. Printing Office): 691-693.

Glover C, Robertson A. 1998. Neotectonic intersection of the Aegean and Cyprus tectonic arcs: extensional and strike-slip faulting in the Isparta Angle, SW Turkey. Tectonophysics 298/ 1-3: 103-132.

Gorsel JT and Troelstra SR. 1980. Late Neogene climate changes and the messinian salinity crisis. Géologie Méditerranéenne VII/ 1: 127-134

Gutnic M, Monod O, Poisson A, Dumont J-F. 1979. Géologie des Taurides occidentales (Turquie). Mémoires de la Société Géologique de France LVIII/137: Paris; 112pp.

Graue K. 2000. Mud volcanoes in dep water Nigeria. Marine and Petroleum Geology 17: 959-974.

Grim RE. 1968. Clay Mineralogy. McGraw-Hill Compagny: 596pp.

Haese RR, Meile C, Van Cappellen P. and De Lange GJ. 2003. Carbon geochemistry of cold seeps: Methane fluxes and transformation in sediments from Kazan mud volcano, eastern Mediterranean Sea, Earth and Planetary Science Letter 212: 361-375

Hayward AB. 1984. Miocene clastic sedimentation related to the emplacement of the Lycian Nappes and the Antalya Complex. In: Dixon JE, Roberston AHF. (eds.), The Geological Evolution of the Eastern Mediterranean, Geological Society, London, Special Publication, 17: 287-300.

Heimann KO and Mascle G. 1974. Les séquences de la série évaporitique messinienne. Comptes Rendus de la Société Académique des Sciences, Paris, série D 279 : 1987-1990.

Henry P, Le Pichon X, Lallemant S, Foucher J-P, Westbrook G and Hobart M. 1990. Mud Volcano Field Seaward of the Barbados Accretionary Complex: A Deep-Towed Side Scan Sonar Survey. Journal of Geophysical Research 95/B6: 8917-8929.

Hieke W, Cita MB, Mirabile GL, Negri A and Werner F. 1996. The summit area (Antaeus/Pan di Zucchero) of the Mediterranean Ridge: a mud diapir field? Marine Geology 132: 113-129.

Higgins GE and Saunders, JB. 1974. Mud volcanoes -their nature and origin. Verhandlungen der Naturforschenden Gesellschaft in Basel 84: 101-152.

Hovland M, Hill A and Stokes D. 1997. The structure and geomorphology of the Dashgil mud volcano, Azerbaijan. Geomorphology 21: 1-15.

Hsü KJ, Cita MB and Ryan WBF. 1973. The origin of the Mediterranean evaporates. In: Ryan WBF, Hsü KJ, Cita MB *et al.* (eds.), Initial reports of the DSDP 13, DC, U.S. Government Printing Office, Washington: 1203-1231.

Huguen C. 2001. Déformation récente à actuelle et argilo-cinèse associée au sein de la Ride Méditerranéenne (Méditerranée Orientale). Thèse, Université Paris 6, Paris.

Huguen C, Benkhelil J, Giresse P, Mascle J, Muller C, Woodside J, Zitter T and the Medinaut Scientific Party. 2001a. Échantillons rocheux provenant de “volcans de boue” de Méditerranée orientale. Oceanologica Acta 24/4 : 349-360.

Huguen C, Mascle J, Chaumillon E, Woodside JM, Benkhelil J, Kopf A, Volkonskaya A. 2001b. Deformational styles of the eastern Mediterranean Ridge and surroundings from combined swath mapping and seismic reflection profiling. Tectonophysics 343/1-2: 21-47.

Huguen C, Zitter T, Woodside J and Mascle J. 2003. Central Mediterranean Ridge mud features: emplacement and evolution hypothesis from deep-tow side scan sonar records and deep dives (MEDINAUT and MEDINETH cruises). Deep Sea Research I, *submitted*.

Ivanov MK, Limonov AF and Cronin BT (editors). 1996. Mud volcanism and fluid venting in the eastern part of the Mediterranean Ridge, Initial results of the geological and geophysical investigations during the fifth UNESCO-ESF "Training-Through-Research" Cruise of RV Professor Logachev (July-september 1995), UNESCO reports in marine science 68, UNESCO: Paris, 126 p.

Ivanov MK, Limonov AF and Woodside JM (editors). 1992. Geological and geophysical investigations in the Mediterranean and Black Seas, Initial results of the "Training-Through-Research" Cruise of RV Gelendzhik in the Eastern Mediterranean and black sea (Jun-July 1991), UNESCO reports in marine science 56, UNESCO: Paris, 208 p.

Jolivet L, Goffé B, Bousquet R, Oberhänsli R and Michard A. The tectono- metamorphic signature of detachments in high pressure mountains belts: Tethyan examples.Earth and Planetary Science Letters 160: 31-47.

Jurado-Rodriguez MJ and Martinez-Ruiz F. 1998. Some clues about the Napoli and Milano mud volcanoes from an integrated log-core approach. In: Robertson AHF, Emeis KC, Richter C, and Camerlenghi A (eds.), Proceedings of the ODP, Scientific Results, 160: College station, TX (Ocean Drilling Program), 607-624.

Kahle H-G, Cocard M, Peter Y, Geiger A, Reilinger R, McClusky S, King R, Barka A, Veis G. 1999. The GPS strain rate field in the Aegean Sea and western Anatolia. Geophysical Research Letters 26/16: 2513-2516.

Kastens KA, Mascle J *et al.* 1987. Proceedings of the Ocean Drilling Program, Initial Reports, Mediterranean I, 107: College Station, TX (Ocean Drilling Program): 1013pp.

Kenyon NH, Ivanov MK, Akhmetzhanov AM, Akhmanov GG. 2000. Multidisciplinary study of geological processes on the North East Atlantic and Western Mediterranean margins, preliminary results of geological and geophysical investigations during the TTR-9 cruise of R/V Professor Logachev, June-July 1999. IOC Technical Series 56, UNESCO: Paris, 102pp.

Kenyon NH, Ivanov MK, Akhmetzhanov AM, Akhmanov GG. 2001. Interdisciplinary approaches to geosciences on the North East Atlantic margin and Mid-Atlantic Ridge, preliminary results of investigations during the TTR-10 cruise of R/V Professor Logachev, July-August 2000. IOC Technical Series 60, UNESCO: Paris, 104pp.

Kempler D, Ben-Avraham Z. 1987. The tectonic evolution of the Cyprus arc. Annales Tectonicae 1: 58-71.

Kempler D, Garfunkel Z. 1994. Structures and kinematics in the northeastern Mediterranean: A study of an irregular plate boundary. Tectonophysics 234: 19-32.

Kissel C, Averbuch O, Frizon de Lamotte D, Monod O, Allerton S. 1990. First paleomagnetic evidence of a post-Eocene clockwise rotation of the western Taurus belt, east of the Isparta reentrant (southwestern Turkey). Earth and Planetary Science Letters 117: 1-14.

Kissel C, Poisson A. 1986. Etude paléomagnétique préliminaire des cénozoïques des Bey Daglari (Taurides occidentales, Turquie). Comptes Rendus de l'Academie des Sciences de Paris, Série II 304/8: 711-716.

Koçyiğit A, Ünay E, Saraç G. 2000. Episodic graben formation and extensional neotectonic regime in west Central Anatolia and the Isparta Angle: a case study in the Aks¸ehir–Afyon graben, Turkey. In Tectonics and magmatism in Turkey and the surrounding area, Bozkurt E, Winchester JA, Piper JDA (eds.). Geological Society, London, Special Publications 173: 405–421.

Koçyiğit A, Yusufoğlu H, Bozkurt E. 1999. Evidence from the Gediz graben for episodic two-stage extension in western Turkey. Journal of Geological Society, London 156: 605-616.

Kopf A. 2002. Significance of mud volcanism. Reviews of Geophysics, 40,2: DOI 10.1029/2000RG000093.

Kopf A and Behrmann JN. 2001. Extrusion dynamics of mud volcanoes on the Mediterranean Ridge accretionary complex. In: Vendelille BC, Mart Y and Vigneresse JL (eds.), Salt, shales and igneous diapirs in and around Europe, Geological Society, London, Special Publications 174: 169-204.

Kopf A and Deyhle A. 2002. Back to the roots: Boron geochemistry of mud volcanoes and its implication for mud mobilization depth and global Boron cycling. Chemical Geology 192: 195-210.

Kopf A, Robertson AHF and Volkmann N. 2000. Origin of mud breccia from the Mediterranean Ridge accretionary complex based on evidence of the maturity of organic matter and related petrographic and regional tectonic evidence. Marine Geology 166: 65-82.

Kopf A, Klaeschen D and Mascle J. 2001. Extreme efficiency in dewatering accretionary prisms. Earth and Planetary sciences Letters 189: 295-313.

Kulm L D and Suess E. 1990. Relationship between carbonate deposits and fluid venting: Oregon accretionary prism. Journal of Geophysical Research 95/B6: 8899-8915.

Kvenvolden K.A. 1998., A primer on the geological occurrence of gas hydrate. In Henriet J-P and Mienert J (eds.) Gas Hydrates: Relevance to World Margin Stability and Climate Change, Geological Society, London, Special Publications, 137: 9-30.

Lance S, Henry P, Le Pichon X, Lallemant S, Chamley H, Rostek F, Faugères J-C, Gonthier E and Olu K. 1998. Submersible study of mud volcanoes seaward of the Barbados accretionary wedge: sedimentology, structure and rheology. Marine Geology 145: 255-292.

Le Pichon X and Angelier J. 1979. The Hellenic Arc and Trench system; a key to the neotectonic evolution of the Eastern Mediterranean. Tectonophysics 60: 1-42.

Le Pichon X, Angelier J, Aubouin J, Lybéris N, Monti S, Renard V, Got H, Hsü K, Mart Y, Mascle J, Matthews D, Mitropoulos D, Tsoflias P, Chronis, G. 1979. From subduction to transform motion: a seabeam survey of the Hellenic trench system. Earth and Planetary Science Letters 44: 441-50.

Le Pichon X, Augustithis SS and Mascle J. 1982a. Geodynamics of the Hellenic Arc and Trench. Tectonophysics 80: 304pp.

Le Pichon X, Lybéris N, Angelier J, Renard V. 1982b. Strain distribution over the Mediterranean Ridge: a synthesis incorporating new Sea-Beam data. Tectonophysics 86: 243-274.

Le Pichon X, Foucher JP, Boulègue J, Henry P, Lallemant S, Benedetti M, Avedik F, and Mariotti A. 1990. Mud Volcano Field Seaward of the Barbados Accretionary Complex: A Submersible Survey. Journal of Geophysical Research 95/B6: 8931-8943.

Le Pichon X, Chamot-Rooke N, Lallemant S. 1995. Geodetic determination of the kinematics of central Greece with respect to Europe: Implications for Eastern Mediterranean Tectonics. Journal of Geophysical Research 100/B7: 12675-12690.

Le Quellec P, Mascle J. 1978. Hypothèse sur l'origine des monts Matapan (Marge Ionienne du Péloponèse). Comptes Rendus de l'Académie des Sciences de Paris, série D 288: 31-34.

Lefèvre R. 1967. Un nouvel élément de la géologie du Taurus Lycien: les nappes d'Antalya (Turquie). Comptes Rendus de l'Académie des Sciences de Paris, série D 265: 1365-1368.

Liebetrau V, Eisenhauer A, Fietzke J and Garbe-Schönberg D. 2003. Growth rates of authigenic carbonates in a cold seep environment Geophysical Research Abstracts, 5: 11900.

Limonov AF, Woodside JM and Ivanov MK (editors). 1994. Mud volcanism in the Mediterranean and Black Seas and shallow structures of the Eratosthenes Seamount, Initial results of the geological and geophysical investigations during the third UNESCO-ESF "Training-Through-Research" Cruise of RV Gelendzhik (Jun-July 1993), UNESCO reports in marine science 64, UNESCO: Paris, 173 p.

Limonov AF, Kenyon NH, Ivanov MK and Woodside JM (editors). 1995. Deep-sea depositionnal systems of the Western Mediterranean and mud volcanism on the Mediterranean Ridge, Initial results of the geological and geophysical investigations during the fourth UNESCO-ESF "Training-Through-Research" Cruise of RV Gelendzhik (Jun-July 1994), UNESCO reports in marine science 67, UNESCO: Paris, 171p.

Limonov AF, Woodside JM, Cita MB and Ivanov MK. 1996. The Mediterranean Ridge and related mud diapirism: a background. Marine Geology 132: 7-19.

Loubrieu B, Satra S and Cagna R. 2000. Cartographie par sondeur multifaisceaux de la Ride Méditerranéenne et de ses domaines voisins. Ifremer/CIESM. Editions Ifremer, Cartes & Atlas, 2 cartes pliées au 1/1500000.

Lykousis V, Woodside J, de Lange G, Alexandri S, Sakellariou D, Nomikou1 P, Ioakim C, Dählmann A, Casas D, Rousakis G, Ballas D, Kormas K, Kioroglou1 S and Perissoratis C. 2003. Mud volcanoes and related gas hydrates in Anaximander Mountains (Eastern Mediterranean). New discoveries from the 01/May03 cruise of R/V AEGAEO (ANAXIMANDER PROJECT). (Abst) OMARC conference, Paris, 15-17/09 2003.

Maksimovich GA 1940. Classification of volcanoids. Doklady Akademii Nauk SSR 29/8-9: 596-600.

Maldonado A and Stanley DJ. 1981. Clay mineral distribution patterns as influenced by depositional processes in the southeastern Levantine Sea. Sedimentology 28: 21-32.

Mascle J and Chaumillon E. 1998. An overview of Mediterranean Ridge collisional accretionary complex as deduced from multichannel seismic data. Geo-Marine Letters 18: 81-89.

Mascle J, Le Cleach A, Jongsma D. 1986. The Eastern Hellenic margin from Crete to Rhodes: example of progressive collision. Marine Geology 73: 145-168.

Mascle J, Huguen C, Benkhelil, J, Chamot-Rooke N, Chaumillon E, Foucher J-P, Griboulard R, Kopf A, Lamarche G, Volkonskaia A, Woodside J, Zitter T. 1999. Images may show start of European-African plate collision. Eos, Transactions, American Geophysical Union 80: 37.

McClusky S, Balassanian S, Barka A, Demir C, Ergintav S, Georgiev I, Gurkan O, Hamburger M, Hurst K, Kahle H, Kastens K, Kekelidze G, King R, Kotzev V, Lenk O, Mahmoud S, Mishin A, Nadariya M, Ouzounis A, Paradissis D, Peter Y, Prilepin M, Reilinger R, Sanli I, Seeger H, Tealeb A, Toksoz MN, Veis G. 2000. Global Positioning System constraints on plate kinematics and dynamics in the eastern Mediterranean and Caucasus. Journal of Geophysical Research 105/ B3: 5695-5719.

McEwan DMC, Ruiz AA and Brown G. 1961. Interstratified clay minerals. In: Brindley GW and Brown G (eds.), Crystal Structures of Clay Minerals and Their X-ray Identification. Mineralogical Society London Monograph 5: 393–445.

McKenzie DP. 1972. Active tectonics of the Mediterranean region. Geophysical. Journal of the Royal Astronomical Society 30: 109-185.

Mélières F, Foucault A and Blanc-Valleron M-M. 1998. Mineralogical record of cyclic climate changes in Mediterranean Mid-Pliocene deposits from Hole 964A (Ionian Basin) and from Punta

Piccola (Sicily). In: Robertson AHF, Emeis KC, Richter C, and Camerlenghi A (eds.), Proceedings of the ODP, Scientific Results, 160: College station, TX (Ocean Drilling Program), 219-226.

MEDINAUT/MEDINETH Shipboard Scientists: Aloisi G, Asjes S, Bakker K, Bakker M, Charlou J-L, De Lange G, Donval J-P, Fiala-Medioni A, Foucher J-P, Haanstra R, Haese R, Heijs S, Henry P, Huguen C, Jelsma B, de Lint S, van der Maarel M, Mascle J, Muzet S, Nobbe G, Pancost R, Pelle H, Pierre C, Polman W, de Senerpont Domis L, Sibuet M, van Wijk T, Woodside J and Zitter T. 2000. Linking Mediterranean brine pools and mud volcanism. Eos, Transactions, American Geophysical Union 81/51: 625, 631-633.

Milkov AV. 2000. Worldwide distribution of submarine mud volcanoes and associated gas hydrates. Marine Geology 167/1-2: 29-42.

Milkov A, Vogt P, Cherkashev G, Ginsburg G, Chernova N and Andriashev A. 1999. Sea-floor terrain of Hakon Mosby Mud Volcano as surveyed by deep-tow video and still photography. Geo-Marine Letters 19: 38-47.

Millot G. 1964. Géologie des argiles. Masson editor, Paris: 499 pp.

Mitchell NC. 1993. A model for attenuation of backscatter due to sediment accumulation and its application to determine thicknesses with Gloria sidescan sonar. Journal of Geophysical Research 98/B12: 22477-22493.

Monod O. 1976. La "Courbure d' Isparta": une mosaïque de blocs autochtones surmontés de nappes composites à la jonction de l'arc héllenique et de l'arc taurique. Bulletin de la Société Géologique de France XVIII/2: 521-531.

Moores EM, Vine FJ. 1971. Troodos massif, Cyprus and other ophiolites as oceanic crust: evaluation and implications. Royal Society Philosophical Transactions A268: 433-466.

Morris A, Robertson AHF. 1993. Miocene remagnetisation of Mesozoic Antalya complex units in the Isparta angle, SW Turkey. Tectonophysics 220: 243-266.

Nesteroff WD, Lort JM, Angelier J, Bonneau M, Poisson A. 1977. Esquisse structurale en Méditerranée orientale au front de l'Arc Egéen. In: Biju-Duval B, Montaret L. (eds.), Symposuim on the Structural History of the Mediterranean Basin, Editions Technip: Paris.

Nur A, Ben Avraham Z. 1978. The Eastern Mediterranean and the Levant: Tectonics of continental collision. Tectonophysics 46: 297-311.

Olivet JL, Bonnin J, Beuzart P and Auzende JM. 1982. Cinématique des plaques et paléogéographie: une revue. Bulletin de la Société Géologique de France 24 :875-892.

Olu-Leroy K, Sibuet M, Levitre G, Gofas S, Salas C, Fiala-Médioni A, Foucher J-P and Woodside JM. 2003. Cold seeps communities in the deep eastern Mediterranean Sea : composition and spatial distribution on mud volcanoes. Deep-Sea Research I, *in press.*

Orange DL, Greene HG, Reed D, Martin JB, McHugh CM, Ryan WBF, Maher N, Stakes D and Barry J. 1999. Widespread fluid expulsion on a translational continental margin: Mud volcanoes, fault

zones, headless canyons, and organic-rich substrate in Monterey Bay, California. Geological Society of America Bulletin 111/7: 992-1009.

Papazachos BC and Comninakis PE. 1971. Deep structure and tectonics of the Eastern Mediterranean. Tectonophysics 46: 285-296.

Papazachos BC and Papaioannou CA. 1999. Lithospheric boundaries and plate motions in the Cyprus area. Tectonophysics 308: 93-204.

Papazachos BC, Hatzidimitriou PM, Panagiotopoulos DG, Tsokas GN. 1995. Tomography of the crust and upper mantle in southeast Europe. Journal of Geophysical Research 100/B: 12 405-12 422.

Papazachos BC, Karakostas VG, Papazachos CB and Scordilis EM; 2000; The geometry of the Wadati-Benioff zone and lithospheric kinematics in the Hellenic Arc. Tectonophysics 319(4): 275-300.

Pancost RD, Sinninghe Damsté JS, Lint S de, Maarel MJEC van der, Gottschal JC and the Medinaut Shipboard Scientific Party. 2000. Biomarker evidence for widespread anaerobic methane oxidation in Mediterranean sediments by a consortium of methanogenic archae and bacteria. Applied and Environmental microbiology 66: 1126-1132.

Pancost RD, Hopmans EC, Sinninghe Damsté JS and the MEDINAUT Shipboard Scientific Party. 2001. Archeal lipids in Mediterranean cold seeps: molecular proxies for anaerobic methane oxidation. Geochimica and Cosmochimica Acta 65: 1611-1627.

Paquet H. 1969. Évolution géochimique des minéraux dans les altérations et les sols des climats méditerranéens et tropicaux à saisons contrastées. Mém. Serv. Carte Géol Alsace-Lorraine, 30, 212 pp.

Payne AS, Robertson AHF. 1995. Neogene supra-subduction zone extension in the Polis graben system, west Cyprus. Journal of the Geological Society, London 152: 613-628.

Pérez-Beluz F, Alonso B and Ercilla G. 1997. History of mud diapirism and trigger mechanisms in the Western Alboran Sea. Tectonophysics 282: 399-422.

Pletsch T. 1998. Origin of lower Eocene palygorskite clays on the Côte d'Ivoire-Ghana transform margin, Eastern Equatorial Atlantic. In: Mascle J, Lohmann GP, and Moullade M. (eds.), Proceedings ODP, Scientific Results, 159: College Station, TX (Ocean Drilling Program). 141- 156.

Poisson, A. 1977. Recherches géologiques dans les Taurides occidentales (Turquie). Thèse, Université Paris 11, Paris.

Poisson A, Orsay A, Akay E, Dumont J-F, Uysal S. 1984. The Isparta Angle: a Mesozoic paleorift in the Western Taurides. In: Tekeli O, Gönçüoglu C (eds.), International Symposuim on geology of the Taurus Belt, Ankara, Special Publication MTA: 11-26.

Premoli-Silva I, Erba E, Spezzaferri S and Cita MB. 1996. Age variation in the source of the diapiric mud breccia along and across the axis of the Mediterranean Ridge Accretionary Complex. Marine Geology 132: 175-202.

Rabaute A, Chamot-Rooke N and The DOTMED Team. 2003. Tectonics and mud volcanism at the western Mediterranean Ridge – backstop contact. Geophysical Research Abstracts 5, 12007.

Ransom B, KastnerM and Bennett RH. 1998. Organic matter in California continental margin sediments; where is it,how does it get there, and how much is preserved? Geological Society of America 28th annual meeting, Geological Society of America 28(7): 520.

Reed DL, Silver EA, Tagudin JE, Shipley TH and Vrolijk P. 1990. Relations between mud volcanoes, thrust deformation, slope sedimentation, and gas hydrate, offshore north Panama. Marine and Petroleum Geology 7: 44-55.

Reilinger RE, McClusky SC, Oral MB, King RW, Toksoz MN. 1997. Global positioning system measurements of present-day crustal movements in the Arabia-Africa-Eurasia plate collision zone. Journal of Geophysical Research 102/B5: 9983-9999.

Rensbergen P van, Morley CK, Ang DW, Hoan TQ and Lam NT. 1999. Structural evolution of shale diapirs from reactive rise to mud volcanism: 3D seismic data from the Baram delta, offshore Brunei Darussalam. Journal of the Geological society, London 156: 633-650.

Robert C and Chamley H. 1991. Development of early Eocene warm climates, as inferred from clay mineral variations in oceanic sediments. Palaeogeography, Palaeoclimatology, and Palaeoecology 89: 315-331.

Robertson AHF. 1993. Mesozoic-Tertiary tectonic evolution of Neothethyan carbonate platforms, margins and small oceans basins in the Antalya Complex, SW Turkey. In: Frostick L E, Steels R (eds.), Sedimentation, tectonics, and eustasy, Sea-level Changes at active Margins, Special Publication of the International Association of Sedimentology: 415-465.

Robertson AHF. 1998a. Tectonic significance of the Eratosthenes Seamount: a continental fragment in the process of collision with a subduction zone in the eastern Mediterranean (Ocean Drilling Program Leg 160). Tectonophysics 298: 63-82.

Robertson AHF. 1998b. Mesozoic-Tertiary tectonic evolution of the easternmost Mediterranean area: integration of marine and land evidence. In: Robertson AHF, Emeis K-C, Richter C, Camerlenghi A (eds.), Proceedings of the Ocean Drilling Program, Scientific Results, 160: College Station, TX (Ocean Drilling Program), 723-782.

Robertson and Kopf, 1998a. Origin of clasts and matrix within the Milano and Napoli mud volcanoes, Mediterranean Ridge accretionary complex. In: Robertson AHF, Emeis KC, Richter C and Camerlenghi A (eds.), Proceedings of the ODP, Scientific Results, 160:College Station, TX (Ocean Drilling Program), 575-595.

Robertson and Kopf, 1998b. Tectonic setting and processes of mud volcanism on the Mediterranean ridge accretionary complex: evidence from Leg 160. In: Robertson AHF, Emeis KC, Richter C and Camerlenghi A (eds.), Proceedings of the ODP, Scientific Results, 160:College Station, TX (Ocean Drilling Program), 663-680.

Robertson AHF and Woodcock, NH. 1979. Mamonia Complex, southwest Cyprus: Evolution and emplacement of a Mesozoic continental margin. Geological Society of America Bulletin 90: 651-665.

Robertson AHF and Woodcock, NH. 1980. Strike-slip related sedimentation in the Antalya Complex, SW Turkey. Special Publication of the Intenational Association of Sedimentologists 4: 127-145.

Robertson A Emeis KC, Richter C, BlancValleron MM, Bouloubassi I, Brumsack HJ, Cramp A, DeLange CJ, DiStefano E, Flecker R, Frankel E, Howell MW, Janecek TR, JuradoRodriguez MJ, Kemp AES, Koisumi I, Kopf A, Major CO, Mart Y, Pribnow DFC, Rabaute A, Roberts A, Rullkotter, J.H., Sakamoto T, Spezzaferri S, Staerker TS, Stoner JS, Whiting BM and Woodside JM. 1996. Mud volcanism on the Mediterranean Ridge: Initial results of Ocean Drilling Program Leg 160, Geology 24(3): 239-242.

Robertson AHF, Emeis KC Richter C and Camerlenghi A (Editors). 1998. Proceedings ODP, Scientific Results, 160. TX (Ocean Drilling Program), College Station.

Rotstein Y and Kafka AL. 1982. Seismotectonics of the southern boundary of Anatolia, Eastern Mediterranean region: subduction, collision and arc jumping. Journal of Geophysical Research 87: 7694-7706.

Rotstein Y and Ben-Avraham Z. 1985. Accretionary processes at subduction zones in the Eastern Mediterranean. Tectonophysics 112: 551-561.

Ryan WBF, Kastens KA, Cita MB. 1982. Geological evidence concerning compressional tectonics in the Eastern Mediterranean. Tectonophysics 86: 213-242.

Ryan WBF, Stanley DJ, Hersey JB, Fahlquist DA, Allan TD. 1970. The tectonic and the geology of the Mediterranean sea. In: Maxwell AE (ed.), The sea, J Wiley and sons: New-York; 387-392.

Sage L, Letouzey J. 1990. Convergence of the African and Eurasian plate in the Eastern Mediterranean. In Petroleum and tectonics in mobile Belt, Letouzey J (ed.). Editions Technip: Paris; 49-68.

Sager WW, MacDonald IR and Hou R. 2003. Geophysical signatures of mud mounds at hydrocarbon seeps on the Louisiana continental slope, northern Gulf of Mexico. Marine Geology 198: 97-132.

Salas C and Woodside JM. 2002. *Lucinoma Kazani* n. sp. (Mollusca: Bivalvia): evidence of a living benthic community associated with a cold seep in the Eastern Mediterranean Sea. Deep-Sea research I 49: 991-1005.

Scholz CH, Dawers NH, Yu JZ, Anders MH, Cowies PA. 1993. Fault growth and fault scaling laws: preliminary results. Journal of Geophysical Research 98, 21951-21961.

Schulz H-M, Emeis K-C and Volkmann N. 1997. Organic carbon provenance and maturity in the mud breccia from the Napoli mud volcano: Indicators of origin and burial depth, Earth and Planetary Science Letters 147/1-4: 141-151

Şengör AMC, Görür N, Şaroğlu F. 1985. Strike-slip faulting and related basin formation in zones of tectonic escape: Turkey as a case study. In: Biddle KT, Christie-Blick N (eds.), Strike-slip deformation, basin formation and sedimentation, The Society of Economic Paleontologists and Mineralogists, Special Publication 37: 27-264.

Seyitoğlu G, Scott BC, Rundle CC. 1992. Timing of Cenozoic extensional tectonics in west Turkey. Journal of the Geological Society, London 149: 533-538.

Spakman W, Wortel MJR, Vlaar NJ. 1988. The Hellenic subduction zone: a tomographic image and its geodynamic implications. Geophysical Research Letters 15: 60-63.

Staffini F, Spezzaferri S and Aghib F. 1993. Mud diapirs of the Mediterranean Ridge: sedimentological and paleontological study of the mud breccia. Riv. It. Paleont. Strat. 99/2: 225-254.

Sumner RH and Westbrook GK. 2001. Mud diapirism in front of the Barbados accretionary wedge: the influence of fracture zones and North America-South America plate motions. Marine and Petroleum Geology 18: 591-613.

Taymaz T and Price S. 1992. The 1971 May 12 Burdur earthquake sequence, SW Turkey: a synthesis of seismological and geological observations. Geophysical Journal International 108: 589-603.

Taymaz T, Tan O, Özalaybey S, Karabulut H. 2002. Source characteristics of February 3, 2002 Çay-Sultandağı Earthquake (Mw= 6.5) sequence in SW-Turkey: a synthesis of Seismological Observations of Body-Waveforms, Strong Motions, and Aftershock Seismicity Survey Data. 1st International Symposium of İstanbul Technical University the Faculty of Mines on Earth Sciences and Engineering, İstanbul-Turkey, Abstracts. p 60.

ten Veen JH and Meijer PT. 1998. Late Miocene to Recent tectonic evolution of Crete (Greece), geological observations and model analysis. Tectonophysics 298: 191-208.

ten Veen JH and Postma G. 1999. Rollback controlled vertical movements of outer-arc basins of the Hellenic subduction zone (Crete, Greece). Basin Research 11/3: 243-366.

ten Veen JH and Kleinspehn KL. 2002. Geodynamics along an increasingly curved convergent plate boundary: late Miocene-Pleistocene Rhodes, Greece. Tectonics 21/3: DOI 10.1029/2001TC001287.

ten Veen JH, Woodside JM, Zitter TAC, Dumont J-F, Mascle J and Volkonskaia A. 2003. Neotectonic evolution of the Anaximander Mountains at the junction of the Hellenic and Cyprus arcs. Tectonophysics, *in press*.

Tomadin L and Lenaz R. 1989. Eolian dust over Mediterranean and their contribution to the present sedimentation. In: Leinen M. and Sarnthein M. (eds.), Paleoclimatology and Paleometeorology: modern and past patterns of global atmospheric transport, Kluwer Academic Publisher: 267-282.

Truffert C, Chamot-Rooke N, Lallemant S, de Voogd B, Huchon P and Le Pichon X. 1993. The crust of the Western Mediterranean Ridge from deep seismic data and gravity modelling. Geophysical Journal International 114: 360-372.

Venkatarathnam K and Ryan WB. 1971. Dispersal patterns of clay minerals in the sediments of the Eastern Mediterranean Sea. Marine Geology 11: 261-282.

Vernette G, Mauffret A, Bobier C, Briceno L and Gayet J. 1992. Mud diapirism, fan sedimentation and strike-slip faulting, Carribean Colombian Margin. Tectonophysics 202: 335-349.

Vidal N, Alvarez-Marron J, Klaeschen D. 2000a. Internal configuration of the Levantine Basin from seismic reflection data (eastern Mediterranean). Earth and Planetary Science Letters 180/1-2: 77-89.

Vidal N, Klaeschen D, Kopf A, Docherty C, Von Huene R, Krasheninnikov VA. 2000b. Seismic images at the convergence zone from south of Cyprus to the Syrian coast, eastern Mediterranean. Tectonophysics 329/1-4: 157-170.

Vogt PR, Crane K, Pfirman S, Sundvor E, Cherkis N, Flemming H, Nishimura C and Shor A. 1991. SeaMARC II sidescan sonar imagery and swath bathymetry in the Nordic basin. Eos Transactions 72: 486

Vogt PR, Gardner J and Crane K. 1999. The Norwegian-Barents-Svalbard (NBS) continental margin: Intrdoucing a natural laboratory of mass wasting, hydrates, and ascent of sediment, pore water and methane. Geo-Marine Letters 19: 2-21.

Volgin AV and Woodside JM. 1996. Sidescan sonar images of mud volcanoes from the Mediterranean Ridge: possible causes of variations in backscatter intensity. Marine Geology 132: 39-53.

Waelkens M, Sintubin M, Muchez P, Paulissen E. 2000. Archaeological, geomorphological and geological evidence for a major earthquake at Sagalassos (SW Turkey) around the middle of the seventh century AD. In: Mcguire B, Griffiths D, Stewart I. (eds.), The Archaeology of Geological Catastrophes, Geological Society, London, Special Publication 171: 373-383.

Wallmann K, Aghib FS, Castradori D, Cita MB, Suess E, Greinert J and Rickert D. 2002. Sedimentation and formation of secondary minerals in the hypersaline Discovery Basin, eastern Mediterranean, Marine Geology 186: 9-28.

Wessel P and Smith WHF. 1991. Free software helps map and display data. EOS Transaction AGU, 72: 441.WWW page, http://gmt.soest.hawaii.edu/.

Werne JP, Zitter TAC, Haese RR, Aloisi G, Bouloubassi I, Heijs S, Fiala-Medoni A, Pancost RD, Sinninghe Damsté JS, De Lange G, Forney LJ, Gottschal JC, Foucher J-P, Mascle J, Woodside J and the MEDINAUT/MEDINETH Shipboard Scientific Parties. 2003. Life at cold seeps: a synthesis of ecological and biogeochemical data from Kazan mud volcano, eastern Mediterranean Sea. Chemical Geology, *in press.*

Wiedicke M, Sahling H, Delisle G, Faber E, Neben S, Beiersdorf H, Marchig V, Weiss W, Mirbach N von and Afiat A. 2002. Characteristics of an active vent in the fore-arc basin of the Sunda Arc, Indonesia. Marine Geology 184: 121-141.

Wiedicke M, Neben S and Spiess V. 2001. Mud volcanoes at the front of the Makran accretionary complex, Pakistan. Marine Geology 172: 57-73.

Woodcock NH, Robertson AHF. 1982. Wrench and thrust tectonics along a Mesozoic-Cenozoic continental margin: Antalya Complex, SW Turkey. Journal of the Geological society of London 139: 147-163.

Woodside JM. 1977. Tectonic elements and crust of the Eastern Mediterranean Sea. Marine Geophysical Researches 3: 317-354.

Woodside JM and Volgin AV. 1996. Brine pools associated with Mediterranean Ridge mud diapirs: an interpretation of echo-free patches in deep tow sidescan sonar data. Marine Geology 132: 55-61

Woodside JM, Ivanov MK, Limonov AF. 1997a. Neotectonics and fluid flow through seafloor sediments in the Eastern Mediterranean and Black Seas- Part I, Eastern Mediterranean Sea. IOC Technical Series No. 48 (Intergovernmental Oceanographic Commission, Unesco), UNESCO 1997: Paris, 128p.

Woodside JM, Ivanov MK, Limonov AF. 1997b. Neotectonics and fluid flow through seafloor sediments in the Eastern Mediterranean and Black Seas- Part II, Black Sea. IOC Technical Series No. 48 (Intergovernmental Oceanographic Commission, Unesco), UNESCO 1997: Paris, 128p.

Woodside JM, Ivanov MK, Limonov AF. 1998. Shallow gas and gas hydrates in the Anaximander Mountains region, eastern Mediterranean Sea. In: Henriet JP, Mienert J (eds.), Gas hydrates: relevance to world margin stability and climate change, Geological Society, London, Special Publications 137: 177-193.

Woodside JM, Mascle J, Huguen C, Volkonskaia A. 2000. The Rhodes Basin, a post-Miocene tectonic trough. Marine Geology 165/1-4: 1-12.

Woodside JM, Mascle J, Zitter TAC, Limonov AF, Ergun M, Volkonskaia A. 2002. The Florence Rise, the Western Bend of the Cyprus Arc. Marine Geology 185/3-4: 177-194.

Wortel MJR and Spakman W.1992. Structure and dynamics of subducted litosphere in the Mediterranean Region. Proceedings Koninlijke Nederlandse Akademie van Wetenschappen 95: 325-347.

Wortel MJR and Spakman W.2000. Subduction and slab detachment of the Mediterranean-Carpathian Region. Science 290: 1910-1917.

Yağmurlu F, Savascin Y, Ergun M. 1997. Relation of alkaline volcanism and active tectonism within the evolution of the Isparta Angle, SW Turkey. Journal of Geology 105/ 6: 717-728.

Zitter TAC, Woodside JM and Mascle J. 2003. The Anaximander Mountains: a clue to the tectonics of Southwest Anatolia. Geological Journal 38: 375-394